Industria Textilă

ISSN 1222–5347 (57–112)

2/2012

Revistă **cotată ISI** şi inclusă în **Master Journal List** a Institutului pentru Ştiinţa Informării din Philadelphia – S.U.A., începând cu vol. 58, nr. 1/2007/
ISI rated *magazine, included in the* ***ISI Master Journal List*** *of the Institute of Science Information, Philadelphia, USA, starting with vol. 58, no. 1/2007*

Editată în 6 nr./an, indexată şi recenzată în:
Edited in 6 issues per year, indexed and abstracted in:
Science Citation Index Expanded (SciSearch®), Materials Science Citation Index®, Journal Citation Reports/Science Edition, World Textile Abstracts, Chemical Abstracts, VINITI, Scopus

MOHAMMAD REZA MOHAMMAD SHAFIEE, MARYAM SALEHI ESFANDARANI
Producerea unei membrane din compozit nanofibros şi caracterizarea permeabilităţii la aer a acesteia 59–63

B. CENKKUT GULTEKIN, S. MUGE YUKSELOGLU, ONUR ATAK
Capacitatea de vopsire a materialelor SeaCell® active cu coloranţi reactivi, folosind energia ultrasonică 64–67

OCTAVIAN POPESCU, RODICA MARIANA DIACONESCU AURELIA GRIGORIU, ECATERINA VASLUIANU
Optimizarea funcţionalizării materialelor celulozice cu monoclorotriazinii-β-ciclodextrină în mediu 68–74

HUSEYIN ATA KARAVANA
Determinarea unor caracteristici ale blănurilor de iepure alb neozeelandez, destinate îmbrăcămintei din piele 75–78

AUREL POPP, VLADLEN BABCINEŢCHI, MIHAELA CARP
Procedee moderne de înnobilare a vestimentaţiei 79–84

BURÇIN ESER, ARIF TANER ÖZGÜNEY, ARZU ÖZERDEM
Studiu privind utilizarea diferitelor tipuri de agenţi de îngroşare la imprimarea cu jet de cerneală, folosind coloranţi reactivi 85–90

ELENA ONOFREI
Identificarea principalilor factori care influenţează confortul termic, folosind analiza componentelor principale şi selecţia materialului textil în funcţie de destinaţia finală a îmbrăcămintei 91–96

IONUŢ DULGHERIU, CIPRIAN COZMANCIUC
Testări mecanice ale materialelor compozite destinate vestelor de salvare 97–104

CRONICĂ 105–109

DOCUMENTARE 84, 110–112

Recunoscută în România, în domeniul Ştiinţelor inginereşti, de către **Consiliul Naţional al Cercetării Ştiinţifice din Învăţământul Superior** (C.N.C.S.I.S.), în **grupa A** /
Aknowledged in Romania, in the engineering sciences domain, by the ***National Council of the Scientific Research from the Higher Education*** *(CNCSIS), in* ***group A***

it Sumar

Contents

MOHAMMAD REZA MOHAMMAD SHAFIEE, MARYAM SALEHI ESFANDARANI	Producing composite nanofibrous membrane and characterization of its air permeability	59
B. CENKKUT GULTEKIN S. MUGE YUKSELOGLU ONUR ATAK	Dyeability of SeaCell®active fabrics with reactive dyes by using of ultrasonic energy	64
OCTAVIAN POPESCU RODICA MARIANA DIACONESCU AURELIA GRIGORIU ECATERINA VASLUIANU	Optimization of the cellulosic materials functionalization with monochlorotriazinyl-β-cyclodextrin in basic medium	68
HUSEYIN ATA KARAVANA	Determination of some characteristics of New Zealand white rabbit furs for leather garment	75
AUREL POPP VLADLEN BABCINEȚCHI MIHAELA CARP	Modern processes of ennoblement for garment	79
BURÇIN ESER ARIF TANER ÖZGÜNEY ARZU ÖZERDEM	Investigation of the usage of different thickening agents in ink-jet printing with reactive dyes	85
ELENA ONOFREI	Identification of the most significant factors influencing thermal comfort using principal component analysis and selection of the fabric according to the apparel end-use	91
IONUȚ DULGHERIU CIPRIAN COZMANCIUC	Mechanical tests carried out on composite materials specific to safety jackets	97
CRONICĂ	Chronicles	105
DOCUMENTARE	Documentation	84, 110

Revista „INDUSTRIA TEXTILĂ", Institutul Național de Cercetare-Dezvoltare pentru Textile și Pielărie – București

Redacția (Editura CERTEX), administrația și casieria: București, str. Lucrețiu Pătrășcanu nr. 16, sector 3, Tel.: 021-340.42.00, 021-340.02.50/226, e-mail: certex@ns.certex.ro; Fax: +4021-340.55.15. Pentru abonamente, contactați redacția revistei. Instituțiile pot achita abonamentele în contul nostru de virament: RO25RNCB0074029214420001 B.C.R. sector 3, București.

Lucrare executată în colaborare cu Editura AGIR, Calea Victoriei nr. 118, sector 1, București, tel.: 021-316.89.92; 021-316.89.93; fax: 021-316.89.92

Producing composite nanofibrous membrane and characterization of its air permeability

MOHAMMAD REZA MOHAMMAD SHAFIEE MARYAM SALEHI ESFANDARANI

REZUMAT – ABSTRACT

Producerea unei membrane din compozit nanofibros şi caracterizarea permeabilităţii la aer a acesteia

În lucrare este prezentat un procedeu de realizare, într-o singură etapă, a nanofibrelor din compozite de carbon activat într-o soluţie polimerică - poliacrilonitril, folosind metoda electrofilării cu o singură duză. Morfologia suprafeţei nanofibrelor din compozite care conţin cantităţi diferite de nanoparticule de carbon activat este analizată în funcţie de concentraţia de carbon activat din soluţia de filare. Rezultatele arată că, odată cu creşterea concentraţiei de carbon activat din soluţia polimerică, diametrul mediu al nanofibrelor creşte, iar nanofibrele devin mai puţin omogene. Investigaţiile făcute asupra structurii chimice şi a structurii cristaline a nanofibrelor compozite obţinute, prin difracţie de raze X şi spectroscopie în infraroşu cu transformată Fourier (FT-IR), au arătat că, proprietăţile se modifică o dată cu introducerea nanoparticulelor de carbon activat în matricea polimerică. Datorită faptului că există un potenţial crescut ca pânza nanofibroasă obţinută să fie aplicată ca mediu de filtrare pentru măştile de faţă, este necesară şi investigarea unei alte proprietăţi importante, şi anume a permeabilităţii la aer.

Cuvinte-cheie: compozit polimeric, carbon activat, nanofibre, nanoparticule, spectroscopie în infraroşu cu transformată Fourier, difracţie cu raze X

Producing composite nanofibrous membrane and characterization of its air permeability

In this work activated carbon-polyacrylonitrile composite nanofibers are successfully produced by a one step, single nozzle electrospinning method. Surface morphology of composite nanofibers containing different amount of activated carbon nanoparticles is analyzed as a function of activated carbon concentration in the spinning solution. The results reveal that with increasing activated carbon concentration in the polymer solution the mean diameter of nanofibers increases and the nanofibers become less homogenous. Investigating the chemical structure and crystal structure of the resulted composite nanofibers by X-ray diffraction (XRD) and Fourier transform infrared (FT-IR) spectroscopy, showed that characteristic changes happen with introducing active carbon nanoparticles into polymeric matrix. Due to the great potential of the resulted composite nanofibrous web to apply as a filter media in the face masks, air permeability is an important property that is investigated through air permeability tests.

Key-words: polymeric composite, activated carbon, air permeability, nanofiber, nanoparticles, Fourier transform infrared spectroscopy, X-ray diffraction

By decreasing the diameter of polymeric fibers from micrometers to sub microns or nanometers, surface area, flexibility in surface, functionalities and mechanical performance improves greatly, compared with any other known form of the materials [1]. Great properties of nanofibers such as large surface area to volume ratio, exceptional long length, high surface area and uniform diameter make them ideal candidates for new generation of filtration materials, carrier for catalysis, nanofibers reinforcement, tissue engineering, sensors, separations, electrochemical cells, drug delivery and chemical filtration [2–4].

Electrospinning is an efficient, simple, versatile and well-known technique for producing extremely ultrafine fibers ranging from nanometer to micrometer by which high voltage is used to produce an interconnected web of ultrafine polymeric fibers [5]. Electrospinning, compared with other methods for producing nanofibers is a promising process due to its flexibility in designing fiber structures by controlling the spinning parameters [6]. In recent years producing electrospun nanofiber with novel composition and morphologies such as hollow, core-sheath, porous and composite nanofibers has attracted great attention of researchers and scientists [7–10]. The electrospun ultra-fine composite fibers are currently a subject of intensive research due to their great properties such as their small diameter, large area-to-volume ratio, and small pore size, which not only improve the material properties, but also create new characteristics not observed in bulk materials [11].

Because of these reasons, much progress has recently been made in the production of composite nanofibers through electrospinning nanoparticulate dispersions in polymer solutions, such as iron–platinum [12], Cr_2O_3/Al_2O_3 [13], SiO_2 [14] composite nanofibers. With embedding the nanoparticles in the nanofibers structure through electrospinning process, their mechanical, electrical, optical, thermal and magnetically properties could be enhanced and their application in fuel cells, separation, biomedical devices, energy conversion and storage systems could be greatly improved [2]. Mostly inorganic nanoparticles are introduced into nanofibers structure, but in some applications, adding the organic nanoparticles could enhance some special properties of nanofibers [15].

Recently nanoporous materials include mesoporous silica materials, mesoporous carbon materials, nanocarbon materials, nanofiber materials and others, have attracted great attention of scientist and researchers, due to their uniquely large specific surface area, regular pore structure, and highly controllable surface properties [15]. These special characteristics cause great absorbency properties for them. Among different absorbent materials activated carbon is specially known as one of the best absorbent for organic chemicals from waste water, it also could remove inorganic and heavy metal pollutants [16]. Carbon adsorption process could effectively control the problems related to trace organic substances such as taste and odor causing by synthetic organic compounds [17].

In this work in order to produce absorbent nanofibers, activated carbon nanoparticles are introduced into nanofibers, through electrospinning process, and surface morphology, chemical and crystal structure of the resulted composite nanofibers are analyzed. Due to the great potential of the resulted composite nanofibrous web to apply as the filter media in the face masks, air permeability of the resulted membrane is also investigated by air permeability test.

EXPERIMENTAL PART

Materials used

Polyacrylonitrile (PAN) was kindly supplied by Polyacryl Co. The weight-average molecule weight (Mw) being 100,000. N, N-dimethylformamide (DMF) acid and activated carbon (charcoal) was purchased from Merck Company Inc. All these reagents were used without further purification.

Preparation of polymer solutions

In order to obtain homogenous dispersion of activated carbon nanoparticles in the spinning solution, at first activated carbon nanoparticles with different concentration (2, 5, 10 wt % to PAN) were dispersed in DMF by probe ultrasonic stirrer (UP2005) for 30 minute, then polyacrylonitrile was added to the that solution (13.5 wt %) to obtain the final spinning solution. Afterwards, the resulted solution was magnetically stirred for 5 hours, in temperature of 50°C and became ready for the electrospinning process.

Surface analysis

Gold sputtering of the membrane samples were conducted in a vacuum chamber with layers of approximately 20 nm thicknesses, and the morphology of nanofibers were observed by a field emission scanning electron microscope (FESEM HIT S-4160 at 15 kV).

Infrared spectroscopy

The FT-IR spectra were recorded on a Nexus FT-IR Spectrometer 670 from 4000 to 400 cm^{-1} with a 2 cm^{-1} resolution.

X-ray diffraction

X-ray diffraction (XRD) analysis was performed using a Philips PWC 3040 diffractometer, using Cu radiation. The operating voltage and current were 40 kV, and 30 mA. Step size was 0.05, peak positions were determined by high score software.

Air permeability

Air permeability measurement of the resulted composite nanofibrous webs were carried out according to ASTM D737-96 using SDL air permeability tester from Shirley, the condition as follows: pressure drop 100 Pa, surface area of 20 cm^2. Air permeability was measured for ten samples of each nanofibrous web and the mean value was recorded.

Electrospinning of nanofibers

Versatility in spinning a wide range of polymeric fibers and the consistency in producing fibers in submicron range, make electrospinning as a very famous method for producing nanofibers. During electrospinning process, a strong electrostatic field is applied to the polymer solution from the needle, when the electrostatic force is strong enough to overcome the surface tension of the solution, the droplet becomes coined and ejected from the spinneret, the polymer solidifies as it travels toward the collecting plates, and fibers with diameter ranging from nanometer to micron are collected on the collecting plate. The electrospinning set up used in this experiment is shown in figure 1.

The electrospun composite nanofibers are produced at 18 kV, at the working distance (the distance between the tip and collecting drum) of 15 cm. The spinning solution was transferred into a 1 ml plastic syringe and pumped at a constant rate of 0.37 mL/h with a digitally controlled syringe pump (Top 3500). A drum with diameter of 8 cm and length of 30 cm, connected to a variable speed motor was used to collect the uniform nanofibrous web. The speed of the drum was carefully chosen 2 rpm (m/s) to prevent fiber breakage during the collection.

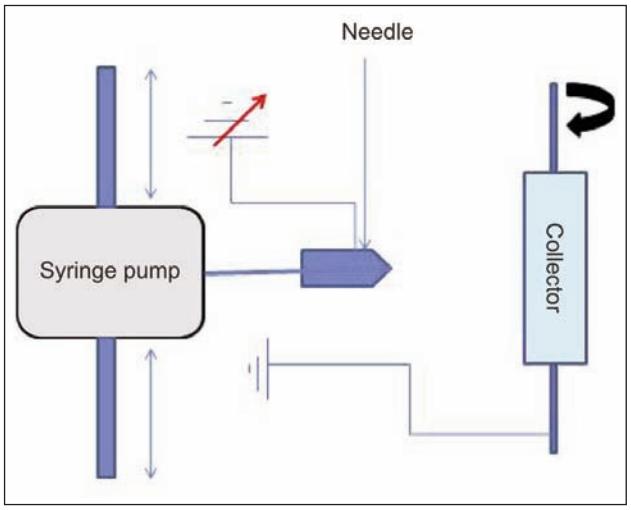

Fig. 1. Electrospinning set up

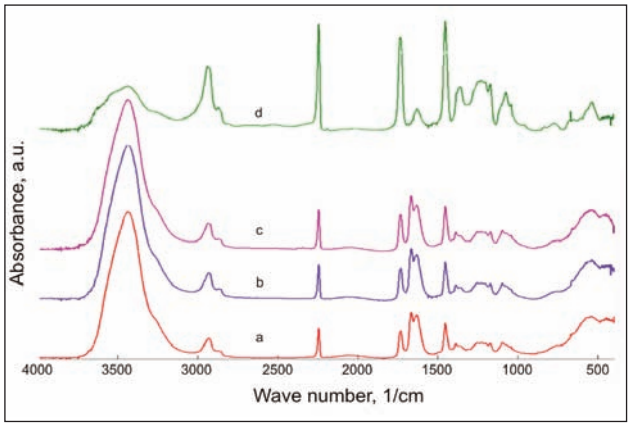

Fig. 2. Infrared spectrum of composite nanofibers containing activated carbon:
a – 2%; ***b*** – 5%; ***c*** – 10%; **d** – 0%

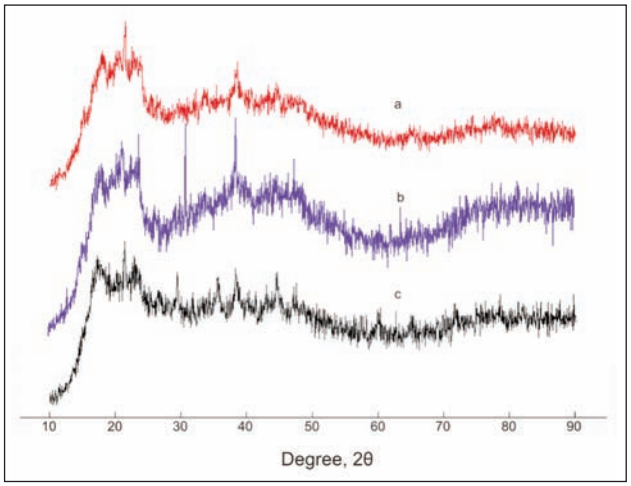

Fig. 3. X-ray diffraction of composite nanofibers containing:
a – 2%; ***b*** – 5%; ***c*** – 10%

RESULTS AND DISCUSSIONS

FT-IR spectroscopy

Chemical structure of composite nanofibers is investigated by Fourier transform infrared (FT-IR) spectroscopy. As shown in figure 2, a number of absorption features appeared at 3 435 cm^{-1} (—OH), 1 740 cm^{-1} (C=O) and the typical absorption peak around 2 248 cm^{-1} was due to the stretching vibration of nitrile groups (–CN–) in PAN chains, and the prominent peaks at 2 925 and 1452 cm^{-1} attributed to the asymmetrical and symmetrical bending vibrations of methylene groups ($–CH_2–$) [19].

Compared with the FT-IR spectra of pure PAN nanofibers, PAN/ activated carbon composite nanofibers present a peak with relatively high intensity around 3 435 cm^{-1}, which is the characteristic peak of (—OH), this peak become appear in the composite nanofibers spectrum due to absorb moisture by activated carbon in nanofibers. This absorbency is because of incorporation activated carbon in the nanofibers structure and absorbing water from environment by them, the intensity of this peak can be affected by the quantity of moisture absorbed by the composite nanofibers, as its appeared in figure 2, with increasing the concentration of activated carbon, the intensity of this peak increases.

For composite nanofibers a new peak in 1650 cm^{-1} becomes appear. This peak is characteristic peak of vibration stretch of C=C in activated carbon. With increasing the concentration of activated carbon in composite fibers, the intensity of this peak increases.

X-ray diffraction

Crystal structure of PAN-carbon active composite nanofibers are characterized using X-ray diffraction (XRD). A typical XRD pattern of the products containing different amount of activated carbon is shown in figure 3. PAN is a polymer that can even crystallize an atactic sample.

One characteristic and sharp crystallize peak around 2 θ = 17° corresponding to (010) plane, indicating the crystalline behavior of PAN [19]. Besides the diffraction peaks of PAN mentioned above, the fibers displayed the features corresponding to the presence of activated carbon in nanofibers. The positions of the XRD reflections are in good agreement with the hexagonal graphite. With increasing the concentration of activated carbon in composite nanofibers crystalline structure of hexagonal graphite will be more appeared.

Surface morphology of the composite nanofibers

The morphologies of resultant samples were examined by field emission scanning electron microscope (FE-SEM). The diameters of fibers were measured for 50 fibers using measurement software. As FE-SEM scans shows there is no bead in nanofibers, and they are relatively even, so the nanoparticles have uniform distribution in nanofiber structure, and they are not aggregated along the nanofibers.

Effect of activated carbon concentration on the fibers diameter

Composite nanofibers containing different amount of activated carbon (2%, 5%, 10%) were electrospun and nanofibers diameter were investigated as a function of activated carbon concentration. As shown in FESEM scans, fibers diameter increasing with increasing the activated carbon concentration in the polymer solution, the mean diameter of composite nanofibers containing 2%, 5%, 10% activated carbon are 121, 159, 166 and their coefficient of variance are 13%, 25%, 30%. Increasing the activated carbon in polymer solution could increase the viscosity of the polymer solution so it causes to increase the fibers diameter. But with increasing the fibers diameter the uniform distribution of nanoparticles in the nanofibers become more difficult and their coefficient of variance is also increase (fig. 4).

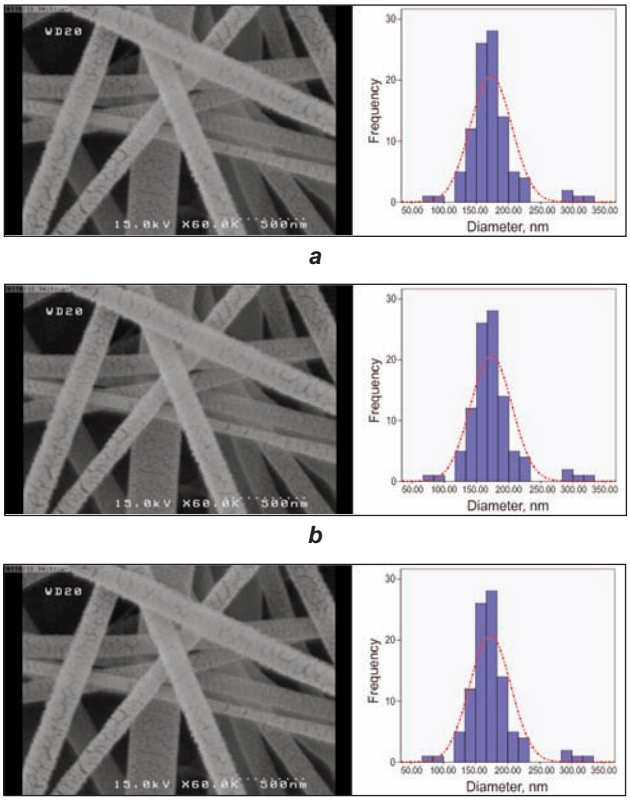

a

b

c

Fig. 4. FESEM scans of resulted composite nanofibers containing:
a – 10%; ***b*** – 5%; ***c*** – 2% and PAN nanofiber

Air permeability

Air permeability is an important performance character of various textile materials such as air filters, fabrics for air bags, clothing, parachutes, sails it also reveal the breathability of the fabrics. The resulted nanofibrous web has a great potential to apply as the filter media in the face masks, so air transmission is an important characteristic for the resulted web that is investigated through the air permeability test. The rate of air flow passing perpendicularly through a known area under an air pressure differential of 100 Pascal between the two surfaces of the nanofibrous web (that was coated on the spunbonded substrate of 17 g/m^2 weight per surface area) is considered as the air permeability of the nanofibrous web. The average air permeability for each sample is determined and the results for the various nanofibrous web reveal that with increasing the concentration of activated carbon in the nanofibers, air permeability of the resulted web is increasing it is due to the variation of the nanofibers diameter. As shown in the last part with increasing the concentration of the activated carbon in the composite nanofibers, the diameter of the nanofibers is increasing. Air permeability of the composite nanofibrous web is shown in figure 5.

Air permeability is related to the porosity or solidity of the web. Peart and Ludwig [20] reported that the number of pores and number of fibers in the web could be influenced by fiber diameter as shown in equation (1), (2):

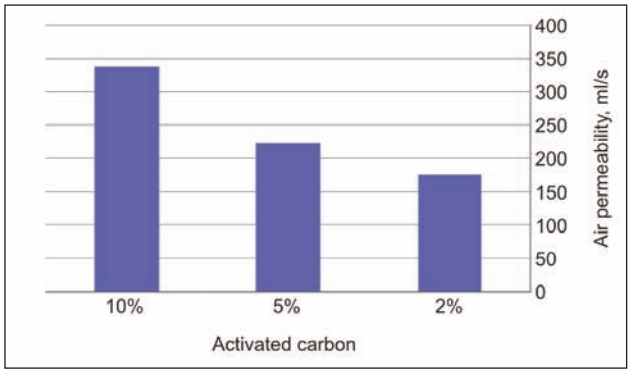

Fig. 5. Air permeability of the membrane composed of composite nanofibers containing activated carbon

$$N_f = \frac{4 M_s}{\pi \rho_f D_f^2 L_f} \quad (1)$$

$$N_p = \frac{16 M_s^2 L_f}{\pi^3 \rho_f D_f^4} \quad (2)$$

where:

N_f is the number of fibers per unit area, of medium, in m^2;

N_p – the number of pores per unit area, of medium, in m^2;

D_f – the fiber diameter, in m;

M_s – the mass of the medium, in gm/cm^{-3};

L_f – the fiber length, in m;

ρ_f – the density of the fiber, in g/cm^{-3}.

As it's appeared in equation (1) and (2), depending on the porosity, fiber diameter is inversely related to flow resistance of the web. With increasing the fibers diameter, air permeability is increases.

CONCLUSIONS

In the presented work, we could successfully produce, activated carbon-PAN composite nanofibers containing different amount of activated carbon. Analyzing the FE-SEM scans of nanofibers shows the nanofibers are relatively even, and there is no bead in their structure, also any aggregation of activated carbon nanoparticles happened along the nanofibers, so the activated carbon nanoparticles have homogenous distribution in the nanofibers structure. Nanofibers diameter is analyzed as a function of activated carbon concentration, the results show that with increasing the activated carbon concentration, nanofibers diameter is increasing also their distribution become wider. FTIR and XRD results indicate that the addition of activated carbon nanoparticles has a significant impact on the chemical and crystal structure of the composite nanofibers. Transport properties of the resulted web were investigated through air permeability tests, the results show that with increasing the activated carbon concentration, air permeability is increasing.

BIBLIOGRAPHY

[1] Huang, Z., Zhang, Z., Kotaki, M., Ramakrishna, S. *A review on polymer nanofibers by electrospinning and their applications in nanocomposites*. In: Composites Science and Technology, 2003, vol. 63, p. 2 223

[2] Sawicka, K. M. Gouma, P. *Electrospun composite nanofibers for functional applications*. In: Journal of Nanoparticle Research, 2006, issue 8, p. 769

[3] Barhate, R. S., Loong, C. K., Ramakrishna, S. *Preparation and characterization of nanofibrous filtering media*. In: Journal of Membrane Science, 2006, vol. 283, p. 209

[4] Boland, E., Wnek, G., Simpson, D., Palowski, K., Bowlin, G. *Tailoring tissue engineering scaffolds using electrostatic processing techniques: a study of poly(glycolic acid) electrospinning.* In: Journal of Macromolecular Science, Pure and Applied Chemistry, 2001, A 38, issue 12, p. 1 231

[5] Subbiah, T., Bhat, G. S., Tock, R. W., Parameswaran, S., Ramkumar, S. S. *Electrospinning of Nanofibers*. In: Journal of Applied Polymer Science, 2005, vol. 96, p. 557

[6] Zhang, S., Shim, W. S., Kim, J. *Design of ultrafine nonwovens via electrospinning of nylon 6: spinning parameters and filtration efficiency.* In: Materials and Design, 2009, vol. 30, issue 9, p. 3 659

[7] Wang, H. Y. *Preparation and characterization of porous TiO_2/ZnO composite nanofibers via electrospinning*. In: Chinese Chemical Letters, 2010, vol. 21, p. 1 119

[8] Qi, Z. *Highly porous fibers prepared by electrospinning a ternary system of nonsolvent/ solvent/ poly (L-lactic acid).* In: Materials Letters, 2009, vol. 63, p. 415

[9] Zhang, Y. Z., Wang, X., Feng, Y., Li, J., Lim, C. T., Ramakrishna, S. *Coaxial electrospinning of (fluorescein isothiocyanate-conjugated bovine serum albumin)-encapsulated poly(ε-caprolactone) nanofibers for sustained release*. In: Biomacromolecules, 2006, issue 7, p. 1 049

[10] Zhang, Y. Z., Huang, Z., Xu., X., Lim, C., Ramakrishna, S. *Preparation of Core-Shell structured PCL-r-gelatin bi-component nanofibers by coaxial electrospinning.* In: Chemistry of Materials, 2004, vol. 16, issue 18, p. 3 406

[11] Ji, L. Saquing, C., Khan, S. A., Zhang, X. *Preparation and characterization of silica nanoparticulate–polyacrylonitrile composite and porous nanofibers.* In: Nanotechnology, 2008, vol. 19, p. 1

[12] Song, T., Zhang, Y. Z., Zhou, T. J. *Fabrication of magnetic composite nanofibers of poly(e-caprolactone) with FePt nanoparticles by coaxial electrospinning.* In: Journal of Magnetism and Magnetic Materials, 2006, vol. 303, p. 286

[13] Yang, X., Shao, C., Liu, Y. *Fabrication of Cr_2O_3/Al_2O_3 composite nanofibers by electrospinning.* In: Journal of Material Science, 2007, vol. 42, p. 8 470

[14] Wu, S., Li, F., Wang, H., Fu, L., Zhang, B., Li, G. *Effects of poly (vinyl alcohol) (PVA) content on preparation of novel thiol-functionalized mesoporous PVA/SiO_2 composite nanofiber membranes and their application for adsorption of heavy metal ions from aqueous solution*. In: Polymer, 2010, vol. 51, p. 6 203

[15] Aryal, S., Kim, C. K., Kim, K. W., Khil, M. S., Kim, H. Y. *Multi-walled carbon nanotubes/TiO_2 composite nanofiber by electrospinning.* In: Materials Science and Engineering, 2008, vol. 28, issue 1, p. 75

[16] Wu, S., Li, F., Wang, H., Fu, L., Zhang, B., Li, G. *Effects of poly (vinyl alcohol) (PVA) content on preparation of novel thiol-functionalized mesoporous PVA/SiO_2 composite nanofiber membranes and their application for adsorption of heavy metal ions from aqueous solution*. In: Polymer, 2010, vol. 51, p. 6 203

[17] Monser, L., Adhoum, N. *Modified activated carbon for the removal of copper, zinc, chromium and cyanide from wastewater*. In: Separation and Purification Technology, 2002, issue 26, p. 137

[18] Knappe, D. U., Matsui, Y., Snoeyink, V. *Predicting the capacity of powdered activated carbon for trace organic compounds in natural waters*. In: Environmental Science & Technology, 1998, vol. 32, p. 1 694

[19] Ma, G., Yang, D., Nie, J. *Preparation of porous ultrafine polyacrylonitrile (PAN) fibers by electrospinning*. In: Polymer Advance Technology, 2009, vol. 20, p. 147

[20] Hutten, I. M. *Handbook of nonwoven filter media.* First edition, Elsevier, 2007, p. 115

Authors:

Assist. prof. MOHAMMAD REZA MOHAMMAD SHAFIEE
Faculty of Material Engineering
Islamic Azad University, Najafabad Branch
e-mail: dr_shafiee@yahoo.com

PhD student MARYAM SALEHI ESFANDARANI
Textile Engineering Department
Amirkabir University of Technology
No. 424, Hafez Ave, Tehran, Iran
e-mail: msalehi_87@aut.ac.ir

Dyeability of SeaCell®active fabrics with reactive dyes by using of ultrasonic energy

B. CENKKUT GULTEKIN S. MUGE YUKSELOGLU ONUR ATAK

REZUMAT – ABSTRACT

Capacitatea de vopsire a materialelor SeaCell®active cu coloranți reactivi, folosind energia ultrasonică

Lucrarea prezintă o tehnică de vopsire a materialelor SeaCell®active cu coloranți reactivi, folosind energia ultrasonică. Pentru studiu, a fost folosit un material textil din SeaCell®active 100%, cu legatură diagonal încrucişat, având masa de 1,22 g/cm^2. În vederea vopsirii acestui material, au fost selectaţi trei coloranți reactivi – albastru, roşu şi galben. Procesul de vopsire a fost efectuat la temperatura de 60°C, timp de 60 de minute, cu un raport de flotă de 40:1. Au fost analizate cinetica vopsirii, viteza de vopsire, capacitatea tinctorială, valorile CIELab, rezistența la spălare, stabilitatea culorii la testele de frecare umedă şi uscată. S-a observat că folosirea energiei ultrasonice la vopsirea țesăturii de SeaCell®active cu coloranți reactivi are un efect important asupra fixării coloranților şi conferă o mai bună capacitate tinctorială.

Cuvinte-cheie: SeaCell active, energie ultrasonică, coloranți reactivi, viteză de vopsire, intensitatea culorii, proprietăți de rezistență, măsurarea culorii

Dyeability of SeaCell®active fabrics with reactive dyes by using of ultrasonic energy

This paper presents a dyeing technique for the SeaCell®active fabrics that are dyed with reactive dyes in the presence of ultrasonic energy. 1.22 g/cm^2 of weight of 100% SeaCell® active fabrics made of herringbone pattern were used for this study. Three reactive dyes (blue, red and yellow) were chosen for the dyeing methods; the dyeing process was carried out at 60°C for 60 minutes and with the liquor ratio of 40:1. The dyeing kinetics were studied along with their dyeing rates, colour yield, CIELab values, washings fastness, colour fastness to dry and wet rubbing tests. It has been observed that the use of ultrasonic energy in reactive dyeing of SeaCell®active fabrics have a considerable effect on the fixation of dyes and have a good colour yield.

Key-words: SeaCell active, ultrasonic energy, dyeability, reactive dye, dyeing rate, colour strength, fastness properties, colour measurement

Ultrasound is sound of frequency which is above of the human audibility that is between 16 Hz and 16 kHz, while ultrasonic frequency generally lies between 20 kHz and 500 MHz. There are many industrial applications of ultrasound such as biology, biochemistry, engineering, geology, medicine, textile wet processes etc. The idea of implementing ultrasonic energy to textiles, especially for the wet finishing processes [1–5] has been familiarized since 1990s; in these works generally ultrasonic energy was utilized to dyeing of textiles. Some researchers also used these ultrasonic frequencies to study dyeability properties of bleached cotton yarns and woven fabrics [6] and washing of medical surgery gowns [7] rather than the conventional methods. Especially, the use of ultrasonic energy in wet finishing processes has a potential in decreasing the amount of the process time, energy, chemicals used in and in improving product quality. Ultrasonic energy was also successfully dyed the wool woven fabrics that are made of both conventional yarns and sirospun yarns [8]. Ultrasonic energy was also used to design some parameters of industrial size of ultrasonic bath for the pre-treatment of cotton fabric and its speed during the production line [9]. The most recent work was used in an apparel industry where ultrasonic welding has more advantages than the other joining methods [10]. So far, we have not seen any new materials/or fibres that are treated with ultrasonic energy.

SeaCell® active fibres are one of these new materials for textile industry and are slightly taking some more places within the range of fibres in textile consumption. For brief information, SeaCell fibre is known as the third generation of regenerated cellulosic fibre and is manufactured using the product and environmental friendly Lyocell technology with algae. The SeaCell fibre production can be either SeaCell® pure or SeaCell® active which has small portions of silver-ions within the fibre matrix. SeaCell fibres have many health advantages to users with excellent physical properties. Especially the SeaCell® active has an antibacterial and fungicidal effect, therefore is generally used for textiles to heal wounds. As SeaCell® active fibres are generally dyed with direct or reactive dyes, we therefore foresee the dyeability of SeaCell® active fabrics with the application of ultrasonic energy which has so far not studied in the literature.

For this purpose, 100% SeaCell® active fabrics were dyed with three reactive dyes and their dyeing kinetics were studied along with their dyeing rates (exhaustion %), colour yield (K/S), CIELab values, washings fastness, dry and wet rubbing tests in this work.

Table 1

C.I. Number	Commercial name	Chemical structure	Producer
C.I. Reactive Blue 221	Sumifix Supra Blue BRF	Formazon	SUMÝTOMO
C.I. Reactive Red 195	Sumifix Supra Red 3BF	Monoazo	SUMÝTOMO
C.I. Reactive Yellow145	Sumifix Supra Yellow 3RF	Monoazo	SUMÝTOMO

EXPERIMENTAL PART

Materials used

100% SeaCell® active bleached fabrics were used in the experimental work. The fabrics were made of herringbone pattern with the weight of 1.22 g/cm^2 with 34 thread/cm in weft density, and 44 thread/cm in warp density. The details of dyes in this study are given in table 1.

Dyeing process

Ultrasonic energy was carried out with the BRANSON ultrasonic probe at 20 kHz. The dyeing profiles for dyes are shown in figure 1. In this dyeing process, the woven SeaCell® Active fabrics were weighed 2 g and dyed according to the weight of fabric with 3% of colour yield of reactive dyes which are C.I. Reactive Blue 221, C.I. Reactive Red 195, and C.I. Reactive Yellow 145 and the liquor ratio was 40:1 (table 2). After the dyeing process, cold washing and 70°C of warm washing carried out, subsequently neutralized with acetic acid and anionic washing (1g/L of washing substances, liquor ratio 40:1 for 20 minutes, 95°C) was implemented and finalized with 70°C of warm and cold rinsing.

Fastness tests

The colour fastness of the dyed materials were carried out the James Heal instrument in accordance with the TS EN ISO 105-C06 [11] and the rubbing tests also proceeded on the James Heal in accordance with the TS 717 EN ISO 105 - X12 [12].

Colour measurement and dyeing kinetics

The colour coordinates of dyed samples were measured on the reflectance spectrophotometer (Datacolor SF 600 plus) coupled to a PC under D65/10° illuminant with specular component included. The colour differences, according to the CIELab (1976) equation, were obtained from the colour measuring software. Four reflectance measurements were made on each sample rotating the samples 90° before each measurement.

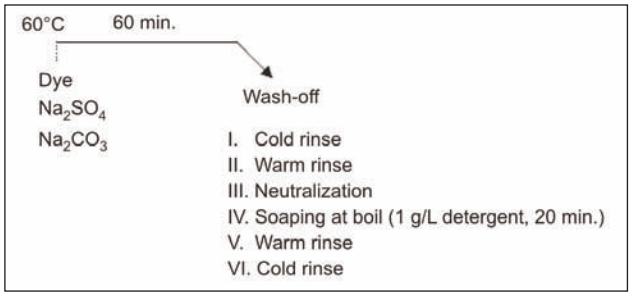

Fig. 1. Dyeing diagrams with the use of ultrasonic energy

Table 2

Dyeing recipe	Colour yield/ Dyeing process
Dyes, % owf	3
Sodium sulphate (Na_2SO_4), g/L	50
Sodium carbonate (Na_2CO_3), g/L	20
Liquor ratio	40/1
Temperature, °C	60
Dyeing duration, minute	60
Weight of material, g	2

The colour difference is expressed as ΔE and is calculated by the following equation (1) [13]:

$$\Delta E^* = ((\Delta L^*)^2 + (\Delta a^*)^2 + (\Delta b^*)^2)^{1/2} \quad (1)$$

where:

ΔE^* is the CIELab colour differences between batch and standard;

ΔL^*, Δa^*, Δb^*, ΔE^* are in commensurate units. ΔL^* denotes the difference between lightness (L^* = 100) and darkness (L^*= 0), Δa^* the difference between green ($-a^*$) and red ($+a^*$), and Δb^* the difference between yellow ($+b^*$) and blue ($-b^*$).

On the other hand, Kubelka-Munk equation relates the absorption function of the substrate K, the scattering function of the substrate S and the reflectance R according to the equation (2), given below [14].

$$\frac{K}{S} = \frac{(1-R)^2}{2R} \quad (2)$$

After the dyeing process, the K/S values of the dyed samples were determined (table 4).

RESULTS AND DISCUSSIONS

Table 3 presents the CIELab values of the dyed SeaCell® active fabrics. As a result of reproduced dyeing of the samples have shown that ΔE^* values are acceptable ($\Delta E^* < 1$). It can be said that there is no difference between the dyed samples of each reactive dyes.

Table 4 gives the colour strength, K/S, of the three reactive dyes. As it is known that, K/S value of a dye is related to the concentration of the dye on the textile material, i.e. the magnitude of the value is a direct measure of dye bath shade. Hence, from the table 4 it can be concluded that the highest K/S values for C.I. reactive Yellow 145, C.I. Reactive Red 195 and C.I. Reactive Blue 122 were 7.09 (400 nm), 7.23 (550 nm) and 6.95 (630 nm), respectively.

Figures 2, 3 and 4 present the dyeing rates of the reactive dyes. From the figure 2, it can be seen that C.I. Reactive Blue 221 has given 90% of exhaustion at the end of 60 minute of dyeing process. On the

Table 3

CIELab values	Dyes		
	C.I. Reactive Blue 221	*C.I. Reactive Red 195*	*C.I. Reactive Yellow 145*
*L**	42.26	50.95	74.32
*a**	–2.03	57.32	22.67
*b**	–30.17	–8.19	68.74
*C**	30.24	57.90	72.38
h	266.15	351.87	71.74
X	11.72	31.39	53.03
Y	12.67	19.23	47.20
Z	29.90	25.35	8.83
*ΔE**	0.606	0.800	0.837

Table 4

Wave length, nm	Dyes		
	C.I. Reactive Blue 221	*C.I. Reactive Red 195*	*C.I. Reactive Yellow 145*
400	2.21	2.66	7.09
410	1.33	1.69	6.52
420	0.86	1.16	6.23
430	0.77	1.03	6.26
440	0.74	0.96	6.21
450	0.81	1.08	5.98
460	0.94	1.42	5.45
470	1.08	1.95	4.79
480	1.26	2.73	3.98
490	1.45	3.51	3.27
500	1.68	4.43	2.45
510	1.95	5.63	1.70
520	2.25	6.60	1.11
530	2.61	6.91	0.70
540	2.99	6.96	0.44
550	3.39	7.23	0.27
560	3.93	6.94	0.17
570	4.58	5.25	0.11
580	5.34	2.86	0.07
590	5.95	1.26	0.05
600	6.34	0.52	0.04
610	6.64	0.22	0.04
620	6.88	0.09	0.03
630	6.95	0.05	0.03
640	6.49	0.03	0.03
650	5.31	0.03	0.02
660	3.80	0.02	0.02
670	2.72	0.02	0.02
680	1.82	0.02	0.02
690	1.28	0.02	0.02
700	0.87	0.02	0.02

other hand, with both C.I. Reactive Red 195 and C.I. Reactive Yellow 145 have shown lower exhaustion rates than the C.I. Reactive Blue 221. This might be due to the C. I. Reactive Blue 221 is in the chemical structure of formazon and the other two reactive dyes are in monoazo structure.

Table 5 gives the fastness, staining and rubbing test results of the SeaCell® active fabrics. The fastness tests of the dyed SeaCell® active fabric samples confirmed that the use of ultrasonic energy have shown

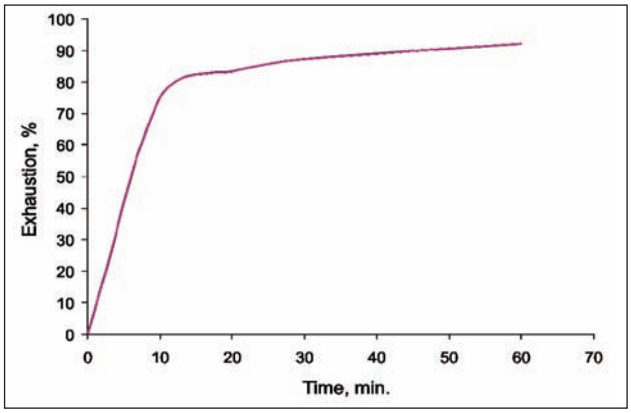

Fig. 2. Dyeing rates for C.I. Reactive Blue 221

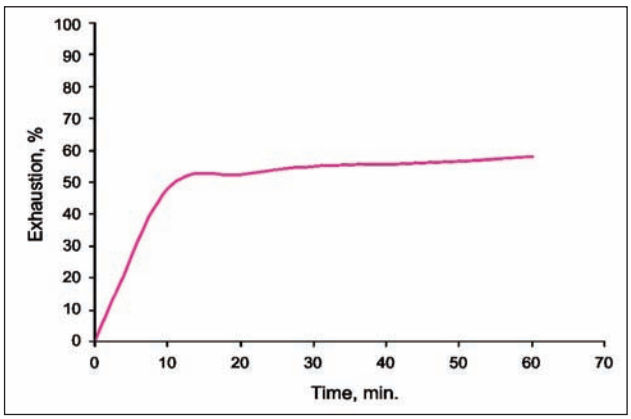

Fig. 3. Dyeing rates for C.I. Reactive Red 195

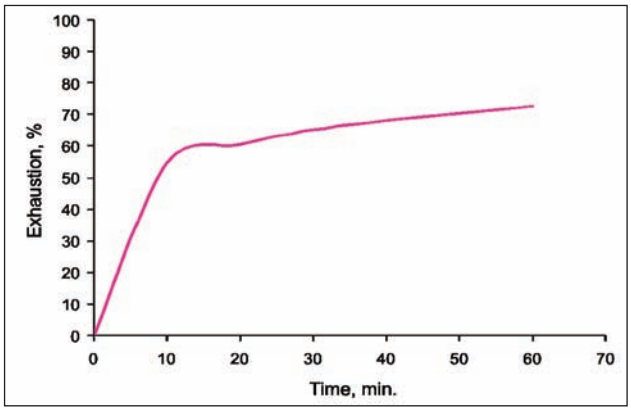

Fig. 4. Dyeing rates for C.I. Reactive Yellow 145

a good fastness properties on the dyed materials. C.I. Reactive Blue 221 has presented a little lower wash fastness on the polyamide than the other mateials. On the other hand, C.I. Reactive Red 195 has also given lower wash fastness on wool and polyamide. Within these reactive dyes, C.I. Reactive Yellow 145 has slightly better wash fastness properties on the SeaCell® active fabrics. The staining results have shown that all three reactive dyed samples have same and also high level of staining properties. However, dry rubbing tests have presented that are much better than the wet rubbing tests of the SeaCell® active fabric samples.

Table 5

Dyes	Wash fastness						Staining	Rubbing	
	Wool	*Acrylic*	*PES*	*PA*	*Cotton*	*Acetate*		*Dry*	*Wet*
C.I. Reactive Blue 221	4	4	4 – 5	3	4	4 – 5	4 – 5	4 – 5	2
C.I. Reactive Red 195	3 – 4	4 – 5	4 – 5	3	4	4 – 5	4 – 5	4 – 5	4
C.I. Reactive Yellow 145	4	4 – 5	4 – 5	3 – 4	4	4 – 5	4 – 5	4 – 5	2

CONCLUSIONS

The use of ultrasonic energy in dyeing of SeaCell® active materials with reactive dyes has a considerable effect on the fixation of dyes and has a good colour yield.

Therefore we believe that the ultrasonic technique has a great potential for the dyeing of SeaCell materials in textiles. In this current work, ultrasonic dyeing technique was carried out at 60°C of temperature and 60 minutes of duration of dyeing and the following outcomes were obtained:

- ultrasonically dyed SeaCell® active fabrics have high level of staining properties.
- colour fastnesses to wet rubbing of the SeaCell® active fabrics are weaker to dry rubbing when dyed with reactive dyes by implementing the ultrasonic energy.
- 60–90% of colour strength is obtained in dyeing of SeaCell® active materials when dyed with the use of ultrasonic energy.
- in generally, vivid colours achievable with the use of ultrasonic dyeing of SeaCell® active materials.
- SeaCell® active fabrics can be easily and successfully dyed with reactive dyes with the application of ultrasonic energy.

Finally, we suggest that in further studies this dyeing process may be optimised and can be employed to a larger scale of production for the novel textile materials, i. e. SeaCell fibres, yarns and fabrics, in textile wet processes.

BIBLIOGRAPHY

[1] Gültekin, C., Akalın, M., Kandola, B. K. *Use of ultrasonic energy in textile finishing*, The 78th World Conference of The Textile Institute, 1997, vol. III, Thessaloniki, Greece, p. 323
[2] Rathi, N. H., Mock, G. N., McCall, R. E. *Ultrasound aided open width washing of mercerized 100% cotton twill fabric.* AATCC Book of Papers International Conference and Exhibition, 1997, Atlanta, p. 25
[3] Shanping, S. *Ultrasound a novel dyeing accelerant*. In: American Dyestuff Reporter, 1988, vol. 77, p.15
[4] Thakore, K. A. *Physico-chemical study on applying ultrasonics in textile dyeing*. In: American Dyestuff Reporter, 1990, vol. 79, p. 45
[5] Öner, E., Başer, İ., Acar K. *Use of ultrasonic energy in reactive dyeing of cellulosic fabrics.* In: JSDC, 1995, vol. 111, p. 279
[6] Mıstık, S. İ., Yükseloğlu, S. M. *Hydrogen peroxide bleaching of cotton in ultrasonic energy*. Ultrasonics, 2005, vol. 43, p. 811
[7] Canoğlu, S., Gültekin, B. C., Yükseloğlu, S. M. *Effect of ultrasonic energy in washing of medical surgery gowns*. In: Ultrasonics, 2004, vol. 42, issues 1-9, p. 113
[8] Yükseloğlu, S. M., Bolat, N. *The use of conventional and ultrasonic energy in dyeing of 100% wool woven fabrics.* In: Tekstil ve Konfeksiyon, April-June 2010, vol. 20, issue 2, p. 162
[9] Duran, K., Korlu, A. E., Perincek, S., Bahtiyari, I. M. *Pretreatment of cotton fabric by aid of continous ultrasonic machine*. In: Industria Textilă, 2009, vol. 60, issue 1, p. 3
[10] Boz, S., Erdoğan, M. Ç. *Ultrasonik enerjinin konfeksiyon sanayiinde kullanımı*. In: Tekstil ve Konfeksiyon, January-March 2011, vol. 21, issue 1, p. 91
[11] TS EN ISO 105-C06. *Textiles for colour fastness – Part C06: Colour fastness to domestic and commercial laundering*. Turkish Standards Institute, November 2001, Ankara, Türkiye
[12] TS 717 EN 105 – X12. *Textiles tests for colour fastness – Part X12: Colour fastness to rubbing.* Turkish Standards Institute, February 2000, Ankara, Türkiye
[13] Sule, A. D. In: Colourage, 1992, vol. 39, issue 11, p. 20
[14] Park, J. *Instrumental colour formulation*. In: Publication of Society of Dyers and Colourists, ISBN 0 901956 1993, vol. 54, issue 6, p. 12

Authors:

B.C. GULTEKIN
ONUR ATAK
Marmara University, Faculty of Technical Education
Department of Textile Education, Göztepe-34722, İstanbul – Turkey
e-mail: cgultekin@marmara.edu.tr; myukseloglu@marmara.edu.tr

S. MUGE YUKSELOGLU
Marmara University, Faculty of Technology
Department of Textile Engineering, Göztepe-34722, İstanbul – Turkey
e-mail: onur.atak@marmara.edu.tr

Optimization of the cellulosic materials functionalization with monochlorotriazinyl-β-cyclodextrin in basic medium

OCTAVIAN POPESCU
RODICA MARIANA DIACONESCU
AURELIA GRIGORIU
ECATERINA VASLUIANU

REZUMAT – ABSTRACT

Optimizarea funcționalizării materialelor celulozice cu monoclorotriazinil-β-ciclodextrină în mediu bazic

Lucrarea prezintă două procedee de preparație a unei țesături din bumbac în vederea grefării cu monoclorotriazinil-β-ciclodextrină şi de modelare matematică a procesului de grefare. Aplicând analiza statistică, au fost selectați principalii coeficienți ai ecuației de regresie, cu ajutorul testului Student şi s-a verificat adecvanța modelului, folosind testul Fisher. De asemenea, s-a determinat influența a trei variabile independente semnificative asupra gradului de grefare şi de optimizare a procesului, utilizând programul MODDE. Modelele matematice obținute au fost folosite pentru simularea procesului analizat, în vederea determinării influenței celor trei variabile independente semnificative asupra gradului de grefare şi de optimizare a procesului.

Cuvinte-cheie: funcționalizare, țesături din bumbac, grefare, monoclortriazinil-β-ciclodetrină, ecuație de regresie

Optimization of the cellulosic materials functionalization with monochlorotriazinyl-β-cyclodextrin in basic medium

Two procedures were studied for the preparation of a cotton fabric destined to grafting with monochlorotriazinyl-β-cyclodextrin and the grafting process was mathematically modeled. By applying the statistical analysis, the significant coefficients of the regression equation were selected (by applying the Student test) and the model adequacy was verified (with Fisher test). By using the MODDE software, the influence of three significant independent variables on the grafting degree was determined, and the process was optimized. The obtained mathematical models were used to simulate the studied process in order to determine the influence of the three significant independent variables on the grafting degree and to optimize the process.

Key-words: functionalization, cotton fabrics, grafting, monochlorotriazinyl-β-cyclodetrin, regression equation

Given their special oligomer structure, with lipophilic cavities and hydrophilic shell, the cyclodextrins offer astonishing possibilities for the supermolecular chemistry, by their capacity to form inclusion compounds. This propriety has been exploited in the textile field for the modification of the products surfaces. The recent attempts to enhance the value of the textile products has materialized, for example, in the production of materials with applications in medicine, which use the cyclodextrins as a reservoir for various bioactive substances that can be released under control, as in the case of transdermal administration.

The purpose of this study is to obtain permanent modifications of the surface of textile cellulosic materials by grafting a derivative of β-cyclodextrin (monochlorotriazinyl-β-cyclodextrin, MCT-β-CD) under optimum grafting conditions and selecting the preparation procedure for the material (cotton) which could be grafted with a sufficient MCT-β-CD quantity and afterward to permit the efficient inclusion of a bioactive substance with beneficial effect on the human body, or of other substances, for example, odorants. The MCT-β-CD possesses a reactive group and is able to perform covalent bounds with cellulose, both in basic medium, according to the reaction (1) at *p*H = 10 – 11 realized with sodium carbonate, caustic soda and other bases [1], and in acid medium, according to the reaction (2) at *p*H = 4 performed with hydrochloric acid.

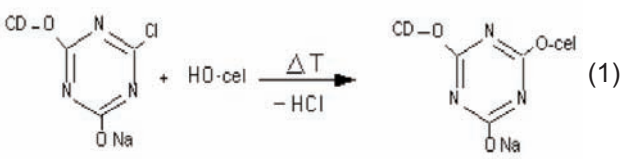

(1)

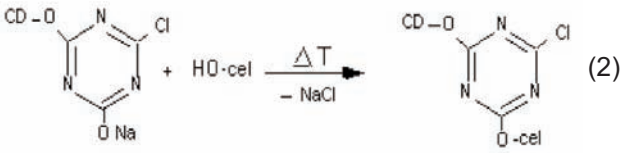

(2)

EXPERIMENTAL PART

Materials used

We used a grey cloth, 100% cotton, with specific mass of 130 g/m², purchased from Iaşitex S.A. – Iaşi, Beisol DO – Bezema, as oxidative desizing agent, Contavan ARL – Bezema, as stabilizer for peroxides, a combination of surfactants for washing, emulsifying and rinsing, Lavotan DSU – Bezema, monochlorotriazinyl-β-cyclodextrin, MCT-β-CD – Wacker Chemie, Germany.

Methods used

The fabric was prepared through two methods:

- a two hour alkaline treatment with 20 g /L NaOH, 5 g/L sodium carbonate, 5 g/L Lavotan DSU, 2 g/L trisodium phosphate, liquor ratio 1:20, preceded by a desizing by impregnation at 65ºC with 7 g/L Beisol DO conc., and 5 g/L Lavotan DSU, liquor ratio 1:10, then storage for 2 hours at 50 – 60°C; as final treatments, repeated washings with hot (90ºC) and cold water up to *p*H = 6.5 – 7 were used;
- cold bleaching with 20 g /L NaOH, 25 g/L peroxide 35%, 5 g /L Beisol DO conc., 5 g/L Lavotan DSU, 4 g/L Contavan ARL, liquor ratio 1:10, storage for 16 hours. As final treatments, repeated washings with hot (90ºC) and cold water up to *p*H = 6.5 – 7 were used.

The MCT-*β*-CD grafting on the cotton fabric prepared by the two modes was carried out in basic medium, which offers a maximum reaction yield. Batches of 40 samples each, made of the fabric prepared in the two manners, conditioned and weighed with 1 mg precision on a Shimadzu Type AW 220 balance, were impregnated according to an experimental program (table 1) with solutions containing 50 – 150 g/L MCT-*β*-CD and 20 – 80 g/L Na_2CO_3, squeezed off to a liquor pick-up of 100%. The samples were dried at the room temperature before the heat fixing accomplished between 100 – 160°C. For each type of fabric preparation, 20 samples were heat treated for 10 minutes, and the other 20 – for 15 minutes. After the heat treatment, the samples were washed with warm and cold water until a neutral *p*H was obtained.

The evaluation of the grafting degree, *Y*, was performed gravimetrically, by weighing the samples before and after treatment (3), after a previous conditioning:

$$Y = \frac{M_t - M_0}{M_0} \cdot 100 \quad [\%] \qquad (3)$$

where:

M_t şi M_0 are the masses of the treated and control samples, respectively.

Experiments programming

In order to obtain, through a reduced number of experiments, maximum information on the parameters which significantly influence the process, a planning method was used for them, called “experiment design”. The parameters which can influence the MCT-β-CD grafting on cotton are: MCT-β-CD concentration, immersion duration, processing duration, drying duration and temperature, alkalies nature and concentration, temperature and duration of heat fixing, and the *p*H value. Among them, based on personal previous studies and the data from specialized literature, three variables of main importance were chosen, namely MCT-β-CD concentration, sodium carbonate concentration and fixing temperature [2]. Two series of experiments with different fixing times (10 and 15 minutes) were performed, on both the cotton prepared through alkaline treatment (F_{10} and F_{15}) and the bleached cotton (A_{10} and A_{15}).

Application of the central composite rotatable design

Considering the three independent variables which have the biggest influence on the grafting process, we proceeded to the application of a 2^3 type central composite rotatable design [6]. In this case, the mathematical model quantifies the influence of the three independent variables, namely the MCT-β-CD concentration – X_1, g/L, sodium carbonate concentration – X_2, g/L, and fixing temperature (X_3, °C), on the grafting degree – *Y*, %), which is the objective function. The ranges of independent parameters variation, and their natural and coded values are presented in table 1.

The parameters coding consists in the transformation of the real variables (X_1, X_2,…, X_n) in dimensionless variables or reduced variables without measurement units, (x_1, x_2, x_3), and was performed based on the relation (4).

Generally, every variable with real dimensions X_i, taken within the considered range, can be transformed in an equivalent dimensionless variable x_i (ranging between –1 and +1), by means of the relation:

$$x_i = \frac{X_i - X_{i0}}{\Delta X_i} \qquad (4)$$

where:

ΔX_i is the length of the half the range of variation of the parameter *i.*

This relation has a special importance for a subsequent inverse transformation (decoding) of the optimum coordinates reduced values. The coordinates are determined with the relation (5):

$$X_i = x_i \Delta X_i + X_{i0} \qquad (5)$$

Table 1

Factor	$X_{i\,min} \rightarrow X_{i\,max}$	X_{i0}	–1.682	–1	0	+1	+1.682
MCT-β-CD concentration, x_1, g/L	50 – 150	100	50	70.27	100	129.72	150
Na_2CO_3 concentration, x_2, g/L	20 – 80	50	20	32.16	50	67.83	80
Fixing temperature, x_3, °C	100 – 160	130	100	112.16	130	147.83	160

Table 2

EXPERIMENTAL MATRIX FOR THE FABRIC PREPARED THROUGH ALKALINE TREATMENT*					
Sample no.	x_1	x_2	x_3	$Y_{e\,F\,10}$	$Y_{e\,F\,15}$
1	–1	–1	–1	1.1082	1.1101
2	1	–1	–1	1.2909	1.6659
3	–1	1	–1	0.7063	0.7102
4	1	1	–1	1.4916	1.7974
5	–1	–1	1	3.8836	4.3290
6	1	–1	1	5.1811	5.2992
7	–1	1	1	1.3868	1.6293
8	1	1	1	3.1876	3.6426
9	–1.682	0	0	1.9244	1.9321
10	1.682	0	0	3.4195	3.9429
11	0	–1.682	0	2.7504	3.5221
12	0	1.682	0	1.1027	1.4380
13	0	0	–1.682	0.5742	0.5801
14	0	0	1.682	3.9058	4.4705
15	0	0	0	3.1132	3.2693
16	0	0	0	3.2036	3.2948
17	0	0	0	3.0306	3.2079
18	0	0	0	3.2104	3.1534
19	0	0	0	3.0469	3.3178
20	0	0	0	3.2127	3.3008

* Values of the grafting degree obtained by experiment at fixing times of 10 min. ($Y_{e\,F10}$) and 15 min. ($Y_{e\,F15}$)

In order to establish the correlation between the grafting degree and the three above mentioned independent variables, the following model of multinomial equation was used [2]:

$$Y = a_0 + a_1x_1 + a_2x_2 + a_3x_3 + a_{11}x_1^2 + a_{22}x_2^2 + a_{33}x_3^2 + a_{12}x_1x_2 + a_{13}x_1x_3 + a_{23}x_2x_3 \quad (6)$$

where:

$a_0, \ldots, a_{23}$ are the regression coefficients.

The table 2 presents the plan of the 2^3 type complex rotatable central experiment (experimental matrix) and the grafting degree values, experimentally obtained on the fabric prepared through alkaline treatment, at fixing times of 10 and 15 minutes ($Y_{e\,F10}$ and $Y_{e\,F15}$), respectively.

The values of the grafting degree experimentally obtained on bleached fabric at fixing times of 10 and 15 minutes ($Y_{e\,A10}$ and $Y_{e\,A15}$) are presented in table 3.

The grafting degree determined with the relation (3) for the four series of experiments is presented in figure 1.

One can notice that in all the four cases, the most favourable values of the three variables where the grafting degree is maximum, can be found at the sixth experiment (X_1 = 129.72 g/L MCT-β-CD, X_2 = 32.16 g/L Na_2CO_3 and X_3 = 147.83°C) for the longest fixing time (15 minutes). At the same time, one can notice that the independent variables have an influence on the grafting degree, hence they are significant.

In order to calculate the regression coefficients, the MODDE 8.0.2.0 program was used, and the calculated values are presented in table 4.

After the determination of all the coefficients, the mathematical models for the fabric prepared through alkaline treatment and for the bleached fabric have the forms:

$$Y_{cF10} = 3.134570 + 0.481838\,x_1 - 0.546405\,x_2 + 1.072310\,x_3 - 0.153191\,x_1^2 - 0.416665\,x_2^2 - 0.305871\,x_3^2 + 0.138238\,x_1x_2 + 0.266287\,x_1x_3 - 0.536137\,x_2x_3 \quad (7)$$

$$Y_{cF15} = 3.260160 + 0.586361\,x_1 - 0.595256\,x_2 + 1.183180\,x_3 - 0.131577\,x_1^2 - 0.293270x_2^2 - 0.277276x_3^2 + 0.196813x_1x_2 + 0.167562x_1x_3 - 0.510987x_2x_3 \quad (8)$$

$$Y_{cF10} = 1.9792100 + 0.5226690\,x_1 - 0.3284510\,x_2 + 0.8836330\,x_3 + 0.1026950\,x_1^2 - 0.0853492x_2^2 - 0.0939736x_3^2 - 0.1151620x_1x_2 + 0.1151870x_1x_3 - 0.1970370x_2x_3 \quad (9)$$

$$Y_{cF15} = 2.0196300 + 0.6940650\,x_1 - 0.3265060\,x_2 + 0.9325580\,x_3 + 0.2593120\,x_1^2 - 0.1108380\,x_2^2 + 0.0486817\,x_3^2 - 0.0933000\,x_1x_2 - 0.0744500\,x_1x_3 - 0.2084250\,x_2x_3 \quad (10)$$

The values computed for the grafting degree, Y_c, are given in table 5.

In order to select the significant coefficients, a statistical analysis of the regression equation was performed. The dispersion of the experimental errors was computed from the relation (11) [3]:

Table 3

EXPERIMENTAL MATRIX FOR BLEACHED FABRIC*					
Sample no.	x_1	x_2	x_3	$Y_{e\,A\,10}$	$Y_{e\,A\,15}$
1	–1	–1	–1	0.6548	0.7022
2	1	–1	–1	1.6370	2.1377
3	–1	1	–1	0.4911	0.6713
4	1	1	–1	1.3096	1.6713
5	–1	–1	1	2.4556	2.8983
6	1	–1	1	4.1955	4.4077
7	–1	1	1	1.8007	1.9898
8	1	1	1	2.7830	3.2099
9	–1.682	0	0	1.4733	1.5511
10	1.682	0	0	3.0285	4.0435
11	0	–1.682	0	2.2919	2.3001
12	0	1.682	0	1.1459	1.1501
13	0	0	–1.682	0.2300	0.5794
14	0	0	1.682	3.1590	3.7734
15	0	0	0	2.0193	2.0314
16	0	0	0	1.9644	1.9441
17	0	0	0	1.8538	1.9502
18	0	0	0	1.9299	2.0953
19	0	0	0	1.9644	2.0584
20	0	0	0	2.1499	2.0719

* The experimental values of the grafting degree at fixing times of 10 min. ($Y_{e\,A\,10}$) and 15 min. ($Y_{e\,A\,15}$).

Table 4

VALUES OF THE REGRESSION COEFFICIENTS				
Coefficient	***Values for F_{10}***	***Values for F_{15}***	***Values for A_{10}***	***Values A_{15}***
a_0	3.134570	3.260160	1.979210	2.026080
a_1	0.481838	0.586361	0.522669	0.703701
a_2	–0.546405	–0.595256	–0.328451	–0.331514
a_3	1.072310	1.183180	0.883633	0.928780
a_{11}	–0.153191	–0.131577	0.102695	0.258401
a_{22}	–0.416665	–0.293270	–0.085349	–0.111749
a_{33}	–0.305871	–0.277276	–0.093973	0.047771
a_{12}	0.138238	0.196813	–0.115162	–0.111850
a_{13}	0.266287	0.167562	0.115187	0.058000
a_{23}	–0.536137	–0.510987	–0.197037	–0.199875

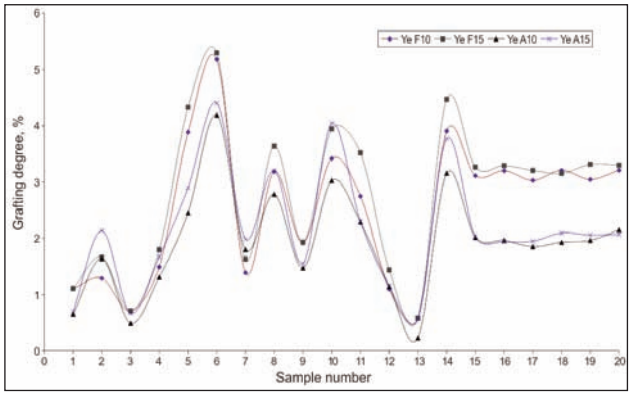

Fig. 1. Experimental grafting degree (%) obtained for the fabric prepared through alkaline treatment, heat fixed for 10 and 15 minutes ($Y_{e\,F10}$ *and* $Y_{e\,F15}$) and for the bleached fabric ($Y_{e\,A10}$ *şi* $Y_{e\,A15}$) under the same conditions

$$s_e^2 = \frac{1}{n_0 - 1} \sum_{i=15}^{20} (Y_{ei} - \overline{Y}_0)^2 \qquad (11)$$

where:

n_0 is the number of repeated experiments made to estimate the experimental error;

$\overline{Y}_0$ – the arithmetic mean of the results obtained for these experiments, and it is defined by:

$$\overline{Y}_0 = \frac{1}{6} \sum_{i=15}^{20} Y_{ei} \qquad (12)$$

For the equation (7), one obtains $\overline{Y}_0$ = 3.1362 and s_e^2 = 0.007112. The dispersion of the regression coefficients was computed with the relation (13), where N is the total number of experiments:

Table 5

VALUES OF THE GRAFTING DEGREE FOR THE FABRIC PREPARED THROUGH ALKALINE TREATMENT AND FOR THE BLEACHED ONE

Sample no.	$Y_{c\,F10}$	$Y_{c\,F15}$	$Y_{c\,A10}$	$Y_{c\,A15}$
1	1.1195	1.2371	0.627719	0.6658
2	1.2741	1.6811	1.673007	2.1809
3	0.8225	0.6750	0.595215	0.6262
4	1.5301	1.9062	1.179855	1.6939
5	3.8038	4.2904	2.558685	2.8071
6	5.0236	5.4046	4.064721	4.5542
7	1.3622	1.6842	1.738033	1.9680
8	3.1350	3.5857	2.783421	3.2677
9	1.8907	1.9017	1.390618	1.5735
10	3.5116	3.8742	3.148876	3.9408
11	2.8748	3.4317	2.290201	2.2675
12	1.0367	1.4292	1.185292	1.1523
13	0.4656	0.4856	0.227076	0.5990
14	4.0728	4.4658	3.199618	3.7234
15	3.1346	3.2602	1.979210	2.0261
16	3.1346	3.2602	1.979210	2.0261
17	3.1346	3.2602	1.979210	2.0261
18	3.1346	3.2602	1.979210	2.0261
19	3.1346	3.2602	1.979210	2.0261
20	3.1346	3.2602	1.979210	2.0261

$$s_b^2 = \frac{s_e^2}{N} = 3.56 \cdot 10^4 \qquad (13)$$

The significance of the regression coefficients was verified with the Student test, t, using the relation (14):

$$t_i = \frac{|a_i|}{s_b} \qquad (14)$$

where:
$s_b = 0.018868$.
The values of the variable t for each coefficient are presented in table 6. The critical value of the Student test for $\alpha = 0.05$ and $\nu = N - l = 10$ (where l represents the number of coefficients from the equation of the model) is $t_{\alpha,\nu} = 2.23$ [3]. If $t > t_{\alpha,\nu}$, it is admitted with a 95% probability that the corresponding coefficient is significant and the sign + is attached to it. The coefficients considered as insignificant ($t < t_{\alpha,\nu}$) receive the sign minus. In the regression equations, only the significant coefficients are preserved, i.e. the terms which significantly influence the reaction yield.
As the result of the application of the Student test also for the equations (8), (9) and (10), all the coefficients appear as significant and the mathematical model remains the one described by the equation (6).
The verification of the model adequacy was performed by means with the Fisher test. The regression dispersion as compared to the experimental data is computed with the relation (15) [3]:

$$s^2 = \frac{1}{N - l} \sum_{i=1}^{20} (Y_{ei} - Y_{ci})^2 \qquad (15)$$

Table 6

VERIFICATION OF THE SIGNIFICANCE OF COEFFICIENTS OF THE REGRESSION EQUATION (7)

Coefficient	Absolute value of the coefficient	t	$t_{\alpha,\nu}$	Signi-ficance
a_0	3.134570	166.1315		+
a_1	0.481838	25.5373		+
a_2	0.546405	28.9593		+
a_3	1.072310	56.8322		+
a_{11}	0.153191	8.1191	2.228	+
a_{22}	0.416665	22.0832		+
a_{33}	0.305871	16.2111		+
a_{12}	0.138238	7.3266		+
a_{13}	0.266287	14.1132		+
a_{23}	0.536137	28.4151		+

where:
$N = 20$ is the total number of experiments;
$l = 10$ – the number of coefficients.
For the equation (17), the experimental values, $Y_{e\,F10}$, from table 2 and the calculated ones, $Y_{c\,F10}$, from table 5 are used, which gives $s^2 = 0.0155$.
The value of the Fisher test is computed with the relation (16):

$$F = \frac{s^2}{s_e^2} \qquad (16)$$

By replacing the values in the relation (16), one obtains for the equation (7), $F = 2.18$. Since the test value from the table for $\alpha = 0{,}05$; $u_1 = N - l = 10$ and $u_2 = n_0 - 1 = 5$ is $F_{\alpha,u1,u2} = 4.8$ [3] and therefore $F < F_{\alpha,u1,u2}$, the adequacy for the regression equation is confirmed.
For the equations (18), (19) and (20) one also obtains for F values smaller than $F_{\alpha,u1,u2}$, which confirms the adequacy of these equations.

RESULTS AND DISCUSSIONS

By analyzing the grafting degrees determined from experiments and based on simulations performed by means of mathematical models (7–10), one can notice that, as as compared to the bleached fabric, the fabric prepared through alkaline treatment is more favourable to MCT-β-CD grafting. The influence of the three independent variables on the grafting degree was determined by using the MODDE software (fig. 2). For the fabric prepared through alkeline treatment with a fixing time of 15 minutes, one can notice a positive influence of the independent variables x_1 – MCT-β-CD concentration, and x_3 – fixing temperature, and a negative influence of x_2 – concentration of sodium carbonate, which is a reason to establish an optimum. One can notice from figure 3 that the temperature effect is twice as the influence of the MCT-β-CD concentration, and the effect of x_2 is negative. The same influence was noticed for the other series of tests.

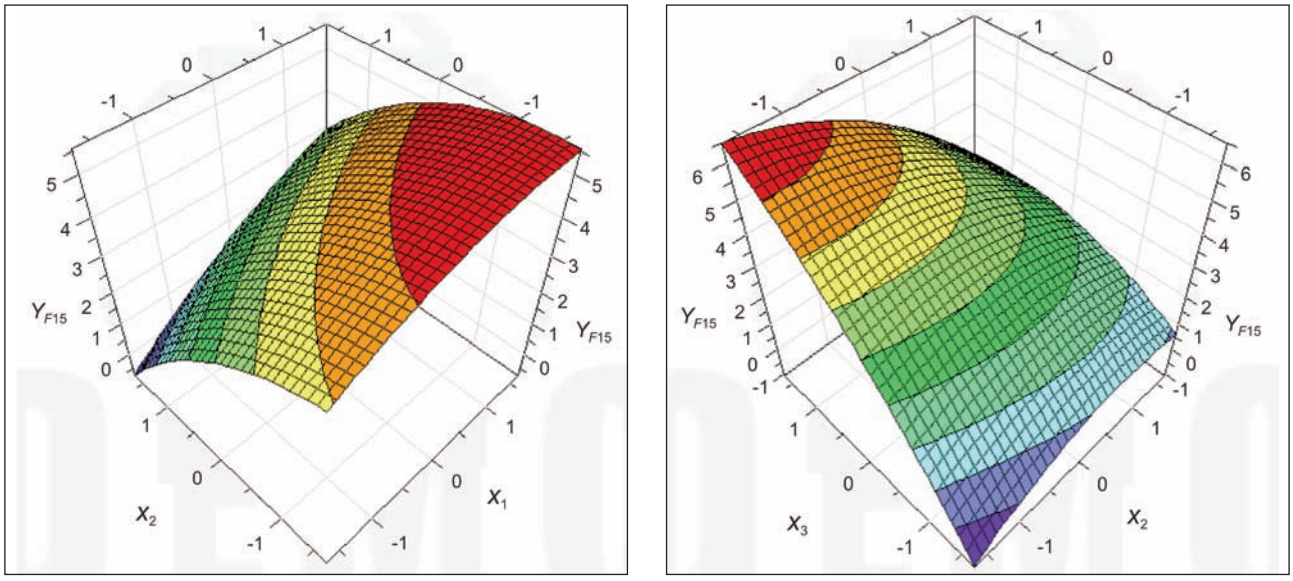

a *b*

Fig. 2. Influence of the independent variables, on the grafting degree Y_{F15}:
a – x_1, x_2 for $x_3 = 1$; ***b*** – x_2, x_3 for $x_1 = 1$

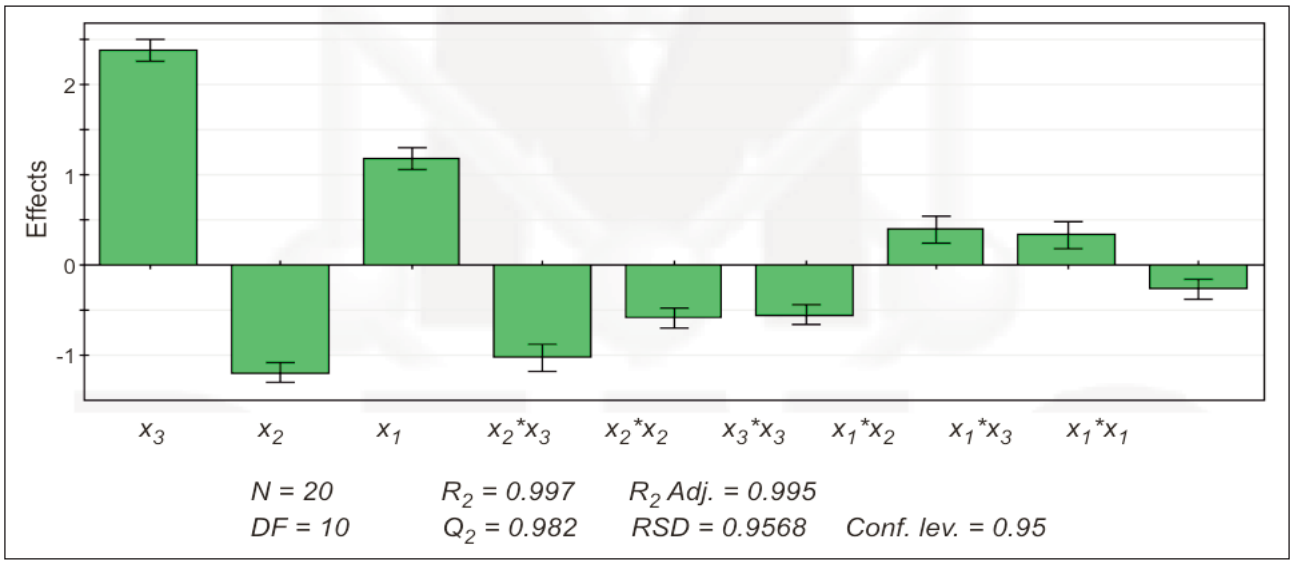

Fig. 3. Efects for Y_{F15}

Then, the optimization of the grafting degree for the chosen system was approached. The optimization problem was formulated as a maximizing one and it was solved by means of the descending simplex [4, 5] within the MODDE software. The obtained results show that the maximum grafting degree Y_{F15} = 5.4934% is obtained for x_1 = +1 and x_3 = +1 (technologically accepted maximum values corresponding to the real values X_1 = 129.72 g/L MCT-β-CD and X_3 = 147.83°C) and x_2 = 1.5487, which corresponds to the real value X_2 = 22.38 g/L Na_2CO_3. The experimental verification confirmed this result.

CONCLUSIONS

In order to establish the adequate preparation procedure for MCT-β-CD grafting on cotton, an experimental study was performed to determine the highest grafting degree, this being the alkaline treatment. It has also been experimentally established that the duration of thermal fixation has a favourable influence on the grafting degree, yet it is technologically limited. The developed mathematical models have been used for simulation, for a more complete knowledge of the studied system within the experimentally investigated field. We were thus able to estimate the influence of the independent variables, finding out in all the cases, that the grafting degree increases with MCT-β-CD concentration and fixing temperature, the both increases presenting technological limits. It was noticed that going beyond the optimum concentration of the sodium carbonate results in the diminution of the grafting degree. The optimization of the grafting degree for the chosen system

has shown that its maximum value is Y_{F15} = 5.4934% and it is obtained under the condition that x_1 = +1, x_2 = 1.5487 and x_3 = +1 (corresponding to the real values X_1 = 129.72 g/L MCT-β-CD, X_2 = 22.38 g/L Na_2CO_3 and X_3 = 147.83°C), which was verified and confirmed by experiment.

Acknowledgement

This work was acomplished with the financial support of the project POSDRU CUANTUMDOC "DOCTORAL STUDIES FOR EUROPEAN PERFORMANCES IN RESEARCH AND INNOVATION" ID79407, project financed by the European Social Fund and the Romania Gouvernment.

BIBLIOGRAPHY

[1] Grigoriu, A., Racu, C., Diaconescu, R., Grigoriu, A. M. *Modelling of the simultaneous process of wet spinning-grafting of hemp fibres destined to medical textiles*. In: Industria Textilă, 2010, vol. 61, nr. 3, p. 112

[2] Grigoriu, A. M. *Cercetări în domeniul compuşilor de incluziune a ciclodextrinelor şi derivaților acestora, cu aplicații în industria textilă*. Teză de doctorat. Universitatea Tehnică Gheorghe Asachi, Iaşi, 2009

[3] Akhnazarova, S., Kafarov, V. *Experiment optimization in chemistry and chemical engineering*. Mir Publishers, Moscow, 1982, p. 188

[4] Racu, C ., Diaconescu, R., Grigoriu, A. M., Grigoriu, A. *Optimization of hemp yarn grafting degree for medical textiles during simultaneous wet spinning-grafting*. In: Cellulose Chemistry and Technology, 2010, vol. 44, issue 9, p. 365

[5] Zaharia, C., Diaconescu, R., Surpăteanu, M. *Optimization study of a wastewater chemical treatment with PONILIT GT-2 anionic polyelectrolyte*. In: Environement Engeneering Management Journal, 2006, vol. 5, issue 6, p. 1 273

[6] Diaconescu, R. M., Grigoriu, A. M., Luca, C., Georgescu, P. *Study on the response surface modelling by central composite design and optimization of paper nanocoating*. In: Revista de Chimie, Bucureşti, 2011, vol. 62, issue 5, p. 522

Authors:

Drd. ing. OCTAVIAN POPESCU
Prof. dr. ing. AURELIA GRIGORIU
Drd. ing. ECATERINA VASLUIANU
Universitatea Tehnică Gheorghe Asachi
Facultatea de Textile, Pielărie şi Management Industrial
Bd. D. Mangeron nr. 53, 700050 Iaşi
e-mail: opopescu@tex.tuiasi.ro;
augrigor@tex.tuiasi.ro; evasluianu@tex.tuiasi.ro

Prof. asociat dr. ing. RODICA MARIANA DIACONESCU
Universitatea Tehnică Gheorghe Asachi
Facultatea de Inginerie Chimică şi Protecţia Mediului
Bd. D. Mangeron nr. 71A, 700050 Iaşi
e-mail: rodicamdiaconescu@yahoo.com

Determination of some characteristics of New Zealand white rabbit furs for leather garment

HUSEYIN ATA KARAVANA

REZUMAT – ABSTRACT

Determinarea unor caracteristici ale blănurilor de iepure alb neozeelandez, destinate îmbrăcămintei din piele

Scopul studiului îl constituie investigarea disponibilității producerii de blănuri din piei de iepure alb, provenit din Noua Zeelandă, acestea reprezentând un produs auxiliar al acestei specii de iepure de carne, precum şi determinarea unor caracteristici ale blănurilor de iepure, ce prezintă importanță pentru industria de îmbrăcăminte din piele. Cele 25 de blănuri de iepure din rasa neozeelandez alb au fost prelucrate conform unei rețete speciale pentru blănuri de iepure. Conform rezultatelor obținute în urma analizelor fizico-chimice, s-a constatat că aceste blănuri sunt adecvate producerii articolelor de îmbrăcăminte. Prin urmare, a fost elaborată o rețetă pentru producerea blănurilor de iepure, care poate fi aplicată şi celor provenite de la iepurele alb neozeelandez.

Cuvinte-cheie: piele gelatină de iepure, piele de iepure, iepure alb neozeelandez, blană de iepure, îmbrăcăminte din piele

Determination of some characteristics of New Zealand white rabbit furs for leather garment

The aim of the study was to investigate availability in rabbit fur production of New Zealand white rabbit pelts that they are by-product of a meat species rabbit and, to determine some important characteristics in point of leather garment industry of rabbit furs. New Zealand white rabbit furs were manufactured from 25 New Zealand white rabbit pelts according to special recipe for rabbit fur production. According to findings from physical tests and chemical analysis, it was detected that these furs are suitable for garment usage. Therefore, developed recipe for production of rabbit furs is also suitable for New Zealand white rabbit pelts.

Key-words: rabbit pelt, rabbit skin, New Zealand white rabbit, rabbit fur, leather garment

Leather industry is a branch of industry which makes production by using raw hides or skins as the most significant by-product of the meat and meet products industry. In consequence of increased meat need both in the world and in our country, in addition to cattle, sheep & goat and poultry, animals like rabbit not only the meat but also other by-products of which can be put to good use are bred. Rabbit is a very economical animal from whose meat, pelt, manure and fiber benefit can be derived [1–3].

Meat is definitely the main goal of rabbit production. Two by-products are usually also recovered from the skin: the pelt and the shorn hair, with no particular production constraint. Rabbit fur production is not comparable with the production of other fur species. Mink, which tops the list of species bred essentially for its fur, supplies a world total of about 25 million to 35 million pelts a year whereas rabbit pelts are estimated at one billion. In France alone annual rabbit skin production tops 70 million.

In the world, first-grade furs of Rex, which is bred for its pelt, are used in the production of garments such as coats, stoles and hats. On the other hand, lower-grade furs are put to good use in the production of toys and slippers, and pelts for shorn hair in glue and feed industries.

In our country, many of about 1 200 business enterprises that raise Angora rabbit for its fiber had economic troubles because Angora fiber is put on the world market by China at a very cheap price and started to breed rabbit for its meat. For this purpose, they preferred New Zealand rabbit, which is one of the best species in terms of meat yield.

The aim of the study was to investigate availability in rabbit fur production of the pelts of New Zealand white rabbits, which are bred for their meat, and to determine some important characteristics in point of leather industry of rabbit furs.

MATERIAL AND METHODS

The study material comprised of 25 defect- and fault-free wet-salted New Zealand white rabbit pelts. Rabbit pelts were processed according to the production recipe given in table 1 and made into furs.

A number of physical tests and chemical analysis were conducted so as to determine the characteristic structure of rabbit furs. Rabbit furs' shrinkage temperature was determined according to TS 4120 EN ISO 3380 (2005) [4], tensile strength and percentage extension according to TS 4119 EN ISO 3376 (2006) [5], tear load-double edge tear according to TS 4118-2 EN ISO 3377-2 (2005) [6], tear load-single edge tear according to TS 4118-1 EN ISO 3377-1 (2005) [7], stitch tear resistance according to TS EN ISO 23910 (2008) [8], fat content according to TS EN ISO 4048 (2009) [9] and chromic oxide content according to TS EN ISO 5398-1 (2008) [10]. The results that were obtained were evaluated in SPSS 15.0 statistics programme.

CHROME TANNING PROCESS RECIPE OF NEW ZEALAND WHITE RABBIT PELTS						
Process	**Chemical additives**	**Temperature, °C**	**Amount**		**Time, min.**	**Remarks**
			1:X	g/L		
Soaking	Water	25	1:20			15 minutes run; 60 minutes stop; 15 minutes run; 60 minutes stop; 20 minutes run; wait a night; morning 15 minutes run; drain and wash
	Salt			20.0		
	Wetting agent			0.5		
	Anionic surfactant			1.5		
	Degreasing agent			1.5		
	Wool bleaching agent			1.0		
	Bactericide			0.2		
Washing	Water	35	1:20			
	Anionic surfactant			1.0		
	Degreasing agent			1.0		
	Sodium bicarbonate			0.3	30	drain, pour, fleshing
Pickle	Water	35	1:20			
	Salt			60.0	15	
	Electrostable oil			3.0	30	
	Formic acid			0.7	40	*p*H: 4.3
	Electrostable oil			2.0	90	
	Formic acid			5.0	3 x 15 + 120	*p*H: 3.0
	Polyaldehyde			2.0	60	wait a night
	Morning run 15 minutes, drain, horse up, wait a day					
Depickle	Water	35	1:20			
	Salt			60.0	10	
	Electrostable oil			1.5	10	
	Electrostable oil			1.5		
	Anionic surfactant			0.5	30	
	Formic acid			0.5	45	*p*H: 3.3-3.6
Tanning	Polyaldehyde			2.0	30	
	Basic aluminium complex salt			3.0	30	
	Basic chromium sulphate			4.0	30	
	Basic chromium sulphate			4.0	30	
	Autobasification agent			1.0	30	
	Basic chromium sulphate			2.0		
	Chromium syntan			5.0	120	
	Acrylic syntan			2.0	60	
	Sodium formate			4.5	3 x 20 + 120	*p*H:3.8
	Wait a night, morning run 20 minutes, drain					
Washing	Water	30	1:20		30	pour, horse up, wait a night
Neutralisation	Water	35	1:20			
	Sodium Formate			2.0	30	
	Sodium bicarbonate			1.5	3 x 15 + 75	*p*H: 6.0
	Drain, wash, drain					
Fatliquoring	Water	50	1:20			
	Combined synthetic oil			4.0		
	Sulphated oil			4.0		
	Phospho-ester oil			2.0		
	Emulsifying agent			0.5	120	
	Formic acid			1.3	2 x 15 + 60	
	Wait a night, morning run 15 minutes, drain, hang drying, mechanical process					

Table 2

SOME PHYSICAL TESTS AND CHEMICAL ANALYSIS RESULTS OF NEW ZEALAND WHITE RABBIT FURS	
Properties	Mean ± S.D.
Shrinkage temperature, °C	78.00 ± 4.58
Tensile strength, N/mm^2	12.44 ± 5.61
Elongation, %	58.02 ± 22.85
Tear load-double edge (N) thickness 0.38 mm	25.75 ± 20.61
Tear load-double edge (N) thickness 0.38 mm	9.53 ± 2.70
Stitch tear resistance, N/mm	61.72 ± 15.87
Fat content, %	12.85 ± 0.64
Chromic oxide content, %	1.96 ± 0.11

RESULTS AND DISCUSSIONS

In general, the shrinkage temperature of collagen protein is accepted as an empirical measure of tanning degree or the degree of transformation from raw hide or skin to finished product [11]. The shrinkage temperature of processed leather differs depending upon both the type and the rate of tanning and retanning agents used in processing and accepted as an indicator of collagen fibers' stabilization [12]. Considered by leather manufacturers and researchers as an indicator of collagen and leather stabilization and in turn tanning, shrinkage temperature was accepted as a measure of tanning in this study. Table 2 demonstrates that the average shrinkage temperature of the rabbit furs subject to the research was found to be 78°C. It was ascertained that this value is above the ones indicated in literature for tanned rabbit furs [13] but below the ones indicated in literature for chrome-tanned garment leather [12, 14].

One of the most important criteria in determining the suitability of processed leathers for area of use is tensile strength, which is applied to almost all types of leathers. Not only the fiber-like structure that forms collagen tissue but also the modification of this tissue with tanning agents have a strong effect on leather's strength properties [15]. A good tensile strength value is generally a desired specification for all leather types and a good indicator of leather quality [16]. Depending upon their areas of use, processed leathers are expected to have strength and flexibility to certain degrees. Upon the examination of table 2, the average tensile strength of the rabbit furs obtained by processing New Zealand white rabbit pelts was found to be 12.44 N/mm^2. In view of the studies performed on rabbit furs and the acceptable quality standards of garment leathers, it is understood that this value is satisfactory [13, 17–19].

It is useful to take elongation value into consideration as well as tensile strength because a low elongation value results in easy tear while a high elongation value causes leather goods to become deformed very quickly or even lose usability. It was determined that the rabbit furs obtained from the researches have an elongation value of 58.02% (table 2). This value is slightly higher than the one mentioned in literature [13, 17–19].

The measure of processed leather's performance and strength during use is determined by means of tear load. Here, the cohesive force between leather fibers is considerably effective [20]. Table 2 shows that the rabbit furs subject to the study have an average double edge tear load and an average single edge tear load of 25.75 N and 9.53 N, respectively. These values are in conformity with the tear load expected from garment leather [19, 21, 22].

Another criterion important for garment leather is stitch tear strength. Thanks to this physical test, the robustness of leather's fiber structure is determined and thus an opinion is formed about the strength of processed leather's seams during both manufacturing and use [20]. As can be seen in table 2, the stitch tear strength of rabbit furs is 61.72 N/mm. This value is higher than the limit values recommended for garment leather [19].15 minutes run;

Tanning is based on the formation of tight cross links between the collagen in leather's fibrillary structure and tanning agents. Depending upon intended leather type, one or a combination of mineral, vegetable and synthetic tanning agents is used in tanning. One of the most commonly used tanning agents is basic chromic salt, a mineral tanning agent. The chromic oxide content of a leather tanned with chromic salts is a measure that indicates the degree of tanning process [23]. The chromic oxide content of a chrome-tanned garment leather should be minimum 2.50% [19, 24]. The chromic oxide value of the rabbit furs obtained as a result of the research was found to be 1.96% (table 2). This result explains why the value established in the shrinkage temperature test is low.

During leather production, natural fats in raw hides or skins are removed and these hides or skins undergo different fat liquoring processes depending upon both place and area of use of processed leathers and desired softness. The fat content of garment leathers ranges from 4% to 16% depending upon tanning degree and type of the raw hide or skin used in processes [19, 24–26]. As can be seen in table 2, the fat content of the processed leather subject to the study is 12.85%.

CONCLUSIONS

Those who live in a country where winters are extremely cold and long need to use fur garments in their daily life so as to protect their body from harsh weather conditions. However, due to the influence of institutions and organizations such as environmentalist non-governmental organizations and societies for the protection of nature and animals, the number of

fur animals and in return of raw pelts for fur gradually decreases in the world.

In this study, rabbit fur was produced using the rabbit pelt obtained by slaughtering New Zealand white rabits, which are bred for meat on the grounds of being cheaper than raw pelts from fur animals. The data acquired as a result of some physical tests and chemical analyses conducted on rabbit furs demonstrate that these furs may be used for garment purposes. Accordingly, it was determined that the rabbit fur processing recipe created within the framework of this study is suitable for New Zealand white rabbit pelts.

Moreover, by putting the pelts of New Zealand white rabbits, which are bred for meat, to good use in the leather industry, contribution shall be made to the economy of both New Zealand white rabbit breeders and of the country.

BIBLIOGRAPHY

[1] Sönmez, R., Koçak, Ç. *Rabbit breeding*. Ege University Pres, 1978, p. 75

[2] Gültanın, N. *Investigation on some physical and chemical properties of New Zealand, Chincilla, California and Angora rabbits wool*. Ankara University Pres, 1979, p. 50

[3] Atav, R., Yurdakul, A. *The use of dendrimers to obtain low temperature dyeability on mohair and Angora fibers.* In: Industria Textilă, 2011, vol. 61, issue 2, p. 57

[4] TS 4120 EN ISO 3380. *Leather – Physical and mechanical tests. Determination of shrinkage temperature up to 100ºC*. Turkish Standart Institution, 2005, p. 9

[5] TS 4119 EN ISO 3376. *Leather – Physical and mechanical tests. Determination of tensile strength and percentage extention*. Turkish Standart Institution, 2006, p. 9

[6] TS 4118-2 EN ISO 3377-2. *Leather – Physical and mechanical tests. Determination of tear load. Part 2: Double edge tear*. Turkish Standart Institution, 2005, p. 7

[7] TS 4118-1 EN ISO 3377-1. *Leather – Physical and mechanical tests. Determination of tear load. Part 1: Single edge tear*. Turkish Standart Institution, 2005, p. 8

[8] TS EN ISO 23910. *Leather – Physical and mechanical tests. Measurement of stitch tear resistance*. Turkish Standart Institution, 2008, p. 13

[9] TS EN ISO 4048. *Leather – Chemical tests – Determination of matter soluble in dichloromethane and free fatty acid content*. Turkish Standart Institution, 2009, p. 17

[10] TS EN ISO 5398-1. *Leather - Chemical determination of chromic oxide content. Part 1: Quantification by titration*. Turkish Standart Institution, 2008, p. 17

[11] Nayudamma, Y. *Shrinkage phenomena*. O'Flaherty, F., Roddy, W.T., Lollar, R.M. (eds.), The Chemistry and Technology of Leather. Vol. II, Reinhold Publishing Corporation, New York, 1958, p. 28

[12] Gustavson, K. H. *The chemistry of tanning processes*. Academic Press Inc., New York, 1956

[13] Burde, R. *Physicochemical evaluation of the factors governing the organoleptic classification of rabbit pelts*. In: Journal of The American Leather Chemists Association, 1962, vol. 57, issue 6, p. 255

[14] Lange, J. *Qualitaetsbeurteilung von leder, lederfehler, -lagerung and -pflege*. Bibliothek Des Leders, Umschau-Verlag, Frankfurt am Main, 1982, Band. 10

[15] Olivannan, M. S., Muthulingam, P., Sadulla, S., Kumar, A., Rao, J. B., Salvarangan, R. *Process for the manufacture of suede garment leathers from chrome crust goat skins*. In: Leather Science, 1977, vol. 24, issue 8, p. 272

[16] Venkatachalam, P. S. *Alum combination tannage*. Lecture Notes on Leather, 1962, p. 208

[17] Yazıcıoğlu, T. and Dikmelik, Y. *Investigation on rabbit pelts which were processed with and without alum*. In: The Journal of Agricultural Faculty of Ege University, 1977, vol. 14, issue 3, p. 391

[18] Sharphouse, J. H. *Leather technican's handbook*. Leather Producers' Association, Northampton, 1989

[19] UNIDO. *Acceptable quality standards in the leather and footwear industry*. UNIDO Publication Sales No. UNIDO.95.4.E, Vienna, 1996

[20] Kanagy, R. *Physical and performance properties of leather*. In: O'Flaherty, F., Roddy, W. T., Lollar, R. T. (eds.), The Chemistry and Technology of Leather, Reinhold Publishing Corporation, New York, 1965, p. 369

[21] Rajamaran, R., Poorneswari, S., Bangaruswamy, S., Rao, J. B., Santappa, M. *Influence of different tanning systems on the characteristics of leather*. In: Leather Science, 1978, vol. 25, issue 9, p. 394

[22] Slabbert, N. P. *Mimosa-Al tannages-an alternative to chrome tanning*. In: Journal of The American Leather Chemists Association, 1981, vol. 76, issue 7, p. 231

[23] Sarı, Ö. *Lecturer notes on tanning materials*. Ege University, 2005 (unpublished)

[24] BASF. *Pocket book for the leather technologists*. BASF Aktiengesellschaft, 67056 Ludwigshafen, Germany, 1996

[25] Bitlisli, B.O., Karavana, H.A., Başaran, B., Sarı, Ö., Yaşa, İ., Birbir, M. *The effect of conservation defects on the suede quality of double-face leather*. In: Journal of The American Leather Chemists Association, 2004, issue 12, p. 494

[26] Karavana, H. A., Başaran, B., Aslan, A., Bitlisli, B. O. *Some technological parameters of deacon skins originates from New Zealand*. In: Journal of Animal Production, 2009, vol. 50, issue 2, p. 41

Authors:

Assist. prof. dr. HUSEYIN ATA KARAVANA
Ege University, Engineering Faculty
Leather Engineering Department
35100 Bornova-Izmir, Turkey
e-mail: huseyin.ata.karavana@ege.edu.tr

Modern processes of ennoblement for garment

AUREL POPP

VLADLEN BABCINEȚCHI
MIHAELA CARP

REZUMAT – ABSTRACT

Procedee moderne de înnobilare a vestimentației

Cercetările teoretice şi experimentale prezentate în lucrare se încadrează în obiectivul general de reevaluare şi reconsiderare a importanței noilor tehnologii neconvenționale în clasificarea îmbrăcămintei conform unor niveluri de performanță prestabilite. Sunt descrise unele tehnologii nonconvenționale referitoare la procesele bazate pe înaltă frecvență, sudarea cu ultrasunete, tăierea cu laser şi gravarea, precum şi pe utilizarea de prese la cald, toate acestea având un rol important în procesele de înnobilare a îmbrăcămintei şi conducând la îmbunătățirea calității acesteia.

Cuvinte-cheie: înnobilare, laser, înaltă frecvență, presare la cald, design

Modern processes of ennoblement for garment

The theoretical and experimental research of this paper fits into the overall objective of reevaluation and reappraisal of the importance that the new non-conventional technologies have for the placement of clothing for certain levels of performance. Are being described the related non-conventional technologies of the following processes, that are based on: high frequency, ultrasonic welding, laser cutting and graving, and the use of hot presses that have an important place in the processes for the ennoblement of clothing which leads to improving their quality.

Key-words: ennoblement, laser, high frequency, hot presses, designe

Theoretical and experimental research in this paper fit within the overall review and reconsideration of the importance that the non-conventional technologies have for the placement of clothing for certain levels of performance.

Initiated long time ago, these alternatives, in fact very diverse, offer many advantages such as:

- reducing the material consumption;
- reducing the time of execution;
- eliminate specific unwanted effects of presentation value, and the improvement of overall value by applying different processes on different part of the final garment.

Both theoretical and experimental research related to this field are encouraged by the enrichment of raw materials that was developed to specific and diverse composite materials appearing in relation to new types of fibers, chemical finishing and surface treatments.

These non-conventional processes are able to transfer the level of performance on the raw materials in the final garment, especially if they are assembled classically, with decorative or constructive types of ennoblement.

Starting from these premises the paper highlights in particular the way in which the different parts or decorative molds and unconventional technologies are applied to different areas of the product.

The technologies that allow this ennoblement on raw materials are: the high frequency welding current, ultrasonic welding, laser engraving and cutting, hot stamping, screen printing etc.

EXPERIMENTAL PART AND RESULTS

Regarding the high frequency currents welding, depending on how the mold is created we can find two different technologies that are divided into categories.

The first one – high frequency currents that are used to weld materials together and they make this operation according to the designed molds that is doing the welding of the materials. The mold is designed according to the product specifications and the welding machine can get any kind of drawing using high frequency currents. Welding occurred when the two materials are pressed together while high frequency current is passing through them and combine them.

High frequency currents had a great significance in terms of plastics assembly at first, and second in the application on the product of decorating details or signs due to the correct parameters of the assembly electrodes.

Based on the principle of the modern capacitor, the welding energy is produced using high frequency current that are converted into heat that appears due to friction when intermolecular chains rub together due. Temperature registered in the welding materials is variable, the highest value is occurring in mid thickness of welded materials.

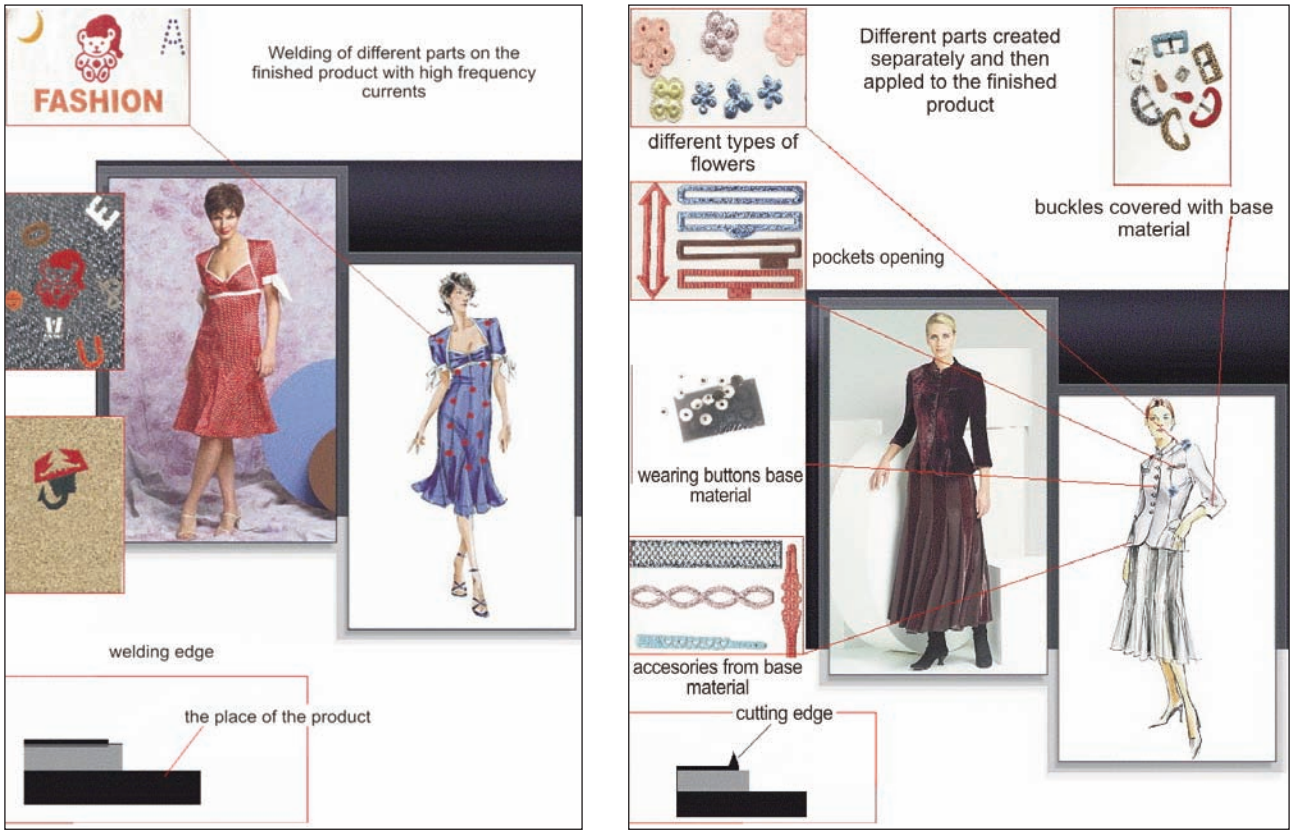

a *b*

Fig. 1:
a – high frequency welding applied on the finish product;
b – high frequency welding current applied on different accessories

Although welding machines with high frequency currents can be fitted with specially shaped electrodes which can achieve buttonholes, buttons, complete connections for some parts, the method is also used as mold design and for the application of different design in agreement with the existing technologies.
Another category of high-frequency current is used to obtain shaped products according to drawing and materials, which generally must have a thickness major than 3 mm. The difference between these dies and the first is that the welding is used to obtain finished products. The mold is provided on the edge not only with the pressing edge but with a cutting edge to. In this case u can achieve: flowers, buckles, buttons, and other accessories for clothing according to the form of the mold.
In the figure 1*a* and 1*b*, welding lines are continuous and correspond to designs applied on the material or product and which have an important role in terms of surface finishing.
The next type of processing of textile materials is the laser machine. This has a wide applicability because of a large amount of drawing that can be made with cutting or engraving at different depths. The technology is using light that is amplified so a stimulated emission of radiation occurred that vaporize the material in a spot at 50 000°C.
Without insisting on the principles at the base of this process, the generation and propagation of the laser beam indicated that it has a wide applicability in the sense that a wide range of materials are obtained either engraved or cut that have in general give added value to the final product.
In industrial practice it is noted the wide variety of designs that are digitized in a graphics program such as CorelDraw. Then the laser interface design is imported, he read as an extension of (PLT) active extension to process the digitized laser.
The drawings are made according to customer requirements and digitized in several colors for the interface, the laser can be set to use for each color a different power to cut the material or to engrave oxidizing the material, such as denim.
In the figures below there are some examples of drawing produced with burning by engraving, in figures 2*a* and 2*b*, that shows how the product application are achieved with this process.
Therefore, in addition to achieving engraving on the finished product directly to the facility we can obtain different holes with a range of diameters on the final product that change the product parameters. This designs or models are made separately to different part of the product and then applied to the finished garment.
Another high performance technology in terms of finishing products are based on hot pressing, using an installation that has a working pressure cylinder with a piston-based hydraulic oil pomp that has the ability

a *b*

Fig. 2:
a – laser engraving and cutting on final product; ***b*** – different types of laser cutting

to be able to warm up side plans and process the material with different effects.

With the design mold placed on the material this processed need several corrections at the lower cylinder for ensuring that the material will not be damaged. It is therefore very important to properly adjust the height of the mold during the processing and the pressure applied under high temperature, also adjusted depending on the specific heat of the material. Due to the high speed of processing, the method is especially effective when working with a large lot.

The method is based on accuracy and durability of the mold that is made of very hard materials design and obtained by converting an area or a drawing in three dimensional drawing with specialized programs such as type 3, Rhinoceros or 3DMax.

Following the hot pressing, the method is useful for materials with hard surfaces, helping to heat the material without piercing damage, and after soaking it better resists compression and plastic deformation depending on the destination. The materials can be various due to very large scales of pressures that can be selected from the machine. This applies to both the textile and leather materials, with possibility of extension on wood and plastic product that resists plastic deformation. In the example below the jacket parts are hot pressed for obtaining the following transformations on the surface:

- smaller parts of the product made with a hot mold;
- doubling of base material with separate parts and then stitched on the final product.

The examples are showed in figure 3*a* and figure 3*b*.

Another way of refining the surface is the screen-printing. This can be made on fabrics or other flat material through a machine with ultraviolet rays. The drawings are made in a range of colors from white to black with intermediate gray scales. Adobe Photoshop graphics program has settings to convert monochrome design in intermediate shades of grayscale. Printer design is brought to a piece of thin plastic with is necessary to be well centered on the material in order to obtain accurate color deposit. The aim is to obtain a product design centered exactly on the marks.

The drawing thus obtained is located above the source of radiation, where it is reflected on a canvas specially prepared for the purpose of screen-printing and in the places where ultraviolet rays are enhanced by dark colors will create holes, in gray or black depending on which one is drawing on plastic film. The holes will create drawing on the canvas according to the colors contained in the original design.

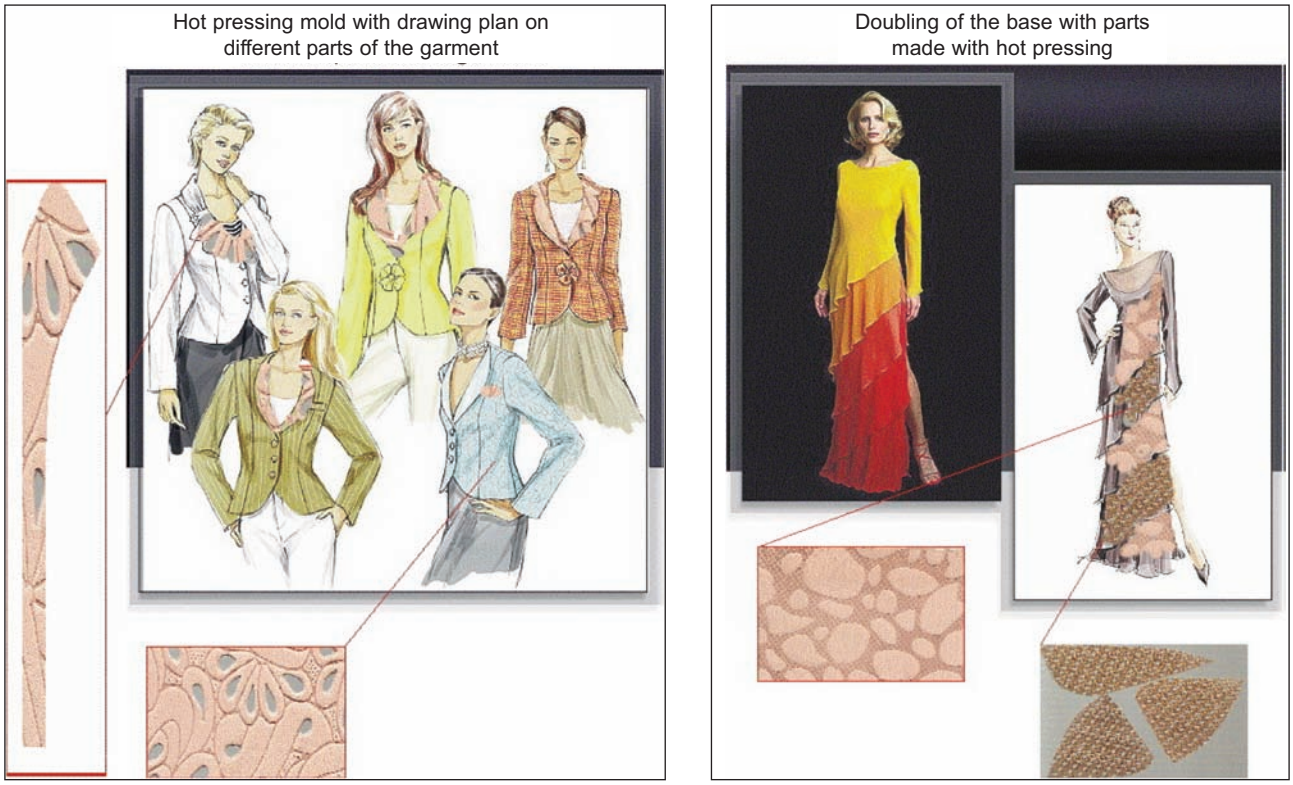

a ***b***

Fig. 3:
a – hot pressing on the product parts; ***b*** – hot pressing on different parts, applied to the product

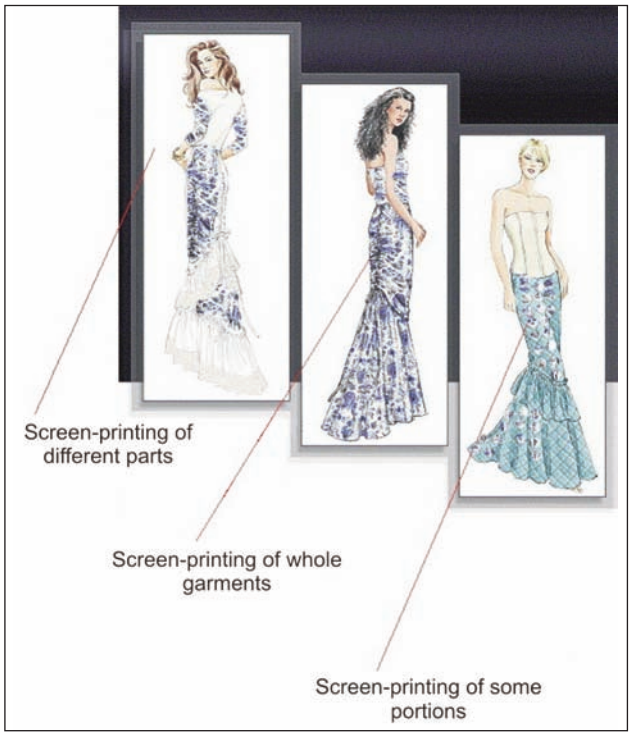

Fig. 4. Screen – printing on different parts

Drawings made in this way give a pleasant aspect of the product color by their complexity and the number of colors that can be used to create the final drawing on the garment.

Screen-printing machine has a great importance in the textile industry, leather and substitutes because there can make a huge number of prints in a limited time, on materials with different configurations. The collective balance machine can print the same design on different parts without having to change anything from one item to another.

Screen printing can be done in the following ways (fig. 4):

- highlights screen – printing full;
- sleeve screen – printing;
- collar, pockets and cap with screen – printing.

A special technology is based on plotter machine is used for the ennoblement of textiles, with the indication that this is just a trolley print cartridges that print larger dimensions on different materials, drawings, writings or pictures. They can be from the internet or on orders from customers. Can also be achieved in a photo editing program such as CorelDraw, AdobePhotoshop, ACDSee, 3Dmax, Rhinoceros and others.

Size of materials that can be printed on a plotter is the size of the working rail car that the machine is equipped, namely the distance you can move the cartridges. In truck with advertising on materials can make smaller or banner can get the width of 4.99 (m). We have to keep in mind that drawings can be made of materials with very long waves, with drawings of parts are produced after specific operations based on frames and cutting room. Example of item processed with plotter is showed in figure 5.

Special features are used to facilitate the application of crystals to finis product, representing different

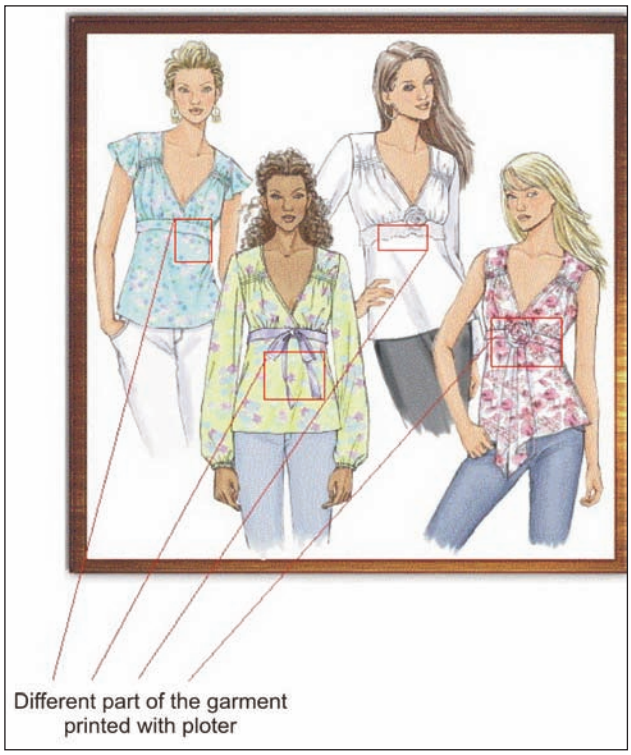

Fig. 5. Example of garments with Ploter processing

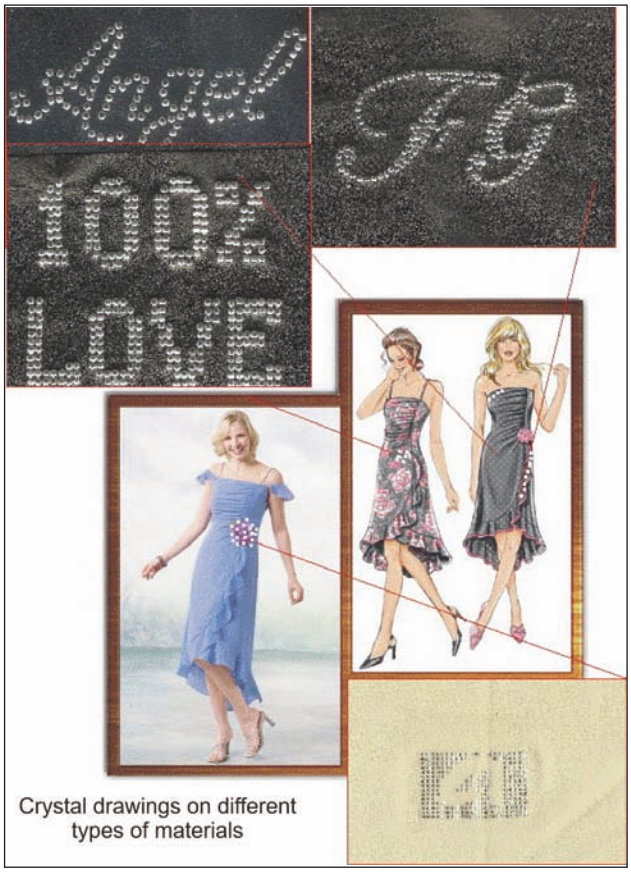

Fig. 6. Different ways to apply crystals on textile materials

drawing or details. Application of crystals on a textile product or some of its parts can be done in several ways, depending on desired design and materials that we need to processes.

For simple designs that have in their composition less than 50 crystals we can use a machine gun fixed with load pressure crystal on a cylinder with holes. These holes are filled with crystals with the help of the brushes that push them on the drum. The gun absorbs the crystal stream while the air keep it on the top, then the operator command and its stick the crystal on the material with high pressure. When the thermo - adhesive film is cooled the crystal sticks to the material.

In addition to the drawings with pressure gun, another variant of the application can be used. The drawings are done on a adhesive polymer film that can withstand higher temperatures than the melting point of the textile material, this is applied on the back of the crystal. In this way, drawing on film is placed on the material and after is press with a hot surface machine. Different ways for apply the crystals are showed in figure 6.

CONCLUSIONS

The general conclusions that can be extracted from this paper, is that the non-conventional treatment are in this moment an interesting topic, and that they fullfil the new requirements given for clothing products. A diversity of ennoblement processes cover a wide range of applications and their knowledge is a prerequisite to improve the quality of the final product.

It also notes the complexity and diversity of the processes underlying the phenomena analyzed their theoretical foundation is necessary for the understanding and interpretation of experimental results.

Accurate determination of specific parameters described technology is important in conditions requiring a connection between treatment parameters and features all done. Experimental research can be extended in the sense that other results can be presented on the screen-printing, plotter based technology, application of crystals, studs etc. Compared with other technologies, the ennoblement methods described are considerable advantages such as:

- high productivity;
- low workload;
- strength and joint density line;
- economy;
- improving working conditions;
- reduction of working volume.

BIBLIOGRAPHY

[1] Loghin, C., Ursache, M., Mureşan, R., Mureşan. A. *Surface treatment applied to textile materials and implications on their behavior in wet conditions.* In: Industria Textilă, 2010, nr. 6, p. 284

[2] Mitu, S., Mitu, M. *Bazele tehnologiei confecțiilor.* Vol. I, II. Editura Performantica, Iaşi, 2005

[3] Matenciuc, C. C., Dulgheriu, I. *Quality evaluation model for clothing materials*. In: Industria Textilă, 2011, issue 2, p. 99
[4] Papaghiuc, V. *Procese şi maşini pentru confecţii textile – Procese şi maşini pentru pregătirea tehnică a fabricaţiei şi croirea materialelor textile*. Editura Performanica, Iaşi, 2003
[5] Papaghiuc, V. *Procese şi maşini pentru coaserea materialelor textile*. Editura Gh. Asachi, Iaşi, 2000
[6] Zanoagă, M. *Compoziţia unui termoadeziv. Un sistem multicomponent complex*. In: Industria Textilă, 2001, issue 2, p. 116
[7] Preda, C., Lupu, I. *Textile neconvenţionale*. Lexicon tehnic explicativ. Editura Bit, Iaşi, 2003
[8] Chiriac, V. *Asamblarea prin termolipire a confecţiilor textile*. Editura Tehnică, Bucureşti, 1991
[9] Preda, C., Lupu, I. *Materiale textile neconvenţionale pentru îmbrăcăminte*. Editura Bit, Iaşi, 2000

Authors:

Drd. ing. AUREL POPP
Drd. ing. VLADLEN BABCINEŢCHI
Drd. ing. MIHAELA CARP
Universitatea Tehnică Gheorghe Asachi
Facultatea de Textile-Pielărie şi Management Industrial
Bd. D. Mangeron nr. 53, 700050 Iaşi
e-mail: apopp@tex.tuiasi.ro;
vbabcinetschi@tex.tuiasi.ro;
mcarp@tex.tuiasi.ro

DOCUMENTARE

Modă

TENDINŢE ALE MODEI PENTRU SEZONUL DE PRIMĂVARĂ-VARĂ 2013

O nouă ediţie a târgului ***München Fabric Start*** a avut loc în perioada 31 ianuarie – 2 februarie 2012. Circa 800 de expozanţi din peste 35 de ţări au expus ţesături din fibre naturale şi sintetice – destinate articolelor de îmbrăcăminte pentru femei, bărbaţi, copii şi articolelor de îmbrăcăminte sport, precum şi altor produse şi accesorii (fig. 1).

În cadrul pavilionului *Organic Selection* au fost expuse peste 400 de ţesături organice, certificate din punct de vedere ecologic. Experţi cu reputaţie în domeniu au oferit vizitatorilor servicii şi asistenţă în domeniul aprovizionării durabile. *Eco Village* a oferit informaţii de specialitate la cel mai înalt nivel.

Pentru a oferi asistenţă şi consultanţă de specialitate, au fost prezente organisme internaţionale de certificare, precum *IMO, IVN, Bluesign, Made-By, Textile Exchange* şi *Ceres.*

Pentru această ediţie a târgului München Fabric Start a fost instalalată o nouă platformă pentru furnizorii de ţesături de înaltă calitate destinate cămăşilor, sub denumirea „Shirtings by Munich Fabric Start“. În Pavilionul 4 al M.O.C., au fost prezente firme de renume, precum *Testa, Leggiano, Getzner Textil,*

Fig. 1

Brennet, Söktas, Virtuose şi *Bossa*, într-un sistem exclusivist de standuri, cu mobilier de înaltă calitate.

De asemenea, în jur de 80 de experţi internaţionali au prezentat ultimele tendinţe în domeniul denimului, pentru sezonul de primăvară-vară, în Zona Albastră a Pavilionului Zenith. În plus, ei au prezentat tendinţele iniţiale pentru sezonul de toamnă-iarnă 2013/ 2014, ca parte a evenimentului expoziţional TIST.

Viteza şi flexibilitatea sunt argumente convingătoare în favoarea perceperii Europei ca principală bază de producţie. Sub noua platformă „Ready Made Solutions“, în Zona Albastră a Pavilionului Zenith au fost prezentate, pentru prima dată, într-un format compact, produse finite ale expozanţilor.

Sursa: www.munichfabricstart.com

Investigation of the usage of different thickening agents in ink-jet printing with reactive dyes

BURÇİN ESER ARIF TANER ÖZGÜNEY ARZU ÖZERDEM

REZUMAT – ABSTRACT

Studiu privind utilizarea diferitelor tipuri de agenți de îngroşare la imprimarea cu jet de cerneală, folosind coloranți reactivi

În general, alginatul de sodiu este utilizat ca substanță de îngroşare în pasta de pretratare, folosită pentru imprimarea cu jet de cerneală, pe bază de coloranți reactivi. Scopul acestui studiu îl constituie investigarea modului de utilizare a diferitelor tipuri de agenți de îngroşare ca înlocuitori ai alginatului de sodiu în pasta de pretratare, folosită la imprimarea digitală cu jet de cerneală a țesăturilor din bumbac. De asemenea, au fost studiate posibilitățile de creştere a capacității tinctoriale, a clarității şi a rezistenței, precum şi realizarea unor procese mai ecologice, prin scăderea concentrației de uree. În acest scop, au fost efectuate experimente cu trei tipuri de agenți de îngroşare (alginat de sodiu, carboximetil celuloză sodică şi derivat de acid poliacrilic). Rezultatele au arătat că celuloza de sodiu carboximetil poate fi utilizată în pasta de pretratare destinată imprimării cu jet de cerneală, pe bază de coloranți reactivi.

Cuvinte-cheie: imprimare cu jet de cerneală, pretratare, țesături din bumbac, coloranți reactivi

Investigation of the usage of different thickening agents in ink-jet printing with reactive dyes

In general sodium alginate is used as a thickener in the pretreatment paste in ink-jet printing with reactive dyes. The aim of this study is to investigate the use of different types of thickeners as a replacement for sodium alginate in the pretreatment paste in digital ink-jet printing of cotton fabrics and the possibilities of achieving higher color yields, better sharpness properties, better fastness properties, and more ecological processes (with the decrease of urea requirements). For this purpose experiments with three types of thickener (sodium alginate, sodium carboxymethyl cellulose and polyacrylic acid derivate) were carried out. The results showed that sodium carboxymethyl cellulose can be used properly in the pretreatment paste for reactive ink-jet printing.

Key-words: ink-jet printing, pretreatment, cotton fabrics, reactive dyes

In inkjet printing, reactive inks are one of the most popular inks due to its excellent water solubility, relatively low price, high wash and crock fastnesses, and beautiful brightness [1].

The production process of ink-jet printing for cotton fabric with reactive dyes is different from that of the conventional printing process [2, 3]. In conventional textile printing of cotton fabric, reactive dye is applied along with alkali and all necessary chemicals in the form of a print paste. The print is then heat treated or steamed to fix the dye on the cotton, and finally washed to remove any unreacted dye, chemicals, and thickener. However for ink-jet printing, none of the conventional printing chemicals such as alkali, urea and thickener can be directly incorporated into the ink formulation [2, 4–6], because inclusion of auxiliary chemicals and thickeners into the low viscosity ink has proved troublesome [7]. As a result, the cotton fabric should be pretreated with those printing chemicals used in the conventional textile printing. The chemicals necessary for fixing reactive dye should be padded onto the cotton fabric prior to the ink-jet printing stage [8].

The main constituents of the pretreatment paste are usually thickener, alkali and urea. Thickeners are employed in printing to preserve the sharpness of edges and outlines by countering the natural wicking effect of the substrate. In addition they hold moisture to enable dyes and chemicals to dissolve and enter the fibers during the steaming stage after printing and drying. They also modify the flow properties (rheology) of the ink or print paste [7].

Alkali is used in the printing process for the reactive dye color development of all shades. Reactive dyes react with cellulose under alkaline conditions to form covalent bonds between fiber and dye. Sodium bicarbonate is generally recommended because it is cheap, causes least hydrolysis of the dye on storage and gives sufficient pretreatment print paste stability with most of the reactive dyes available in the markets [7, 9–11]. During steaming, sodium bicarbonate loses carbon dioxide and increases the ionization of cellulose which thus promotes the dye-fiber interaction in the fixation stage [9].

Urea is one of the most important content in the pretreatment paste because during the steaming process, it is mainly used to swell the cotton fibers so that the dye can penetrate into them rapidly [12,13]. Therefore, urea acts as a solvent for the reactive dye and also it performs as a moisture-absorbing agent in the pretreatment print paste to increase the moisture regain during the steaming process [11–13]. Thus,

urea accelerates the migration of dye from the thickener film into the cotton fiber and the urea also reduces the yellowing of cotton under hot, dry alkaline conditions [9]. However, the use of urea poses ecological problems associated with the high nitrogen content of the printing effluent. Therefore, printers are being forced to reduce or eliminate urea from the printing paste formulation [14].
Another commonly incorporated constituent of the pad liquor is sodium meta nitrobenzene sulphonate (Ludigol®, BASF), a mild oxidizing agent, which is included to avoid the risk of reduction, and hence decolourisation, of the dye during steaming [7].
In the last decade, a large number of studies have been carried out on the pretreatments for ink-jet printing with reactive inks [3, 8, 9, 15–17]. However, most of these studies have made use of sodium alginate thickeners, and very few studies have been carried out with different types of thickeners.
In the literature on ink-jet printing there is a lack of studies on the subject of developing cost effective and low urea consuming pretreatment recipes. Thus, the aim of this study is to investigate the use of different types of thickeners as a replacement for sodium alginate in the pretreatment print paste for digital ink-jet printing for cotton fabric and the possibilities of achieving higher color yields, better sharpness properties, better fastness properties, and more ecological processes with the less urea consumption.

EXPERIMENTAL PART

Desized, scoured, and bleached woven cotton fabric was used in the study. The pretreatment pastes were prepared with thickener, sodium bicarbonate, urea, Ludigol® and water. Three types of thickeners, which are commercially available in the market, were chosen to use in this study. These are sodium carboxymethyl cellulose, sodium alginate and polyacrylic acid derivate thickeners.
The amounts of thickener in the pretreatment pastes were changed related to the thickener type, and were recommended by the suppliers. These amounts are given in table 1.
To determine the optimum amount of sodium bicarbonate for the experiments on the investigation of the effect of thickener types and the amount of urea on the printing properties, which is the main subject of this study, a group of pre experiments were carried out.

Table 1

THE AMOUNTS OF THICKENER IN THE PRETREATMENT PASTES

Thickener type	Amount of thickener, g/kg
Sodium alginate (4% solution)	300
Sodium carboxymethyl cellulose (10% solution)	300
Polyacrylic acid derivative	150

In these pre experiments, the amount of urea in the pretreatment paste was constant at 100 g/kg, and the amount of sodium bicarbonate varied as 10–20–30–40 g/kg. The amount of sodium bicarbonate, which gave the best color yield was determined and used in the main experiments.
The amount of urea in the pretreatment pastes varied from 0 g/kg to 125 g/kg. Additionally, each pretreatment paste contains 10 g/kg Ludigol®, and rest amount of water. The total weight of each paste was 250 g.
Well-mixed pre-treatment pastes were padded onto the cotton fabrics with a pick-up ratio of 80% and a padding speed of 3 rpm. Immediately afterwards, the fabrics were dried for 2 minutes at 100°C.
A pattern was designed in order to evaluate the color yield and the sharpness properties, and printed onto the pre-treated fabrics with red, blue, yellow, black and cyan reactive inks (provided by Aleph S.r.l., Italy), at 360 x 360 dpi, using Mimaki Tx3-1600 (Mimaki Engineering Co., Ltd.) ink-jet printer with a piezoelectric drop on demand print head.
After the patterns dried, the printed fabrics were steamed for 10 minutes at 102°C with a laboratory-type steamer (Mathis) for the fixation of dyes. Finally the fabrics were washed off to remove unfixed dyes and residual materials on the surface.
Color yield of the printed fabrics expressed as K/S values, were measured with Hunter Lab ColorQuest II spectrophotometer. Four measurements were carried out from the front and reverse sides of the fabrics and the average values were evaluated.
In order to compare the sharpness of the prints, the width of the printed lines, which have 1 mm width in the pattern, in both warp and weft directions were measured using a stereomicroscope (Leica S8APO) with a magnification of 100.
The colour fastness to washing of the printed fabrics was assessed ISO 105-C06 and colour fastness to crocking by the ISO 105-X12.

RESULTS AND DISCUSSIONS

Determining the optimum amount of sodium bicarbonate

For each type of thickener, the maximum *K/S* values obtained with different colors were considered as 100%, and thus the percentage changes in *K/S* values of other fabrics, pretreated with the same thickener type, were evaluated. The percentage changes in *K/S* values are given in figure 1.
As it is seen from the figure 1, the amount of sodium bicarbonate does not have significant effect on the color yield. In general, best color yield values were obtained with 20 g/kg sodium bicarbonate, with the exception that when polyacrylic acid derivate thickener is used, the optimum amount for red color is 10 g/kg, and for cyan and blue is 40 g/kg. Consequently, the amount of sodium bicarbonate that would use in the main experiments was determined as 20 g/kg.

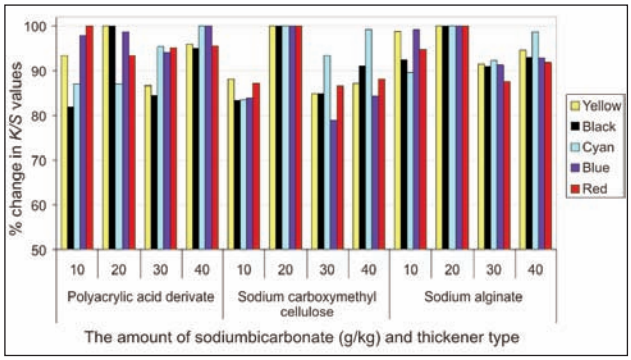

Fig. 1. % change in *K/S* values related to the amount of sodium bicarbonate

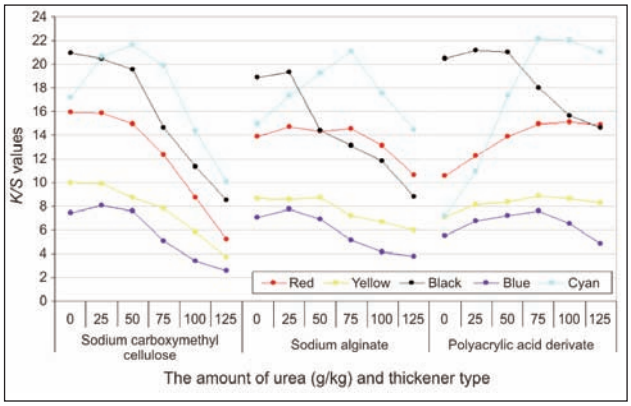

Fig. 2. *K/S* values on the front side of the fabrics

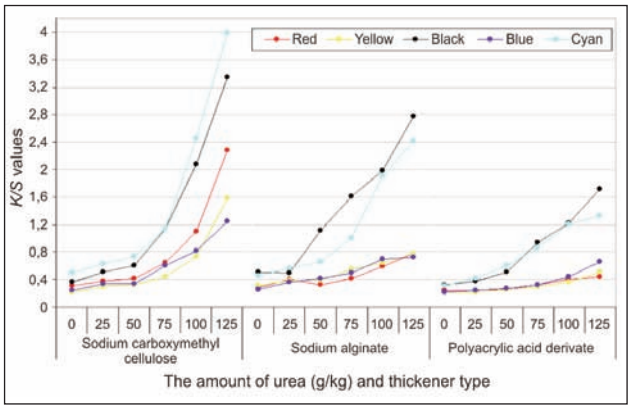

Fig. 3. *K/S* values on the reverse side of the fabrics

The effect of thickener type and the amount of urea on the color yield

K/S values on both front and reverse sides of the fabrics, pretreated with different types of thickeners and different amounts of urea, are given in figure 2 and figure 3.

As it is seen clearly from the figures 2 and 3, the amount of urea in the pretreatment paste is the main factor, effecting the color yield of the ink-jet printed fabrics. The *K/S* values are affected by the changes in the amount of urea significantly.

When sodium carboxymethyl cellulose is used as a thickener, the amount of urea required for the highest *K/S* values is 0–50 g/kg for the color blue, 0–25 g/kg for the colors red, yellow and black, and 50 g/kg for the color cyan. When sodium alginate is used as a thickener, the amount of urea required for the highest *K/S* values is 0–50 g/kg for the colors blue and yellow, 0–75 g/kg for the color red, 0–25 g/kg for the color black, and 75 g/kg for the color cyan. When polyacrylic acid derivate is used as a thickener, the amount of urea required for the highest *K/S* values is 50–75 g/kg for the color blue, 25–125 g/kg for the color yellow, 75–125 g/kg for the color red, 25–50 g/kg for the color black, and 75–100 g/kg for the color cyan. In the case of using urea with upper and lower amounts of these values, the color yield decreases significantly.

For all types of thickener, the color cyan requires more urea for obtaining the highest color yield values, in proportion to the amounts used for the other colors.

In general, when the amount of urea used in the pretreatment paste increases, dye penetration on the reverse side of the fabrics increases correspondingly. This increase is more significant with the thickeners sodium carboxymethyl cellulose and sodium alginate. Although, the penetration on the reverse side of the fabrics can be considered as a reason for the decrease in the color yield on the front side of the fabrics, with the increase in the urea amount, another important reason for this decrease is the moisture absorbing property of urea.

Such a large amount of urea may enhance moisture absorption and also cause hydrolysis of the reactive dye during steaming.

In the view of these results, the amount of urea recommended with the usage of sodium carboxymethyl cellulose is 0 g/kg, meaning that urea-free, when there is no cyan color in the printing pattern, and 25 g/kg for a pattern consists of all colors, including cyan.

Similarly, with the usage of sodium alginate, the amount of urea recommended for a pattern without cyan is 0–25 g/kg, while it is 50–75 g/kg for a pattern including cyan. With the usage of polyacrylic acid derivate, the amount of urea required is more than that required with the usage of other thickener types, and is recommended as 50–75 g/kg in general.

The effect of thickener type and the amount of urea on the sharpness properties

In order to compare the sharpness properties, the width of the printed lines (original width is 1 mm in the pattern) of the fabrics, pretreated with different thickener types and different amounts of urea, was measured on both warp and weft directions, and the results are given in figure 4 and figure 5.

It can be seen clearly from figure 4 and 5 that the sharpness properties of the prints are affected by the amount of urea in the pretreatment paste significantly. For all thickener types, when the amount of urea increases, the bleeding effect in both warp and weft directions and the widths of lines increase correspondingly, and the sharpness of the prints decreases. Furthermore, for the colors red, yellow and blue, the

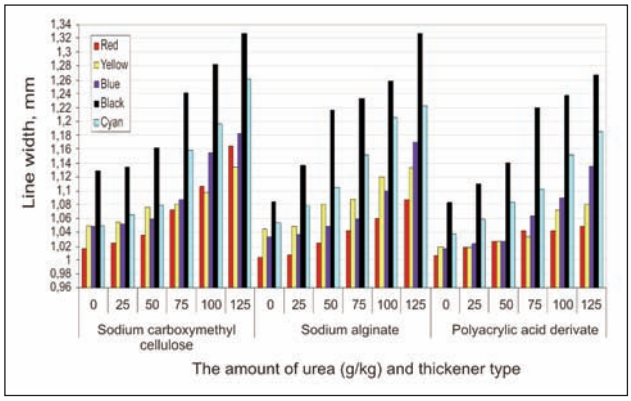

Fig. 4. The width of lines in the warp direction

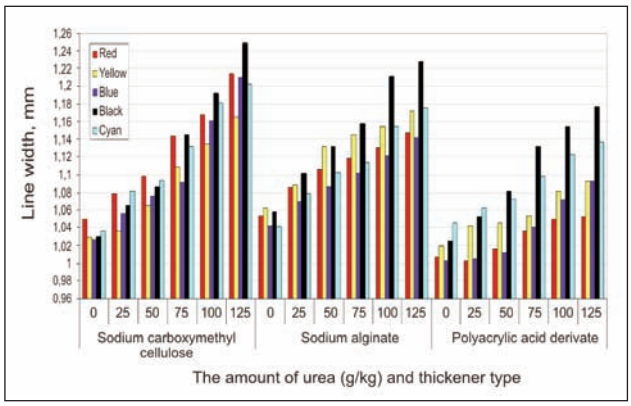

Fig. 5. The width of lines in the weft direction

sharpness properties are much better than cyan and black.

Figure 6 also shows the decrease in the sharpness of the prints visually. The change in the sharpness and the bleeding occurred with the color black when the amount of urea in the pretreatment paste is 0 and 125 g/kg can be seen clearly. This kind of worsening also occurs with other colors depending on the increase of urea amount.

For all types of thickeners and all colors, the best sharpness properties were obtained with the fabrics, pretreated without urea, and the sharpness drops rapidly, with the increase of urea amount. This drop is more significant in the printed fabrics, pretreated with the usage of sodium carboxymethyl cellulose and sodium alginate. On the other hand, the bleeding effect is less, and the sharpness is better in the printed fabrics, pretreated with polyacrylic acid derivate than those pretreated with other thickeners.

The effect of thickener type and the amount of urea on the color fastness properties

Instead of testing all fabrics, the printed fabrics with sufficient *K/S* values were chosen, and color fastness to washing and crocking was tested. The color fastness results of the printed fabrics are given in table 2.

In general the wash and dry crock fastness of all printed fabrics are quite good. However, there are some minor drops (0.5 points) in the dry crock fastness values for the colors cyan and black, when the amount of urea in the pretreatment paste is little or 0 g/kg.

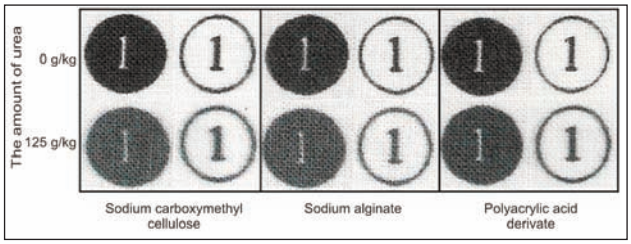

Fig. 6. The change in the sharpness of the prints depending on the amount of urea

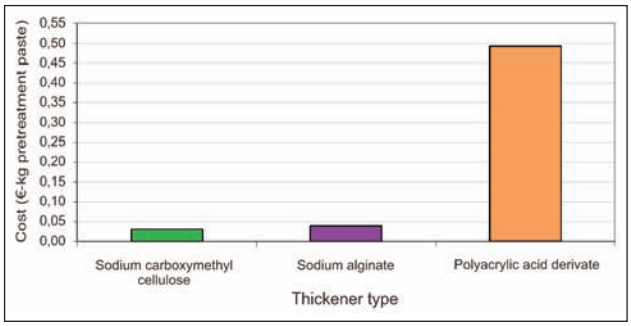

Fig. 7. The cost of thickener required for 1 kg pretreatment paste

Wet crock fastness values for the blue prints are 4 when polyacrylic acid derivate is used, and 4–4,5 when sodium carboxymethyl cellulose and sodium alginate are used as a thickener. For the red prints the values are 4 for all thickener types. For the yellow prints, the values are 3–3,5 when sodium carboxymethyl cellulose is used, 3,5–4,5 when polyacrylic acid derivate is used, and 4–4,5 when sodium alginate is used. For the black prints, the values are 2,5–3 when sodium carboxymethyl cellulose is used, 3–4 when polyacrylic acid derivate is used, and 3,5–4 when sodium alginate is used. The values for cyan prints are lower than those for the other colors, and 2,5 when sodium carboxymethyl cellulose is used, and 3 when sodium alginate and polyacrylic acid derivate are used.

In general, the lower crock fastness values are measured when the amount of urea in the pretreatment paste is little or 0 g/kg. As well as, the reason of obtaining better fastness values with higher amounts of urea is the decrease in the color yield values, but the main reason is that urea enhances the penetration and the fixation of dye molecules into the fibers.

It can be said that there is no effect of thickener type and the amount of urea on the wash and dry crock fastness properties. However, when carboxymethyl cellulose is used lower wet crock fastness values are obtained than those obtained with other thickeners. This difference is 0.5 or 1.0 points.

Evaluation of the thickener costs

In order to compare these thickener types in terms of their costs, the costs of thickener amounts required for 1 kg pretreatment paste were calculated.

As it is seen in figure 7, the cost of polyacrylic acid derivate thickener is approximately 12 times more

Table 2

THE FASTNESS VALUES OF THE PRINTED FABRICS

Ink	Thickener type	Amount of urea, g/kg	Wash fastness		Crock fastness	
			Colour change	*Staining of cotton*	*Dry*	*Wet*
Cyan	Carboxymethyl cellulose	0	5	5	5	2 – 3
		25	5	5	5	2 – 3
		50	5	5	5	2 – 3
	Sodium alginate	0	5	5	4 – 5	3
		25	5	5	4 – 5	3
		50	4 – 5	5	5	3
		75	4 – 5	5	5	3
	Poliacrylic acid derivate	25	5	5	4 – 5	3
		50	5	5	4 – 5	3
		75	5	5	5	3
Blue	Carboxymethyl cellulose	0	5	5	5	4
		25	5	5	5	4
		50	5	5	5	4 – 5
	Sodium alginate	0	5	5	5	4
		25	5	5	5	4
		50	5	5	5	4 – 5
		75	5	5	5	4 – 5
	Poliacrylic acid derivate	25	5	5	5	4
		50	5	5	5	4
		75	5	5	5	4
Red	Carboxymethyl cellulose	0	4 – 5	5	5	4
		25	5	5	5	4
		50	4 – 5	5	5	4
	Sodium alginate	0	4 – 5	5	5	4
		25	4 – 5	5	5	4
		50	4 – 5	5	5	4
		75	5	5	5	4
	Poliacrylic acid derivate	25	4 – 5	5	5	4
		50	5	5	5	4
		75	4 – 5	5	5	4
Yellow	Carboxymethyl cellulose	0	5	5	5	3
		25	5	5	5	3
		50	5	5	5	3 – 4
	Sodium alginate	0	5	5	5	4
		25	5	5	5	4
		50	5	5	5	4
		75	5	5	5	4 – 5
	Poliacrylic acid derivate	25	5	5	5	3 – 4
		50	5	5	5	4
		75	5	5	5	4 – 5
Black	Carboxymethyl cellulose	0	5	5	5	2 – 3
		25	5	5	5	3
		50	5	5	5	3
	Sodium alginate	0	5	5	5	3 – 4
		25	5	5	5	3 – 4
		50	4 – 5	5	5	4
		75	5	5	5	4
	Poliacrylic acid derivate	25	5	5	4 – 5	3
		50	5	5	5	3 – 4
		75	4 – 5	5	5	4

than the cost of sodium alginate, and 16 times more than the cost of sodium carboxymethyl cellulose. Therefore, the use of sodium alginate, but especially carboxymethyl cellulose thickeners is recommended, due to their low costs.

CONCLUSIONS

In this study, as well as the use of sodium alginate, carboxymethyl cellulose and polyacrylic acid derivate in the pretreatment print paste for digital ink-jet printing for cotton fabric were investigated.

The results showed that to provide prints with high color yield and good sharpness properties, the type of thickener and the amount of urea should be both taken into consideration. The amount of urea required for the best print properties varies according to the thickener types and also the colors. For all types of thickener, the color cyan requires more urea for obtaining the highest color yield values, in proportion to the amounts used for the other colors.

The sharpness of the prints decreases and the bleeding effect in both warp and weft directions

increases with the higher amounts of urea for all thickener types and colors. It is recommended to keep the amount of urea below 50 g/kg when sodium carboxymethyl cellulose and sodium alginate are used, and below 75 g/kg when polyacrylic acid derivate is used.

The wash and dry crock fastness of the printed fabrics are good enough for all thickener types and all amounts of urea. However, when carboxymethyl cellulose is used lower wet crock fastness values are obtained than those obtained with other thickeners. This difference is 0.5 or 1.0 points, and can be enhance with the use of higher amounts of urea.

To provide the prints with high color yield, and good sharpness and fastness properties, 25 g/kg urea is recommended for sodium carboxymethyl cellulose, 25–50 g/kg for sodium alginate, and 50–75 g/kg urea for polyacrylic acid derivate.

Moreover, the handle properties of the fabrics were evaluated subjectively and hence it can be said that the thickener type didn't have a significant effect on the handle of the fabrics as long as the washing proses carried out efficiently after the printing process.

In conclusion, the use of sodium carboxymethyl cellulose will be the right choice of the thickener type by considering both the printing properties and the costs. Furthermore, it requires less amount of urea, hence provides a more ecological process. Thus, it can be a good alternative to sodium alginate.

BIBLIOGRAPHY

[1] Yang, Y., Naarani, V. *Improvement of the lightfastness of reactive inkjet printed cotton*. In: Dyes and Pigments, 2007, vol. 74, issue 1, p. 154

[2] Aston, S. O., Provost, J. R., Masselink, H. *Jet printing with reactive dyes*. In: J.S.D.C., 1993, vol. 109, p. 147

[3] Fan, Q., Kim, Y. K., Lewis, A. F., Peruzzi, M. K. *Effects of pre-treatments on print qualities of digital textile printing.* In: Book of Papers, IS & Ts NIP18:2002 International Conference Digital Printing Technology, San Diego, USA, 2002, p. 236

[4] Schulz, G. *Textile chemistry of digital printing*. In: Melliand Textilberichte. International Textile Reports, 2002, vol. 83, p. E 30

[5] Siemensmeyer, K., Siegel, B., Ervine, S., Bullock, J. *Solutions for digital textile printing*. In: Book of Papers, IS & Ts NIP 15:1999. International Conference Digital Printing Technology, Orlando, USA, 1999, p. 280

[6] Zhou, X., Li, Y. *Inkjet printing: the easy way to produce textile sample.* In: Internationale Textile Bulletin, 2002, vol. 48, issue 3, p. 64

[7] Hawkyard, C. *Substrate preparation for ink-jet printing*. Digital Printing of Textiles, Ujiie, H., Cambridge: Woodhead Publishing, 2006, p. 201

[8] Yuen, C. W. M., Ku, S. K. A., Choi, P. S., Kan, C. W. *The Effect of the pretreatment print paste contents on colour yield of an ınk-jet printed cotton fabric*. In: Fibers and Polymers, 2004, vol. 5, issue 2, p. 117

[9] Choi, P. S. R., Yuen, C. W. M., Ku, S. K. A., Kan, C. W. *Digital ınk-jet printing for chitosan-treated cotton fabric*. In: Fibers and Polymers, 2005, vol. 6, issue 3, p. 229

[10] Bandyopadbyay, B. N., Sheth, G. N., Moni, M. M. In: International Dyer, 1998, vol. 11, p. 39

[11] Gutjahr, H., Koch, R. R. *Direct print coloration*. Textile Printing, 2nd Edn., Ed. Miles, L.W.C., Bradford: SDC, 1994, p. 139

[12] Achwal, W. B. *Textile chemical principle of digital textile printing*. In: Colourage, 2002, vol. 49, issue 12, p. 33

[13] Chen, W., Wang, G., Bai, Y. *Best for wool fabricprinting – digital inkjet*. In:Textile Asia, 2002, vol. 33, issue 12, p. 37

[14] Ahmed, N. S. E., Youssef, Y. A., El-Shishtawy, R. M., Mousa, A. A. *Urea/alkali-free printing of cotton with reactive dyes*. In: Coloration Technology, 2006, vol. 122, issue 6, p. 324

[15] Yuen, C. W. M., Ku, S. K. A., Choi, P. S. R., Kan, C. W. *Factors affecting the color yield of an ink-jet printed cotton fabric.* In: Textile Research Journal, 2005, vol. 75, issue 4, p. 319

[16] Yuen, C. W. M., Ku, S. K. A., Kan, C. W., Choi, P. S. R. *Enhancing textile ink-jet printing with chitosan*. In: Coloration Technology, 2007, vol. 123, issue 4, p. 267

[17] Yuen, C. W. M., Ku, S. K. A., Kan, C. W., Choi, P. S. R. *A two-bath method for digital ink-jet printing of cotton fabric with chitosan.* In: Fibers and Polymers, 2007, vol. 8, issue 6, p. 625

Authors:

Dr. BURÇİN ESER
Assoc. prof. dr. ARİF TANER ÖZGÜNEY
Department of Textile Engineering
Ege University
35100 Izmir, Turkey
e-mail: arif.taner.ozguney@ege.edu.tr

Assoc. prof. dr. ARZU YAVAŞ
Department of Textile Engineering
Pamukkale University
20100 Denizli, Turkey

Identification of the most significant factors influencing thermal comfort using principal component analysis and selection of the fabric according to the apparel end-use

ELENA ONOFREI

REZUMAT – ABSTRACT

Identificarea principalilor factori care influențează confortul termic, folosind analiza componentelor principale şi selecția materialului textil în funcție de destinația finală a îmbrăcămintei

Pentru analizarea proprietăților de confort termofiziologic al structurilor tricotate, în acest studiu s-a utilizat analiza componentelor principale. În urma analizei, au fost extrase patru componente principale, şi anume: încetinirea uscării, izolația termică intrinsecă a materialului, porozitatea materialului şi absorbția apei. Componentele extrase explică 90% din varianța totală a celor treisprezece variabile originale, astfel încât se poate reduce, în mod considerabil, complexitatea datelor inițiale, prin utilizarea acestor componente, cu o pierdere de doar 10% din informații. Această reducere poate fi folosită, ulterior, pentru modelarea proprietăților de confort termofiziologic al materialului textil şi pentru selectarea celor mai adecvate materiale pentru diferite domenii de aplicație.

Cuvinte-cheie: tricotaje, proprietăți, confort termofiziologic, analiza componentelor principale

Identification of the most significant factors influencing thermal comfort using principal component analysis and selection of the fabric according to the apparel end-use

In this study principal component analysis was used to analyse knitted fabrics in terms of thermo-physiological comfort properties. Four principal component factors were extracted from the analysis: Slowness of drying, Intrinsic fabric thermal insulation, Fabric porosity and Fabric wicking. The extracted components explain 90% of the variability in the original thirteen variables, so we can considerably reduce the complexity of the data set by using these components, with only about 10% loss of information. This reduction can be used thereafter for the modeling of fabric thermo-physiological comfort properties and for the selection of the most adequate fabric for particular applications.

Key-words: fabrics, properties, thermo-physiological comfort, principal component analysis

The clothing comfort can be divided into three different main aspects: thermo-physiological comfort, tactile comfort and ergonomic comfort. During normal wear, i.e., under steady-state conditions, comfort is mostly related to tactile and ergonomic sensations. Under transient wear conditions, caused by physical activity or weather conditions, comfort is mainly related to the thermo-physiological wear comfort that is determined by the movements of heat, moisture and air through a fabric [1, 2].

Functional yarns with a thermo-regulating effect improve thermal and moisture performance of fabrics. In this study, elastic knitted fabrics incorporating yarns with different thermo-regulating effect were analysed in terms of their thermo-physiological comfort properties. Two functional yarns were used: a 30% viscose (Outlast®)/70% cotton yarn, 14.7 tex and a 100% polyester (Dacron) Coolmax® yarn, 14.3 tex. These yarns were selected due to the different approach of achieving the thermo-regulating effect: the first one provided by the incorporation of thermally active materials (paraffinic PCM microcapsules) within the viscose fibre structure [3] and the second one promoted by the fiber design (multi-channelled cross section) [4].

Nine knitted structures plated with elastane (Creora®) 44 dtex were produced combining plain, tuck and float stitches, using an 8-feed single-jersey circular knitting seamless machine MERZ–MBS. Machine details were as follows: gauge – E 28, diameter – 13”, number of needles – 1 152, speed – 1.0 m/s. The yarn input tension for elastane was 4 cN and for the ground yarns 2 cN. The machine setting for the loop length was the same for all fabrics. From these fabrics the best candidates for sportswear applications will be selected.

The principal components method was used to reduce the number of variables in the data set and to identify the most significant factors influencing thermal comfort.

EVALUATED PROPERTIES AND EQUIPMENT USED

- **Fabric mass per unit area** – was determined according to ISO 3801:1977 standard using an electronic balance KERN-770.
- **The thickness of the fabrics** – was determined by Alambeta instrument.
- **Air permeability** – is described as the rate of air flow passing perpendicularly through a known

area, under a prescribed air pressure differential between the two surfaces of a material. Tests were performed according to standard ISO 9237 using a Textest FX-3300 air permeability tester. The air pressure differential between the two surfaces of the material was 100 Pa.

- **Thermal properties** – were evaluated using the Alambeta instrument [5] and tests performed according to standard ISO EN 31092-1994. In all cases, the measuring head temperature was, approximately, 32°C and the contact pressure 200 Pa. Thermal comfort was characterized by three properties: thermal conductivity, thermal resistance and thermal absorptivity.
- **Diffusion capacity**. Expresses the rate of water diffusing in the fabric surface and represents fabric's instantaneous water (perspiration) absorbency and transferring ability. The fabric samples were placed flat on a hydrophobic board with the outer surface facing down. The diffusion area (mm^2) was measured 30 seconds after dripping 0.2 ml of water, using a precise dropper whose tip was 10 mm above the fabric surface. The measurement was repeated at five different points and the average of the diffusion area (mm^2) was taken to indicate the diffusion ability of the fabrics.
- **Vertical wicking.** The water transport rate is determined by a vertical strip wicking test in accordance with DIN 53924. One end of the strip (25 mm wide and 200 mm long) was clamped vertically with the dangling end immersed to about 3 cm in distilled water. A little amount of dye is added in the water, which can enhance the clear observation of the liquid. The height of water in wale-wase at 3 minutes was used to express the vertical wicking of the fabrics.
- **Horizontal wicking.** Expresses fabric's ability to move sweat away from the skin to the outer surface of the fabric, where it evaporates. The apparatus used to determine the transverse wicking consists of a horizontal glass plate fed from below with water through a capillary tube coming from a reservoir placed on an electronic balance. The sample was placed on the glass plate and was held in contact with it (and with water) applying another glass plate on top of it. The changing weight of the reservoir is measured by an electronic balance to determine the rate of liquid uptake by the textile material. Similar apparatus have been used by Buras, McConnell, among others [6].
- **The water vapour permeability –** was determined on SDL Shirley Water Vapour Permeability Tester M-261, according to standard BS 7209-1990. The cup method is a very common method for testing the moisture transfer ability of fabrics [7].
- **Drying capacity**. In this test, fabrics were cut into circular samples of 100 cm^2, placed on a horizontal surface and wetted with 1 ml of distilled water dropped onto it using a precise dropper whose tip was 10 mm above the fabric surface. The remaining water ratio (RWR) and the drying time of fabrics were assessed. In order to determine the drying rate (evaporating curve), the fabrics were weighted in the dry state (dry weight – W_f) and immediately after wetting (wet weight at the initial stage – W_0). The change in weight (W_i) was measured at 10-minute intervals and the remaining water ratio (%) was then calculated, for each interval, using the following equation (1):

$$RWR = (W_i - W_f) / (W_0 - W_f) \times 100\% \qquad (1)$$

The remaining water ratios were used to express the drying ability of the fabrics as wetted by sweat.

Principal components analysis (PCA)

The principal components method was used to reduce the number of variables in the data set and to identify the most significant fabric properties influencing thermal comfort. The central idea of principal component analysis is to reduce the dimensionality of a data set consisting of a large number of interrelated variables, while retaining as much as possible of the variation present in the data set. The principal components method of extraction begins by finding a linear combination of variables (a component) that accounts for as much variation in the original variables as possible. It then finds another component that accounts for as much of the remaining variation as possible and is uncorrelated with the previous component, continuing in this way until there are as many components as original variables. Usually, a few components will account for most of the variation, and these components can be used to replace the original variables [8, 9].

Explicitly, the principal component variables y_1, y_2, …, y_q are obtained from the original variables x_1, …, x_q as follows equation (2) [9]:

$$\begin{aligned} y_1 &= a_{11}x_1 + a_{12}x_2 + \ldots + a_{1q}x_q \\ y_2 &= a_{21}x_1 + a_{22}x_2 + \ldots + a_{2q}x_q \\ &\cdots\cdots\cdots\cdots \\ y_q &= a_{q1}x_1 + a_{q2}x_2 + \ldots + a_{qq}x_q \end{aligned} \qquad (2)$$

where:

the coefficients a_{ij} (i = 1, …, q, j = 1, …, q) are chosen so that the required maximal variance and uncorrelated conditions are respected.

A constraint is applied on these coefficients: the sum of squares of the coefficients is one so that the total variance of all the components is equal to the total variance of all the observed variables. It is often convenient to rescale the coefficients so that their sum of squares are equal to the variance of that component they define.

In the case of components derived from the correlation matrix of the data, these rescaled coefficients give the correlations between the components and the original variables. These values are often presented as the result of a principal components analysis.

Table 1

Structure	Symbol fibre brend	Mass per unit area, g/m^2	Thick-ness, mm	Thermal conduc-tivity, (x 10^{-3}), W/mK	Thermal resis-tance (x 10^{-3}), m^{2}K/W	Thermal absorp-tivity, W s$^{1/2}$/m^2 K	Air perme-ability, l/m^2/s	Index of water vapour trans-mission rate, %	Vertical wicking, mm	Hori-zontal wicking, ml	Diffusion capacity, mm^2	Drying capacity, (*RWR* after 180 min.)
Single jersey	C_{-1}	253.78	1.22	44.63	27.54	112.70	229.30	96.89	7.05	10.46	1299.69	0.00
	O_{-1}	253.2	1.08	54.04	20.26	142.10	258.90	100.14	5.85	9.95	1143.51	8.25
Double one-needle floats	C_{-2}	303.40	1.36	47.10	29.06	107.70	176.90	95.27	4.15	11.34	1234.60	0.21
	O_{-2}	288.26	1.22	55.42	22.04	141.70	221.10	98.46	5.80	9.29	1087.70	12.95
Locknit	C_{-3}	380.02	1.49	48.55	30.68	115.26	97.77	92.18	5.25	10.00	1210.60	6.30
	O_{-3}	370.07	1.41	55.76	25.33	145.16	110.40	95.89	5.85	8.67	852.10	20.83
Double locknit	C_{-4}	363.04	1.48	44.48	30.42	120.79	145.00	92.80	4.50	9.01	1290.00	5.40
	O_{-4}	355.73	1.38	56.53	24.46	146.50	149.80	97.22	5.25	6.24	961.32	20.82
Alternating three-needle floats	C_{-5}	308.43	1.89	47.25	42.56	100.28	168.80	93.93	6.05	15.77	1614.66	5.93
	O_{-5}	296.18	1.57	50.87	30.95	132.66	219.80	98.73	5.90	10.47	900.67	15.08
Two-needle floats (ribbed structure)	C_{-6}	334.5	1.78	48.07	37.81	104.03	221.30	98.20	7.45	14.06	1402.66	7.65
	O_{-6}	304.58	1.58	53.42	29.67	124.33	300.10	102.67	6.60	14.49	989.75	17.10
One-needle floats (ribbed structure)	C_{-7}	314.60	1.46	47.00	30.47	110.20	201.70	97.59	5.60	13.11	1193.80	4.30
	O_{-7}	308.94	1.30	55.04	23.71	142.50	257.30	100.99	6.80	14.12	954.00	16.92
Double piqué	C_{-8}	334.21	1.50	46.87	32.02	104.37	149.20	93.20	6.55	11.44	1217.30	0.49
	O_{-8}	330.3	1.40	65.65	23.98	130.20	158.80	98.10	6.30	5.94		20.75
Single piqué	C_{-9}	282.95	1.33	46.94	28.04	109.00	167.70	93.48	8.40	12.90	1321.30	1.81
	O_{-9}	278.09	1.25	53.17	23.56	137.30	181.20	99.01	6.45	8.04	1056.61	12.08

Note: C_{-1} ... C_{-9} represented symbol for Coolmax®/ Creora®; O_{-1} ... O_{-9} represented symbol for Coolmax®/ Creora®

In most practical applications of principal components, the analysis is based on the correlation matrix, i.e., on the standardized variables, since the original variables are likely to be on very different scales so that linear combinations of them will make little sense.

Principal component scores for an individual *i* with vector of variable values x_i^T can be obtained by simply applying the derived coefficients to the observed variables, generally after subtracting the mean of the variable, i.e., from the equation (3):

$$\begin{aligned} y_{i1} &= a_1^T(x_i - \bar{x}) \\ &\cdots\cdots\cdots\cdots \\ y_{iq} &= a_q^T(x_i - \bar{x}) \end{aligned} \qquad (3)$$

where:

$a_i^T = [a_{i1}, a_{i2}, ..., a_{iq}]$;

$\bar{x}$ is the mean vector of the observations.

Table 2

COMMUNALITIES		
Properties	**Initial**	**Extraction**
Thermal conductivity	1.000	0.922
Thermal resistance	1.000	0.966
Thermal absorptivity	1.000	0.809
Thickness	1.000	0.967
Air permeability	1.000	0.937
Vertical wicking	1.000	0.855
Diffuzion capacity	1.000	0.831
Mass per unit area	1.000	0.843
Horizontal wicking	1.000	0.825
Water vapour permeability	1.000	0.949
Drying ability	1.000	0.950
Fibres	1.000	0.946
Structure	1.000	0.874

Note: Extraction method: principal component analysis

RESULTS AND DISCUSSIONS

The measured characteristic and properties of the fabrics are shown in table 1. Using PCA, based on the correlation matrix, the initial thirteen variables were reduced to four components that explain 90% of the population variance. Extraction communalities are estimates of the variance in each variable accounted for by the components. The communalities (table 2) are all high, which indicates that the extracted components represent the variables well. The variance explained by the initial solution, extracted components, and rotated components ere displayed in table 3.

Eigenvalues greater than 1 have requested to be extracted, so the first four principal components form the extracted solution.

The extracted components explain 90% of the variability in the original thirteen variables, so we can

Table 3

TOTAL VARIANCE EXPLAINE									
Com-ponent	Initial eigenvalues			Extraction sums of squared loadings			Rotation sums of squared loadings		
	Total	*% of variance*	*Cumulative, %*	*Total*	*% of variance*	*Cumulative, %*	*Total*	*% of variance*	*Cumulative, %*
1	5.855	45.039	45.039	5.855	45.039	45.039	4.548	34.985	34.985
2	2.613	20.098	65.136	2.613	20.098	65.136	3.009	23.146	58.131
3	1.920	14.767	79.904	1.920	14.767	79.904	2.559	19.681	77.813
4	1.287	9.904	89.807	1.287	9.904	89.807	1.559	11.995	89.807
5	0.351	2.704	92.511	–	–	–	–	–	–
6	0.313	2.407	94.918	–	–	–	–	–	–
7	0.238	1.830	96.748	–	–	–	–	–	–
8	0.182	1.402	98.150	–	–	–	–	–	–
9	0.153	1.176	99.326	–	–	–	–	–	–
10	0.053	0.405	99.731	–	–	–	–	–	–
11	0.021	0.165	99.895	–	–	–	–	–	–
12	0.012	0.096	99.991	–	–	–	–	–	–
13	0.001	0.009	100.000	–	–	–	–	–	–

Note: Extraction method: principal component analysis

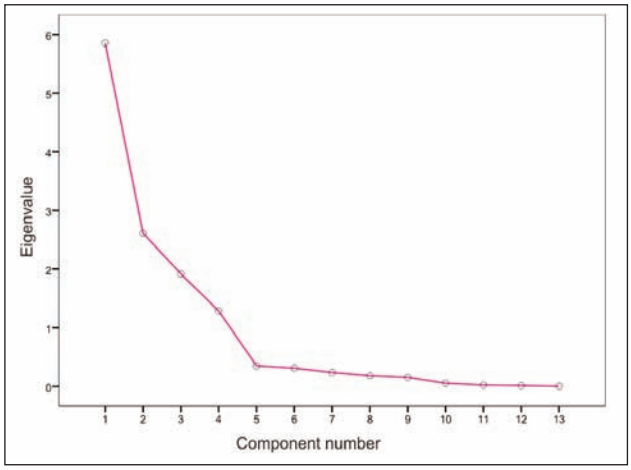

Fig. 1. The scree plote

Table 4

ROTATED COMPONENT MATRIX				
Properties	Component			
	1	*2*	*3*	*4*
Thermal conductivity	0.888	–0.362	0.005	–0.044
Thermal resistance	–0.444	0.869	–0.107	0.038
Thermal absorptivity	0.597	–0.663	0.109	–0.021
Thickness	–0.084	0.963	–0.162	0.076
Air permeability	0.191	–0.010	0.948	0.040
Vertical wicking	–0.192	–0.120	0.290	0.849
Diffuzion capacity	–0.858	0.304	0.038	–0.010
Mass per unit area	0.238	0.436	–0.768	–0.078
Horizontal wicking	–0.429	0.560	0.542	0.186
Water vapour permeability	0.606	–0.088	0.756	0.051
Drying ability	0.972	0.067	–0.022	0.000
Fibres	0.901	–0.273	0.240	–0.045
Structure	0.148	0.240	–0.109	0.885

Note: Extraction method: principal component analysis;
Rotation method: Varimax with Kaiser normalization

considerably reduce the complexity of the data set by using these components, with only about 10% loss of information.

The scree plot (fig. 1) also helped to determine the optimal number of components. Generally, the components on the steep slope must be extracted. The components on the shallow slope contribute little to the solution [8, 9]. Here, the last big drop occurs between the fourth and fifth components, so using the first four components is an easy choice. The results of the Varimax rotation are shown in table 4. To access the variables in each extracted component, the highest loading factor for each fabric characteristic or property is selected. The result is shown in bold type table 4.

The first component is most highly correlated with the remaining water ratio (r = 0.972), fibers (r = 0.901), thermal conductivity (r = –0.888), and negatively correlated with water diffusion capacity (r = –0.858).

Drying, in fact slowness of drying, is a better representative, however, because it is less correlated with the other three components. The first component accounts for 35% of the total variation and can be thermed “Slowness of drying”.

The second component is most highly correlated with the thermal resistance (r = 0.869), fabric thickness (r = 0.963), and thermal absorbtivity, i.e. the initial warm/cool feeling (r = –0.663). These properties represent the intrinsic insulation properties of the fabric. The second component accounts for about 23% of the total variation. It may be thermed “Intrinsec fabric thermal insulation”.

The third component is most highly correlated with air permeability (r = 0.948), index of water vapour transmission rate (r = 0.756) and fabric mass per unit area (r = –0.768). Since the third factor is negatively

related to fabric mass and positively related to the air and water vapor permeability it may be termed as "Fabric permeability". It accounts for about 19% of the total variation.

The fourth component is highly correlated with fabric structure (r = 0,885) and vertical wicking (r = 0.849). The overall effect of change in the fabric construction on fabric wicking is quite prominent which in turn have influence on comfort related properties of the fabric. Hence, fabric structure can be selected so that greater moisture wicking of fabric is achieved. This component can be thermed "Fabric wicking" and it accounts for 12% of the total variation.

From the results obtained it can be concluded that the thermal and moisture management performance of the studied fabrics are greatly affected by raw material properties and by fabric characteristics and structure. The fibres properties (especially fibres hygroscopicity) determine drying ability and fabric construction (thickness, porosity, structure) particularly have influences in what concern wicking ability, permeability and thermal properties.

The components are representative of all thirteen original variables, and the components are not linearly correlated with each other.

Table 5 shows the component score coefficients. For each case and each component, the component score is computed by multiplying the case's standardized variable values by the component's score coefficients. The resulting component score variables are representative of, and can be used in place of, the thirteen original variables with only a 10% loss of information.

A radar plot of the principal components extracted is shown in figure 2. The new variables are automatically scaled to unit standard deviation.

Now, we can easily select the fabric and design a product with appropriate thermo-physiological properties that is suitable for the use as sportswear for summer, and respectively, cold weather.

Table 5

COMPONENT SCORE COEFFICIENT MATRIX				
Properties	**Component**			
	1	***2***	***3***	***4***
Thermal conductivity	0,194	–0,014	–0,036	0,008
Thermal resistance	0,017	0,308	0,027	–0,043
Thermal absorptivity	0,060	–0,192	–0,014	0,037
Thickness	0,136	0,402	0,001	–0,017
Air permeability	0,038	0,100	0,396	–0,080
Vertical wicking	–0,073	–0,139	0,019	0,559
Diffuzion capacity	–0,196	0,002	0,055	–0,044
Mass per unit area	0,150	0,181	–0,287	–0,002
Horizontal wicking	–0,038	0,210	0,262	0,011
Water vapour permeability	0,147	0,116	0,300	–0,041
Drying ability	0,288	0,187	–0,019	0,003
Fibres	0,208	0,047	0,072	–0,028
Structure	0,089	0,043	–0,132	0,600

Note: Extraction method: principal component analysis;
Rotation method: Varimax with Kaiser normalization

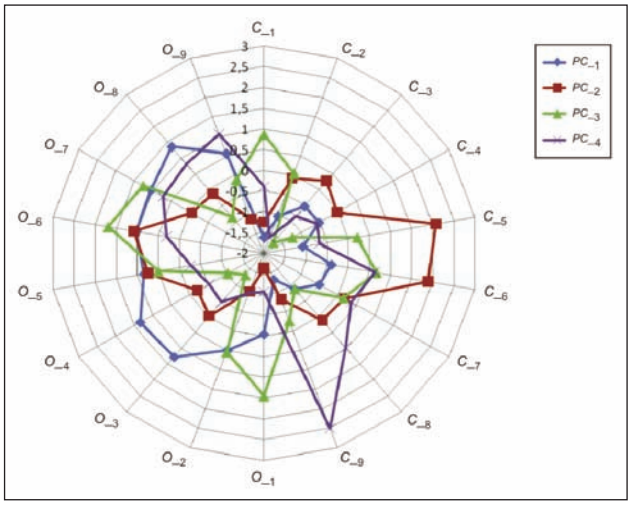

Fig. 2. Radar plot of the new variables:
*C*_1...*C*_9 – Coolmax/Creora knitted fabrics;
*O*_1...*O*_9 – Outlast/Creora knitted fabrics

Outlast® fabrics are considered preferred candidates for warmer climate sportswear, particularly due to their lower thermal resistance and higher air and water vapour permeability. However, as they demonstrated fair drying ability, fabrics can become wet and damped, creating discomfort to the user (heavy, sag, feel cold when activity ends). Therefore, different solutions must be proposed, according to the activity level. If the wearer performs mild activities, skin wetness is very low and thermal comfort is managed by skin temperature. In this case, fabrics permeability and thermal resistance are determining properties for thermal comfort. Fabrics must have high air permeability and low thermal resistance. Fabrics with structures *1* (single jersey), *2* (alternate double one-needle floats) and *7* (one-needle floats with ribbed surface) fulfil these requirements.

If the wearer performs more intense activities, skin temperature and wetness increase rapidly. Under these conditions, besides high air permeability and low thermal resistance, fabrics must provide higher water vapor transfer, high wicking ability, as well as fast drying. Fabric structure *1* (single jersey) seems the most adequate for higher intensity activities, where the user tends to sweat more.

As regards Coolmax® fabrics, the results pointed to a preferential use on sportswear applications for colder ambient conditions, particularly due to their high thermal resistance together with high drying ability. Fabrics with ribbed structure 6 (with 2-needle floats) and 5 (with 3-needle floats) have the higher thermal resistance and the better overall liquid moisture management capacity which makes them the best choice for cold weather sport activities.

Coolmax® fabric *1* (single jersey) has the lowest thermal resistance, good air and water vapour permeability and the best drying capacity. This fabric structure are the most apropriate for Coolmax® sportswear for worm climate conditions.

CONCLUSIONS

This paper presents a quantitative study of thermo-physiological comfort properties carried out on different knitted fabric structures containing Outlast® and Coolmax® yarns, and aiming at the selection the most adequate fabric for sportswear applications.

We have focused on the most significant properties influencing thermo-physiological comfort and have identified them, using principal component analysis.

Four principal component factors were extracted from the analysis: Slowness of drying, Intrinsic fabric thermal insulation, fabric permeability and fabric wicking. The extracted components explain 90% of the variability in the original thirteen variables, so we can considerably reduce the complexity of the data set by using these components, with only about 10% loss of information.

Through the use of an extensive database that correlates characteristics/properties of knitted fabrics, comfort can be predicted by analysing a limited number of properties.

The present study clearly showed that by an assessment of transport properties that are necessary to get the best comfort levels, it is possible to engineer a fabric, by appropriately selecting fiber and fabric constructional parameters, based on their established relationships with different comfort parameters.

Acknowledgements

This work was conducted under support of the FCT – Fundação para a Ciência e a Tecnologia and the 2C2T – O Centro de Ciência e Tecnologia Têxtil, Universidade do Minho, Portugal, within the framework of "Ciência 2008" Program.

BIBLIOGRAPHY

[1] Li, Y. *The Science of Clothing Comfort*. In: Textile Progress, 2001, vol. 31, issue 1/2, ISBN: 1870372247

[2] Fan, J., Tsang, H. W. K. *Effect of clothing thermal properties on the thermal comfort sensation during active sports*. In: Textile Research Journal, 2008, vol. 78, issue 2, p. 111; doi: 10.1177/0731684408080046

[3] Erkan, G. *Enhancing the thermal properties of textiles with phase change materials*. In: Research Journal of Textile and Apparel, 2004, vol. 8, issue 2, p. 57

[4] Li, D., Ni, M. *Moisture properties of Coolmax® fiber blended with regenerated cellulose fibers.* Second International Conference on Information and Computing Science, 2009, vol. 2, p. 129 http://doi.ieeecomputersociety.org/10.1109/ICIC.2009.141

[5] Hes, L. *Thermal properties of nonwovens*.Proceedings of Congress Index 87, Geneva, 1987

[6] Sarkar, M., Fan, J., Qian, X. *Transplanar water transport tester for fabrics*, Measurement Science And Technology, 2000, vol. 18, p. 1 465

[7] Scott, R. A. (ed.) *Textiles for protection.* The Textile Institute, Woodhead Publishing Limited, Cambridge England, 2005

[8] Jolliffe, I. T. *Principal component analysis*. Second Edition, ISBN: 0-387-95442-2, Springer New York, 2002

[9] Landau, S., Everitt, B. S. *A handbook of statistical analyses using SPSS*. ISBN 1-58488-369-3, Chapman & Hall/ CRC Press LLC , USA, 2004

Authors:

Dr. ing. ELENA ONOFREI

University of Minho, Centre for Textile Science and Technology

Campus de Azurém, 4800 - 058 Guimarães, Portugal

Universitatea Tehnică Gheorghe Asachi

Facultatea de Textile, Pielărie şi Management Industrial

Bd. D. Mangeron nr. 29, 700050 Iaşi

e-mail: eonofrei@yahoo.com

Mechanical tests carried out on composite materials specific to safety jackets

IONUȚ DULGHERIU CIPRIAN COZMANCIUC

REZUMAT – ABSTRACT

Testări mecanice ale materialelor compozite destinate vestelor de salvare

Lucrarea dezvoltă aspecte teoretice şi experimentale privind comportarea la diferite solicitări mecanice ale unui sistem de vestă de protecție compusă din mai multe straturi de spumă din polietilenă şi o anvelopă din poliester. Caracteristicile mecanice ale materialului sunt evaluate pe cale experimentală, în urma determinării comportării acestuia la diferite solicitări specifice destinației sale, şi anume absorbția energiei cinetice a unor corpuri/proiectile cu care vine în contact, pentru a proteja zonele de corp uman pe care le acoperă. În urma testărilor efectuate s-au identificat o serie de caracteristici mecanice, care recomandă utilizarea materialului pentru produse şi echipamente de protecție cu astfel de destinații. În acelaşi timp, este foarte important să se cunoască mărimea, dimensiunile, modul de aranjare a acestuia pe suprafața corpului. De asemenea, este necesar să se țină cont de faptul că forța de impact nu trebuie sa creeze o presiune mai mare de 50 gf/cm^2, deoarece această valoare a presiunii nu afectează fluxul sangvin.

Cuvinte-cheie: materiale compozite, spumă de polietilenă, anvelopă din poliester, testări mecanice, compresie, rezistență la tracțiune, energie de deformare

Mechanical tests carried out on composite materials specific to safety jackets

The article develops theoretical and experimental aspects regarding the behaviour of different mechanical loads for a system of protection jacket, composed of several layers of polyethylene foam and a polyester tire. The material's mechanical characteristics are experimentally evaluated from its behaviour, at different loads, specific to the product destination: the kinetic energy absorption of bodies/projectiles that comes into contact, protecting so, the areas of the human body, over which the jacket is placed. Following the tests carried out have identified a number of mechanical characteristics tested material recommended protective products and equipment such destinations, and at the same time is very important to know the size, dimensions, the arrangement on the body, and the fact that the force of impact should not create a pressure greater than 50 gf/cm^2 pressure value which does not affect blood flow task.

Key-words: composite materials, polyethylene foam, polyester tire, mechanical tests, compression, tensile testing, deformation energy

The research justification is given by the evolution and explosion of new raw material, microfibers, nano-fibres, textile surfaces with special features, high new chemical finishing treatments and new types of equipment for special destination and news in assessing the relationship between clothing and environment.

Along with top-level domains like aircraft, automobiles, and medicine, research and development of textile made some sensitive systems that can measure pressure changes of clothing on the human body, variations that can be amplified in different types of unwanted mechanical action. For the users of safety jackets, it is important to choose the level of protection that corresponds more to the potential threats. Choosing a level of protection higher than that required has a positive impact on the wearer's morale, and a negative influence in the price of the equipment and its greater mass, leading to reduced mobility and time to wear endurance [4, 5].

The threat caused by attacks with cutting or pointed objects is becoming increasingly important for people who work in security or storage formations and restoring public order. Legal restrictions on firearms possession in Europe led to greater spread of cold steel.

The characteristics of attacks with a sharp object depend on the type of the weapon and the way of using it (cutting, stabbing). Protection tiles included on the jackets provide total protection from any type of knife or sharp object (arrows). The only protected area of multilayer fabric protection package varies, depending on the shape of the object pointed and of the shot power [3].

Military jackets usually are not able to provide very good protection against attacks with cold steel when they are used for stabbing. On the attack by hitting with the edge of the weapon (e.g. by swords), the effect of protection is significant.

Present research develops theoretical and experimental aspects regarding protection system's behaviour on different mechanical loads for a jacket model, where the breastplate is made of a polyethylene foam, tougher (Z_1 – meaning "first area"), in a layer or two, and a polyester tire (Z_2 – the second area). As well known, the material's mechanical characteristics can only be assessed by experimental

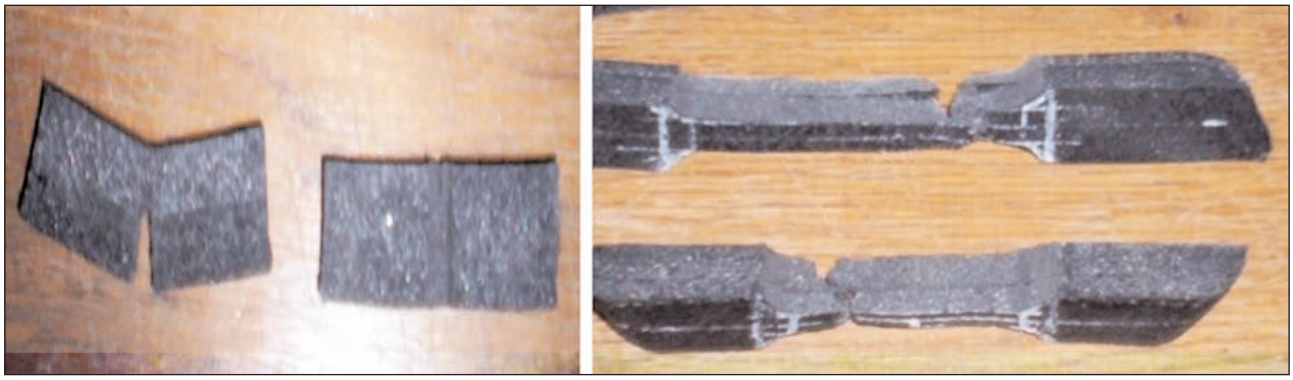

a ***b***

Fig. 1:
a – samples for bending by shock tests; ***b*** – samples broken while tensile testing

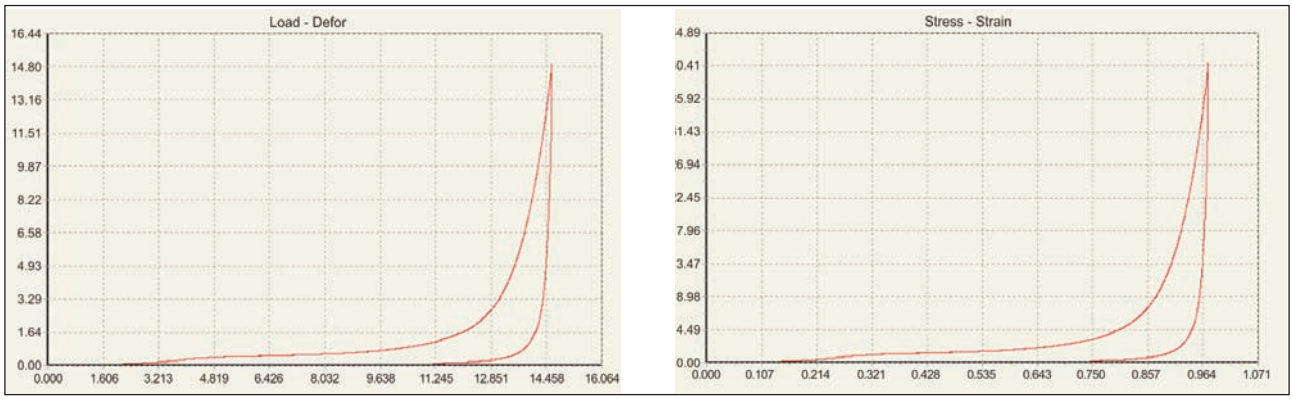

a ***b***

Fig. 2. Compression characteristics, build by the testing device's software:
a – the characteristic of compression-deformation force, in N-mm;
b – the characteristic of compression – specific deformation tension, σ–ε, in MPa – %

researches, following some tests where the material has certain behaviours (specific nature, structure or destination). The present material is designed to absorb the kinetic energy of bodies/projectiles that come into contact, to protect areas of human body, over which is placed [1].

BENDING BY SHOCK TESTING

Three samples were made with a U-shaped notch in order to be tested on bending at impact, using the Charpy Pendulum of 30 daJ. The samples (fig. 1) were cut with a cutter and the notch was made with a thin stone grinder (2 mm), rotated at high speed.

The first sample had the notch on both areas (Z_1 and Z_2). The real section of the sample in the notches plane was: S_0 = 8.1 x 14.8 mm^2 = 119.9 mm^2.

The hammer was raised on a height corresponding to a potential energy of 23 daJ and after launching it was found that the energy absorbed on bending by the shock was low: $W_{abs,1}$ = 0,3 daJ. The sample has not been completely broken.

For the second and third samples, a notch was made to cut that whole-tire layer (Z_2), about 6 mm thickness and the hammer was raised to a maximum height, corresponding to an initial 30 daJ energies. The samples sections in the right area of the notches were (fig. 1 *a, b*):

- on the second sample:
  S_{02} = 7,5 x 10 mm^2 = 75 mm^2, the absorbed energy being: $W_{abs,2}$ = 0,3 daJ;
- on the third sample:
  S_{03} = 7,8 x 16 mm^2 = 124,8 mm^2, the absorbed energy being: $W_{abs,3}$ = 0,5 daJ.

The specific absorbed energy (W_{abs}/S_0) was the same, 4 × 10^{-3} daJ/mm^2, for both samples, without to call this "resilience" as in case of metals. Energy absorbed is small for these samples and do not reflect the properties of fragility. These tests cannot be considered conclusive or characteristics for the material properties.

COMPRESSION TESTING

For compression, a first sample was used, cut as a parallelepiped, with 19.8 mm x 18.5 mm x 15 mm dimensions. Compression was done until the sample came from a thickness of 15 mm, to a thickness of 8.5 mm (specific deformation ε_{max} = (15 – 8,5)/15 = = 0,43 = 43%), the load being applied to the surface with 18.5 mm x 19,5 mm dimensions and with machine's speed at 2 mm/min.

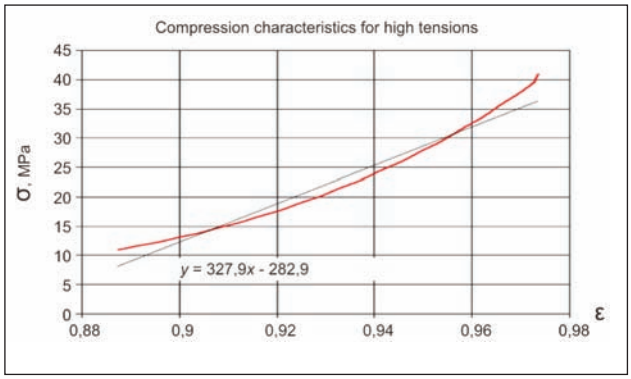

Fig. 3. The characteristic curve made for higher tensions area; elasticity module estimation for compression, in the normal tension interval $E_{comp} \in$[10 MPa, 40 MPa]: E_{comp} = 327.9 MPa

or ε = 96.9913%, and after ending this load, the material returned almost completely to the original thickness.

TESTING THE COMPOSITE TO COMPRESSION WITH A BALL

This attempt was made in order to obtain the phenomenon of loosen/breakage by crushing/ compression. The test is similar to the hardness test, except that in this case it didn't have the purpose of obtaining a fingerprint, only to study of the material's behaviour.

Deducting the calculus relationship of contact pressure

It is considered a ball (steel ball) under the action of *F* force in contact with an elastic plate. A law of

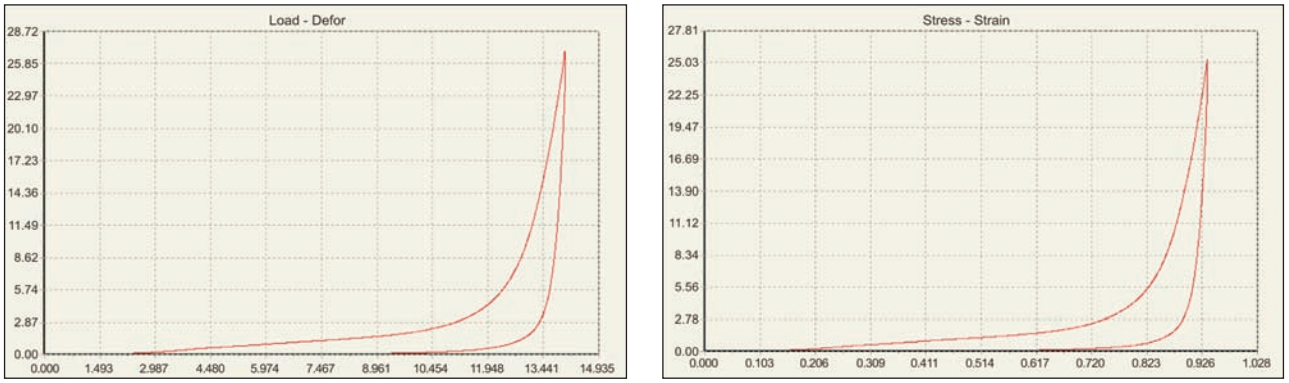

a ***b***

Fig. 4. Compression characteristics made on pad sample:
a – load-deformation; ***b*** – strain-specific deformation (percentage)

On the maximum tension area of σ – ε curve (fig. 3), between σ_1 = 30 MPa and σ_2 = 40 MPa, an elasticity modulus at compression E_{comp} = 584.3681519 MPa, was calculated (nearly double from the average amount of tension between [10 MP, 40 MPa] E_{mediu} = 328 MPa) (fig. 2).

It was noted that the compressed sample returned to the near-original size after a few minutes (after about 20 minutes). On surfaces that have been in contact with the test pan's device were printed the channels that pans have (provided in order to increase the stability of test materials) (fig. 3 and fig. 4).

EVALUATING THE SPECIFIC ENERGY OF DEFORMATION

Specific energy absorbed by the material during the parallelepiped sample load, calculated as the surface area under the σ – ε diagram (fig. 5), the result:

$$U_{1,compr} = \sum_i \frac{(\sigma_{i+1} + \sigma_i)\cdot(\varepsilon_{i+1} - \varepsilon_i)}{2} = \\ = 2.97298 \frac{\text{Nmm}}{\text{mm}^3} = 2.97298 \cdot 10^{-3} \frac{\text{J}}{\text{mm}^3} \quad (1)$$

It should be noted that the material was loaded to a specific deformation (at compression) ε = 0.969913

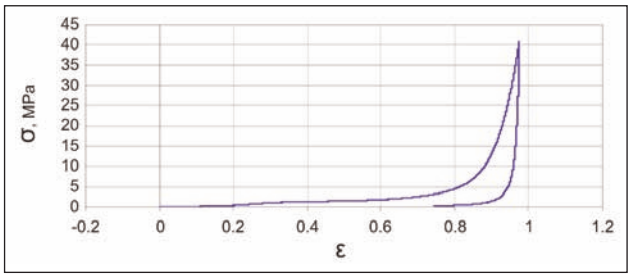

Fig. 5. Compression characteristic curve of the parallelepiped sample

variation of pressure contact, sinus type was adopted; this function has the following boundary conditions (fig. 6):

$$p(\beta) = p_{max} \sin(\alpha - \beta) \quad (2)$$

with boundary conditions:

$$p(0) = p_{max} \sin\alpha \\ p(\alpha) = 0 \quad (3)$$

Elementary force, *dF* is deducted as $p(\beta)$, the resultant pressure, applied on $dA = 2\pi r R d\beta$ (where $r = R\sin\beta$, elementary area, then projected on the vertical:

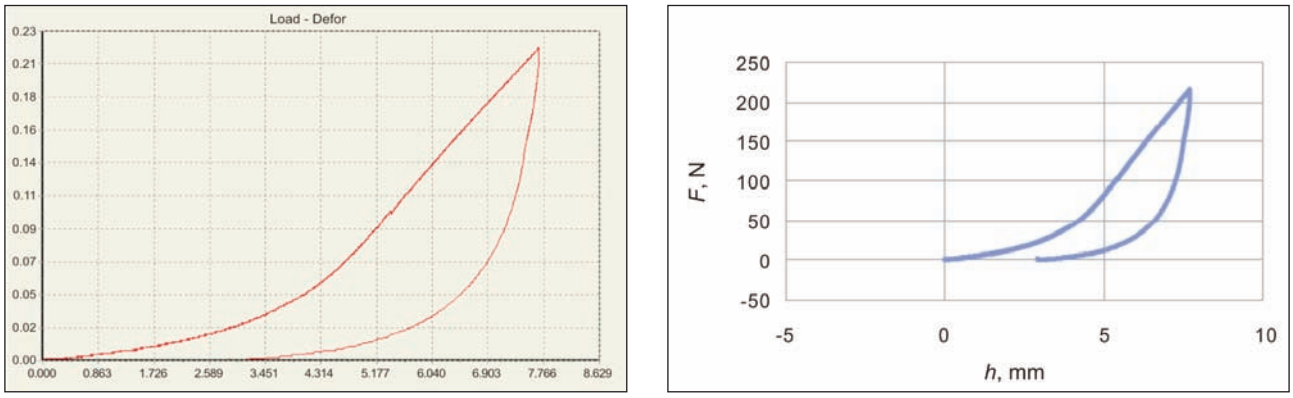

a **b**

Fig. 6. Ball compression, with the ball entering in a depth of 7,6 mm:
a – diagram obtained with the device's software; **b** – diagram obtain with the data stored by device's software

$$dF = (2\pi R \sin\beta \, R d\beta) \cdot [p_{max} \sin(\alpha - \beta)] \cdot \cos\beta \quad (4)$$

This expression is integrated and it is obtained the relationship between force, F, and maximum pressure, p_{max}:

$$F = \int_0^{\alpha} 2\pi R^2 p_{max} \sin\beta \cdot \cos\beta \cdot \sin(\alpha - \beta) d\beta = \\ = \pi R^2 p_{max} \int_0^{\alpha} [\cos(3\beta - \alpha) - \cos(\beta + \alpha)] d\beta \quad (5)$$

$$F = \frac{4}{3} \pi R^2 p_{max} \sin\alpha \cdot (1 - \cos\alpha) \quad (6)$$

After integrating, the result is:

$$\sin\alpha = \frac{d}{2R} = \frac{d}{D} \\ 1 - \cos\alpha = \frac{h}{R} \quad (7)$$

Where can be made some replacements, with the notes form figure 6*b*. Resulting:

$$F = \frac{2\pi}{3} p_{max} \cdot d \cdot h \quad (8)$$

It is noticed that, on the diagram from figure 5*b*, for larger forces of 50 N (and less than 217 N) material deformation is linear (ball's moving, h, varies between 4.1737 mm and 7.6837 mm). This linear deformation can be attributed to the area's properties of tougher consistency, z_1 (9):

$$\Delta P = k \cdot \Delta \quad (9)$$

If it is recorded:

- the proportionality constant on the linear area is calculated (line's inclination) (10):

$$k = \frac{\Delta F}{\Delta h} = \frac{1.67 \text{ N}}{3.51 \text{ mm}} = 47.578 \frac{\text{N}}{\text{mm}} \quad (10)$$

- the maximum pressure, $P_{max,}$ in N/m², for $d = D =$ 15,2 mm, obtaining by (11):

$$p_{max} = \frac{3}{2\pi} \cdot \frac{\Delta F}{\Delta h} \cdot \frac{1}{d} = \frac{3}{2\pi} \cdot 47.578 \cdot \frac{1}{15.2} = \\ = 1.494 \frac{\text{N}}{\text{mm}^2} \quad (11)$$

This pressure represents the normal maximum strain were the polyethylene foam, of tougher consistency, z_1, breaks (static). On experimental level, the ball was pressed till a displacement of the device's cross bar was measured, equal with half of the diameter of the ball: D = 15.2 mm.

From figure 6, it can be deduced that, on the linear area, a force of ΔF = 149.83 N and a variation of displacement Δh = 2.987 mm were recorded. Request compression with a ball to larger forces revealed nonlinearity of material behaviour (fig. 7). To interpret this behaviour it was sought a relationship between force F and maximum pressure that develops on the surface of contact between ball and composite.

Testing the composite to compression with a ball until perforation

Material's behaviour at large ball compressive forces are shown in figure 7. It should be noted that the force reaches an almost vertical rise between the pans when between the test device is just a ball of steel, the composite material being perforated and completely removed from the load compression. In figure 7*a* it is represented the $F - h$ diagram resulted from the sample that was tested at ball compression, when the ball has perforated a distance equal to its radius, and in figure 7*b* was tested at ball compression one unsolicited sample before.

The K factor, determined as a constant in the attempt where the penetrator displacement was made on a distance equal to the radius of the ball, becomes a variable.

To highlight the change from linear behaviour in figure 6, in figure 8 were constructed (superimposed on experimental diagrams) (12):

$$\Delta F = k \cdot \Delta h \quad (12)$$

where:

lines for k = 47 578 N/mm.

If it takes into consideration the K factor defined in (9), by combining with (7) relationship, it will be obtained (13):

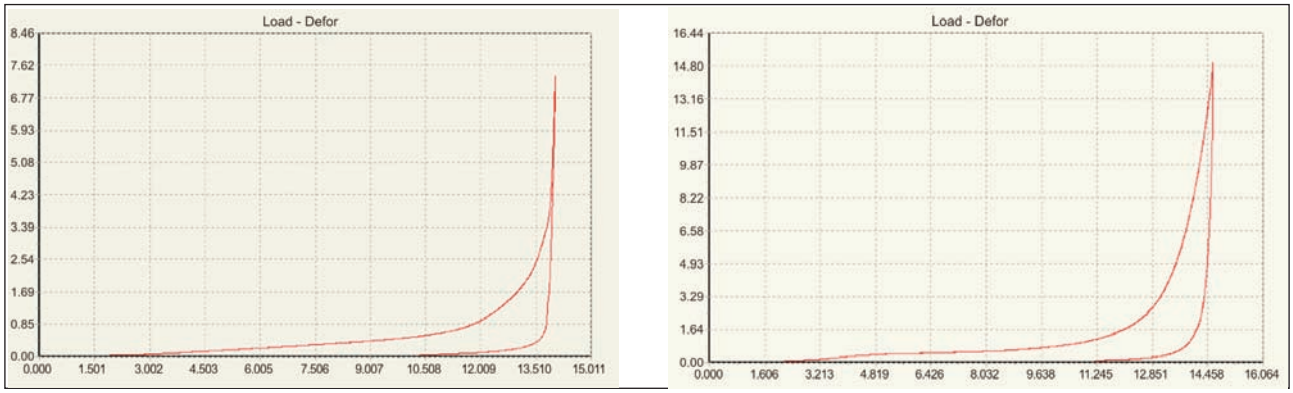

a ***b***

Fig. 7. Ball compression; graphics made by the testing device's software:
a – initial samples compression using a ball, until a displacement of D/2; ***b*** – new samples compression

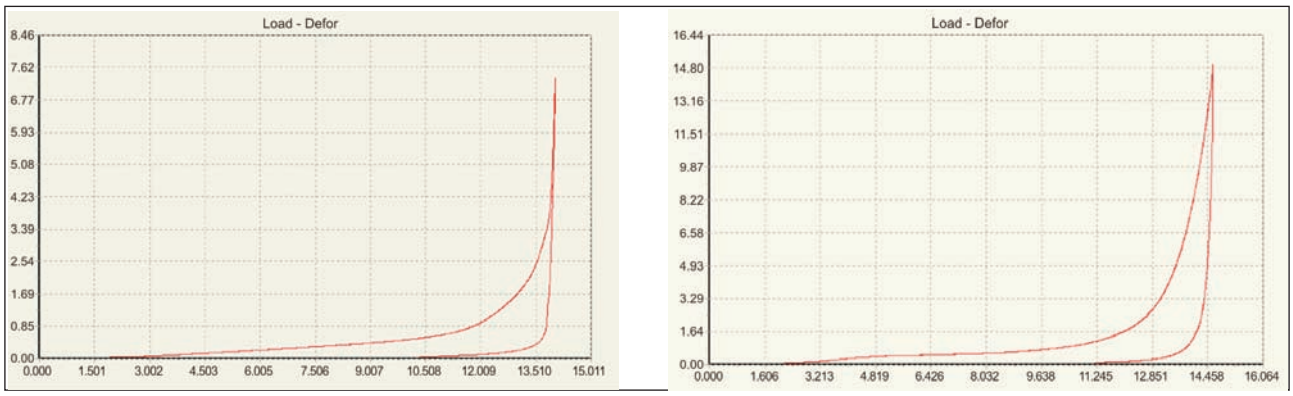

a ***b***

Fig. 8. Compression with a ball and the graphs were made, using the numerical data stored by the testing machine:
a – initial samples compression using a ball; ***b*** – new samples compression

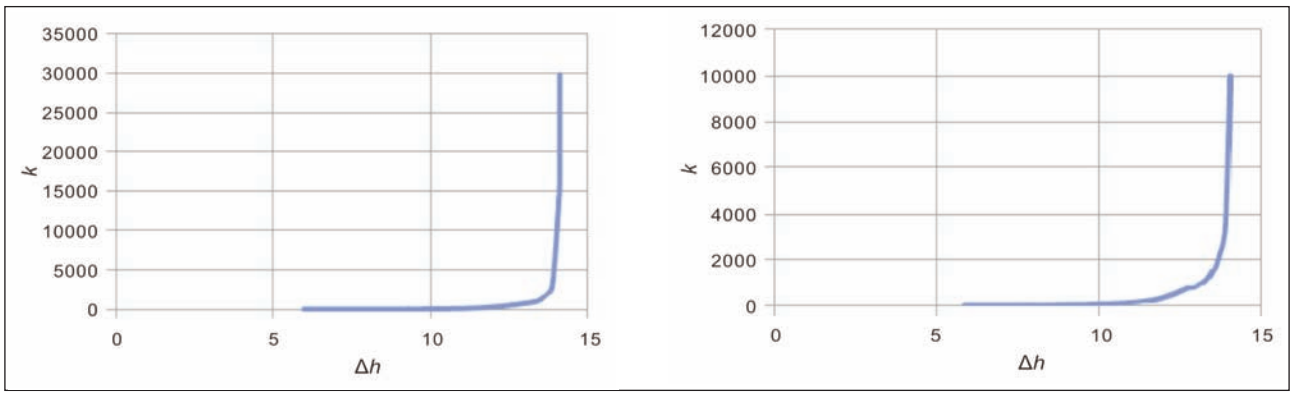

Fig. 9. The variation of *k* factor in case of ball compression

$$k = \frac{\Delta F}{\Delta h} = \frac{2\pi}{3} \cdot D \cdot p_{max} \qquad (13)$$

It is illustrated in figure 9. The variation of *k* factor according to the ball's depth of penetration, for displacements greater than 300 N.

There can be seen in figure 9, that a rapid increase in *K* factor is produced when the crushed composite from the ball's "peak" is depleted. The proximity between the graph $k = f(\Delta h)$ and the vertical, indicates that the test machine compresses the ball (bearing steel). Therefore, the *k* factor, presented in figure 9*a* up to a maximum value of $k = 2\,600$ N/mm (a variation of displacement $\Delta h = 13.7$ mm) and in figure 9*b* the limit value is $k = 3\,200$ N/mm (for the same variation $\Delta h = 13.7$ mm). These values were read on the "dilated" charts, built in Excel. The lower value of the *k* factor, for the corresponding test case presented in figure 7*a*, is explained by the mechanical "memory" of the material, which recorded the

previous load of the sample with the ball pressed on the depth of half the diameter (Δh = 15.2 mm / 2 = = 7.6 mm).
Concluding, one can assign to the composite material, a factor of k = 3 200 N/mm, used to calculate the maximum pressure (the "peak" of the ball) p_{max} = = 100.5189 N/mm^2. This pressure is quite the normal breakdown tension (breaking) of the material: σ_{striv} = = 100.5189 MPa.

DEFORMATION ENERGY

The energy absorbed by the material until breaking, by pressing it with the ball, is the energy transferred by the testing device (14):

$$U_{striv} = \frac{F \cdot h}{2} \quad (14)$$

From the data extracted and processed, the energy value loosened by the test device for composite plastic deformation at compression with a ball was obtained (table 1).
Energy absorbed by the material after plastic deformation at compression with a ball can be calculated by graphical integration based on data recorded on digital test device (15):

$$U = \frac{1}{2} \cdot \sum_i (F_{i+1} + F_i) \cdot (h_{i+1} - h_i) \quad (15)$$

where:

i indicator is the line number in the table data from Excel.

Thus, we obtained the energies calculated in table 2. Of the same order of magnitude as those calculated in table 1. Which can be considered the measure of test car ceded power. The volume of material displaced by the ball can be calculated with (16):

$$V_{dislocat} = \frac{\pi D^2}{4}(g - D) + \frac{1}{2} \cdot \frac{\pi D^3}{6} = \frac{\pi D^2}{4}\left(g - \frac{2D}{3}\right) \quad (16)$$

Table 1

THE ENERGY ABSORBED BY THE COMPOSITE MATERIAL FOR COMPOSITE'S PLASTIC DEFORMATION WITH A BALL

	F, N	**h,** mm	**U_{str},** *Nm* = J
Test 2 - ball	658	13.8337	5.55
Test 3 - ball	660	13.88	4.58

Table 2

THE ENERGY LOOSENED BY THE TESTING MACHINE FOR PLASTIC DEFORMATION OF COMPOSITE AT COMPRESSION USING A BALL

	U_{final}, *Nm* = J
Test 2 - ball	5.897716
Test 3 - ball	6.151698

By substituting in relationship (16): g = 15 mm and D = 15.2 mm values, will result $V_{dislocat}$ = 883.097 mm^3, the volume displaced by the penetrator and calculated with this relationship does not take into account the material driven from surrounding areas, which can reach twice the theoretical values, by calculus. Energy absorbed by plastic deformed material is the product between the volume of deformed material and the specific energy (per volume unit), which is calculated by surface area under the characteristic $\sigma - \varepsilon$ curve. So far, the specific energy wasn't provided, because the tests carried out were not completed by breaking the material.

TENSILE TESTING

Tensile testing was performed in the first stage on samples cut with constant width. It was found that the samples do not get broken due to increased production of transverse contraction that makes the samples escape from the device's tank (fig. 1*b*) [2].
On figure 10 there can be noted that the loads haven't exhausted the carrying capacity of the sample (compared with figure 10*b*, where maximum tension achieved is 1.65 MPa, respectively figure 10*c,* with σ_{max} = 1,32 MPa).
On the WDW device were made tests on samples with a narrowed study area from the extremities. The curves in figure 11 and figure 12 were made by the testing device's software.
Energy consumed at samples tensile break can be expressed as a compressive work of tensile forces (17):

$$U_{tract} = \sum \frac{F_i \cdot \Delta l_i}{2} \quad (17)$$

Has resulted:

U_{tract1} = 6581,676, *Nmm* = 6.581676 J, for the first sample;

U_{tract2} = 10322.42, *Nmm* = 10.32242 J for the second sample.

The results are different because of the different sample's size.
The friction specific breaking energy was calculated with (1) relation. The value obtained in this case is a characteristic of the material at the load of traction, without being related to the application of compressive properties. Compared with the energy obtained

Table 3

VALUES OBTAINED FOR SPECIFIC ENERGY AT TENSILE BREAKING

Sample	**Transversal section dimensions,** mm^2	**Study area length,** mm	**Tensile compressive work,** J	**Breaking specific energy,** J/mm^3
1	15,2 × 9,3	35	6,581676	1,330277 × 10^{-3}
2	15,2 × 10	50	10,32242	1,376322 × 10^{-3}

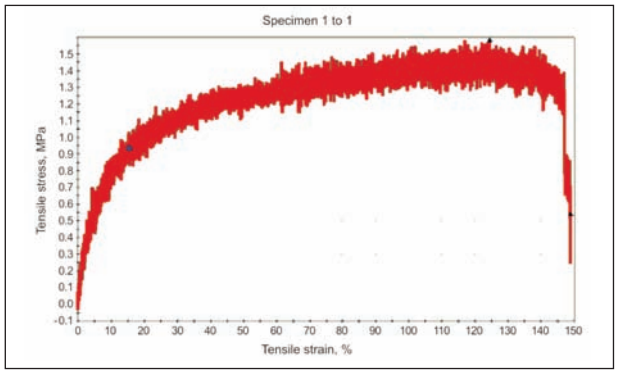

a

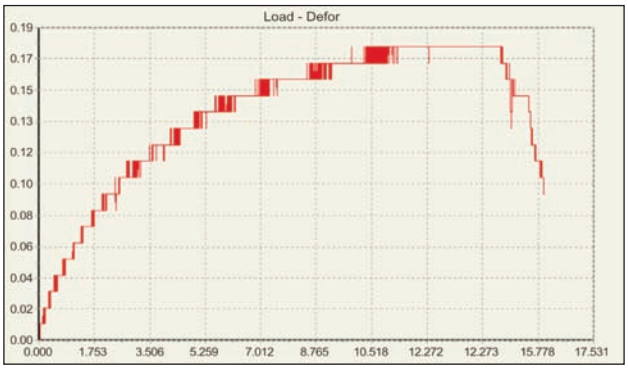

b

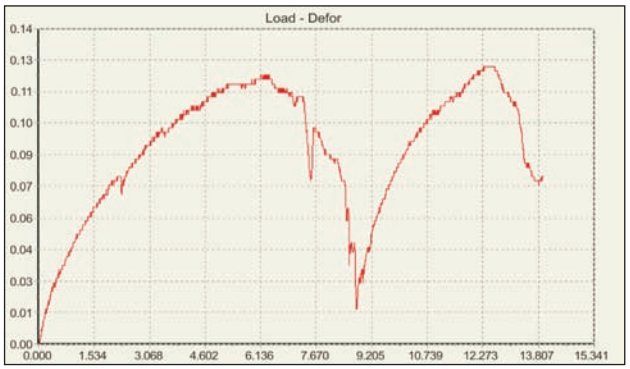

c

Fig. 10. The characteristics built after tensile testing on constant width samples:
a – the test on Instron machine; ***b, c*** – the characteristics built after tensile testing on WDW machine

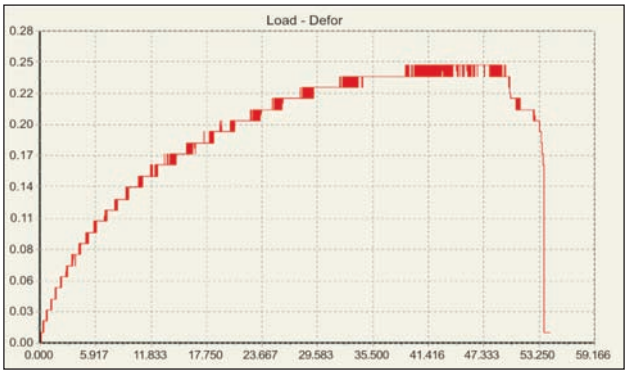

a

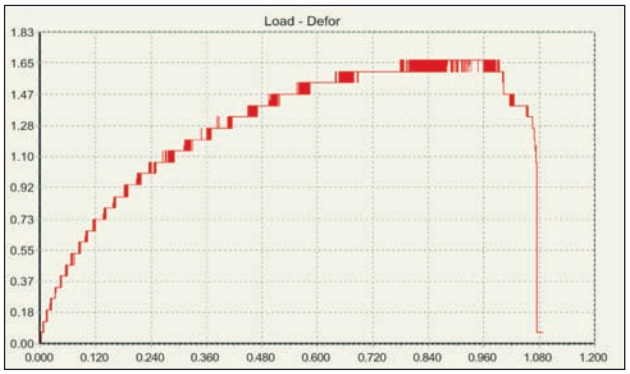

b

Fig. 11. The tensile characteristics for the first sample:
a – load-deformation sample; ***b*** – strain-specific deformation curve

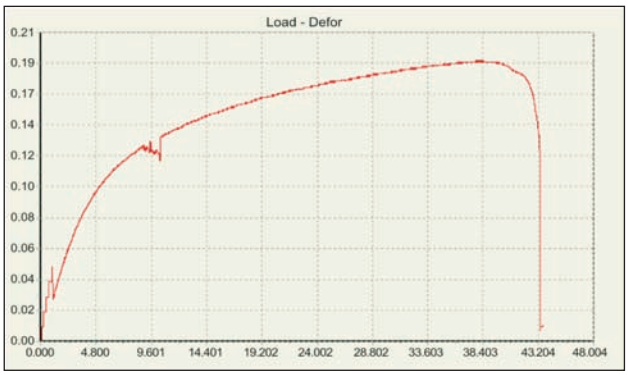

a

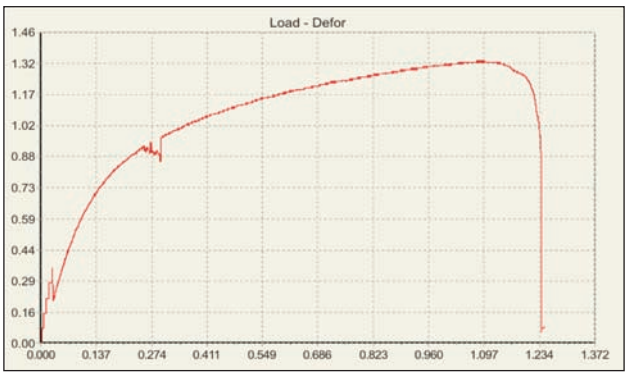

b

Fig. 12. The tensile characteristics for the second sample:
a – load-deformation sample; ***b*** – strain-specific deformation curve

from compression parallelepiped sample, where the request came not to destroy, although tension has reached values much higher than the tensile (and the material presented an almost complete return to its original size), specific energy is lower tensile than half the specific compression energy.

CONCLUSIONS

The composite material studied has presented the following characteristics:

- The absorbed energy value $W_{abs}/S_0 = 4 \times 10^{-3}$ daJ/mm^2 bending by shock load.
- Elasticity module at compression has a medium value of $E_{mediu} = 328$ MPa, for the interval of normal strain, $\sigma_{comp} \in [10$ MPa, 40 MPa] and a maximum value of $E_{comp} = 584.3681519$ MPa, for the interval of strain, $\sigma_{comp} \in [30$ MPa, 40 MPa].
- Specific energy at compression until $\sigma_{max\ ,compr} =$ = 40 MPa, has resulted $U_{1,compr} = 2.973 \times 10^3$ J/mm^3.
- The tests defined a specific size of k composite, $k = \Delta F/\Delta h$, variable by h, which has a maximum value of $k = 3\,200$ N/mm, and is used to determine the crushing strength, $p_{max} = \sigma_{striv} = \frac{3}{2\pi} \cdot \frac{k}{D}$, only only by knowing the penetrator's diameter, D.
- From ball compression test resulted a composite's crushing strength $\sigma_{striv} = 100.5189$ MPa.
- Energy absorbed in ball compression test was $U_{final} = 6.1517$ J, the theoretical volume of material displaced by the ball being $V_{dislocat} = 883.097$mm^3 (specific energy of deformation at compression is less than the $U_{1,compr} = 6.966$ J/mm^3, because it has to be considered the adjacent volume of material deformed without the deformation capacity being exhausted).
- At tensile testing were obtained specific breaking energies of $U_{1,\ tract} = 1.376 \times 10^{-3}$ J/mm^3.
- The composite material has good energy absorption characteristics in case of compression.

Following the tests carried out have identified a number of mechanical characteristics tested material recommended protective equipment products and to protect areas of impact body with arms, and even bullets blunt objects and at the same time is very important, as for such protective equipment to know the size, dimensions, the arrangement on the body and that the impact force creating a pressure not greater than 50 g_f/cm^2 pressure value which does not affect blood flow task.

BIBLIOGRAPHY

[1] Curtu, I., Sperchez, Fl., Munteanu, M. *Rezistența materialelor*. Memorator, Braşov, 1989
[2] Horbaniuc, D. *Déformations palstiques*. Université "Mohanned V", Ecole "Mohammadia" d'Ingénieurs, Rabat, 1976
[3] Mareş, M. *Materiale compozite – proprietăți şi modelare*. Ed. Tehnopress, Iaşi, 2006
[4] Cioară, L., Cioară. I., Toma, D. *Relația structură-proprietăți pentru țesături antistatice, destinate echipamentelor de protecție*. In: Industria Textilă, 2010, vol. 61, issue 2, p. 81
[5] Loghin, C., Nicolaiov, P., Ionescu, I., Hoblea, Z. *Functional design of equipments for individual protection*. In: Management of Technological Changes, 2009, vol. 2, p. 693

Authors:

Dr. ing. IONUȚ DULGHERIU
Universitatea Tehnică Gheorghe Asachi
Facultatea de Textile, Pielărie şi Management Industrial
Bd. D. Mangeron nr. 53, 700050 Iaşi
e-mail: idulgheriu@tex.tuiasi.ro

Dr. ing. CIPRIAN COZMANCIUC
Universitatea Tehnică Gheorghe Asachi
Facultatea de Construcții şi Instalații
Bd. D. Mangeron nr. 43, 700050 Iaşi
e-mail: cozmancicuc@ce.tuiasi.ro

ITMA 2011 – CEA MAI PRESTIGIOASĂ EXPOZIȚIE INTERNAȚIONALĂ DE MAŞINI TEXTILE ŞI ÎMBRĂCĂMINTE. Partea a II-a*

Salonul de la Barcelona focalizat pe inovația la cel mai înalt nivel

În economia contemporană globalizată şi bazată pe cunoaştere, inovația este un element vital, alături de poziția de piață, productivitate, calificarea personalului, calitatea produselor şi serviciilor, rezultatele financiare. De-a lungul celor 60 de ani care au trecut de la prima expoziție internațională de maşini textile inițiată de CEMATEX, *ITMA 2011* şi-a confirmat, în capitala catalană, poziția de lider absolut, prin numărul record de firme expozante care dezvoltă cu prioritate cele mai avansate inovații tehnologice, maşini de înaltă productivitate şi tehnologii de producere a unor articole de îmbrăcăminte inteligentă, în raport cu expozițiile şi târgurile similare din diferite zone ale lumii – *ITMA Asia, CITME, Techtextil South America, Interstoff Asia Esential, Fespa, Fisma, Modtissimo, Heimtextil, IFAI Expo Canada, Filtrex Asia, Texgate, Temac, Shanghai Tex* ş.a., organizate de asociații de maşini textile – chineză (*CTMA*), japoneză (*JTMA*), coreeană (*KOTMA*), taiwaneză (*TAMI*) sau nord-americană (*ATAMA*). Doamna Maria Avery, secretar general al CEMATEX, a spus că ITMA a fost întotdeauna îndreptată spre inovație, însă acest lucru a fost mai evident ca niciodată la recentul salon de la Barcelona.

Pe întregul spațiu al inovației, de 100 000 m^2, oferit de *Fira de Barcelona*, sute de branduri renumite au prezentat cele mai performante maşini textile şi tehnologii de vârf ale sectorului. *ITMA 2011* a oferit o vitrină uriaşă de soluții de ultimă oră pentru factorii de decizie din domeniul textil mondial.

Principalii lideri mondiali tehnologici, care au obținut *medalii de aur* pentru maşini de înaltă productivitate şi tehnologii textile de ultimă oră, sunt:

- ***În domeniul filaturii*** – *Oerlikon Textile, Rieter, Marzoli, Trutzschler, Toyota, Tsudakoma, Howa, N. Schlumberger, SantAndrea Novara, Seydal, Cognetex, Tibeau, Savio, Garnett Controls, Xorella, Laroche, Autefa, Temafa, Hacoba, Asselin, Hergeth, Suessen, Knotex, Fadis, Fehrer AG, Lauffenmuhle GmbH* ş.a., care au expus noile lor dezvoltări de produse şi tehnologii. Au fost prezentate soluții viabile legate de cele mai recente tehnologii neconvenționale de filare, sisteme de monitorizare şi control şi automatizări de ultimă generație la maşina de filat cu rotor, noi tehnologii de schimbare automată a cănilor, comanda şi legarea automată a benzii şi a firului, curățarea rotorului, schimbarea automată a levatei şi transportul automat al bobinelor,

Fig. 1

comanda şi monitorizarea prin teleservice a procesului de filare. Una din cele mai admirate firme de pe glob, *Oerlikon Schlafhorst* (fig. 1), care s-a poziționat fără întrerupere în linia de avangardă a maşinilor de filat, a prezentat la salon câteva din produsele sale de vârf: *Autocoro 8, BD 448, Autocoro 480, Autocoro S360, Corolab XQ* şi *Belcoro Rotor – quality standards*. Noul model de maşină de filat cu rotor Autocoro 8 are cel mai înalt nivel de automatizare şi o productivitate cu 25% mai mare față de modelele similare ale firmelor concurente. Dacă viteza motorului de antrenare a rotoarelor la maşinile de filat fabricate de Rieter ajunge la 140 000 rpm, la Savio 107 500 rpm, la Autocoro 8 micşorarea diametrului şi o tehnologie magnetică perfectă permite creşterea turației rotorului până la 200 000 rpm. Fiecare cap de filare dispune de propria tehnologie de filare. Modelul Autocoro BD 448, cu 448 de posturi de filare este considerat de profesioniştii cea mai inteligentă şi mai ecologică linie tehnologică de filare din lume. Printr-o simplă apăsare pe buton, în doar 10% din timpul care era necesar la maşinile de filat convenționale, productivitatea modelului BD 448 poate creşte cu 25%. Față de vechea generație de BD-uri, consumul de energie este cu 10% mai redus. De asemenea, s-au micşorat cu mult, față de modelele prezentate la salonul de la München, atât numărul de operatori ce supervizează funcționarea agregatelor, cât şi spațiul tehnologic necesar amplasării maşinilor şi costurile logistice. *Oerlikon Zinser* a prezentat tehnologii inovatoare privind filarea cu inele a bumbacului şi a lânii pieptănate, care îmbină tehnologia convențională cu cea compactă. Noul sistem de schimbare a levatelor *Zinser 670 RoWeMat* stabileşte noi recorduri în privința siguranței şi duratei de schimbare a levatelor, iar sistemul de aspirație controlat de inversor asigură

* Partea I a fost publicată în Revista *Industria Textilă*, 2012, vol. 63, nr. 1, p. 52.

o secțiune optimizată a consumului energetic. Fabricantul oferă cumpărătorilor noi modele cu până la 681 de fuse. *Zinser 351 Impact FX* este o maşină de filat cu inele de înaltă performanță, având cea mai mare lungime din lume şi o presiune negativă de compactare constantă pe întreaga lungime a maşinii. Modelul *Zinser 451C* asigură o îmbinare optimă a calității şi productivității. Datorită prelucrării fibrelor de lână în condiții mai prietenoase, răsucirea firelor poate fi redusă cu 10–15%. În acelaşi timp, numărul de fire rupte este cu 50% mai mic, în comparație cu alte modele similare, fabricate de firmele concurente. Filaturile dotate cu maşini de filat *Zinser* realizează productivități net superioare, față de filaturile *Rieter, Savio, Marzoli* sau *Tibeau.*

- ***În domeniul țesătoriei*** *– Picanol, Sulzer Rüti* (fig. 2)*, Dornier, Nuovo Pignone, Toyota, Tsudakoma Air, Sultex, Smit Textile, Vamatex, Hacoba, Jacob Müller, Staubli, Bonas, Suzuki, Gunne, Howa, Van de Wiele, Panter Rapier Weaving, Mathis Group, GTP Global Textile Partner, Groz-Beckert* ş.a. au prezentat, în cadrul salonului, cele mai performante maşini de țesut. Expozanții au oferit utilaje şi echipamente de preparare a țesăturilor, modele de maşini de țesut cu rost multiplu şi maşini de țesut cu rotativă multifazică, cu viteze de lucru impresionante – de până la 1 800 rpm, cu suluri de urzeală cu diametrul de înfăşurare de până la 1 600 mm, cu sisteme automate de căutare a rostului şi de extragere a firului de bătătura rupt cu ajutorul unui robot, la cererea lansată de către maşină, fără acționarea întregii maşini, cu nivel de zgomot sub 10 dB, cu efecte de țesere inteligente, cu platforme electronice dotate cu microprocesoare de mare capacitate, cu sisteme automate de monitorizare şi control al proceselor „*inteligente*“ de țesere, cu sisteme sofisticate CAD/CAM de proiectare şi reproiectare a țesăturilor.

  Liderul tehnologic care a oferit la salon o gamă mai largă de maşini de țesut, caracterizate prin robustețe, versatilitate şi înaltă productivitate a fost *Picanol Group*. Liderul dezvoltă, produce şi lansează, pe piețele din Asia, Europa şi Statele Unite, maşini de țesut de înaltă tehnologie. De la fondarea sa, în 1936, Grupul Picanol a evoluat de la poziția de jucător foarte mic la cea de lider tehnologic în producția modernă de maşini de țesut. În cei 75 de ani de activitate, Picanol a vândut 270 000 de maşini de țesut, grupate în 26 000 de țesătorii. În standul de la Fira de Barcelona, liderul strategic Picanol a expus şase modele de maşini de țesut (*OMNIplus-X, GT-Max, OPTI-Max, OMNIjet, TERRYplus 800, OMNIplus 800 TC airjet*), lansate după ITMA 2007, din care cele mai multe sunt realizate în China, la fabrica din Suzhou, dată în funcțiune în anul 1994. Toate modelele de maşini de țesut prezentate de liderul tehnologic belgian sunt echipate cu dispozitive performante, care monitorizează, controlează şi conduc funcționarea maşinilor de țesut, programează rapoartele de legătură şi culoare, achiziționează, memorează şi salvează datele de producție. Toate modelele sunt dotate cu sisteme digitale de supraveghere, adaptate la particularitățile sistemelor de țesere. În realizarea părților mecanice şi electronice ale maşinii, Picanol s-a bazat pe experiența îndelungată a companiei în ceea ce priveşte tehnologia de țesere, folosind dispozitive cu graifăr. Maşinile sunt echipate cu accesorii destinate reducerii numărului de opriri, atât ca frecvență, cât şi ca durată. Acționarea vatalei şi a graifărului sunt asigurate de un motor standard şi

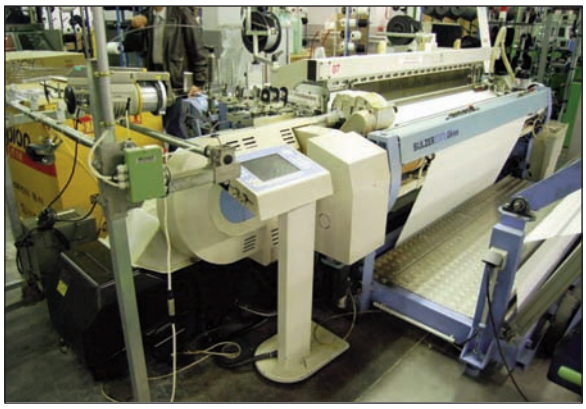

Fig. 2

de un ambreiaj electromagnetic cu fricțiune. Totodată, maşinile sunt dotate cu microprocesoare care monitorizează, controlează şi determină forța de pornire şi de frânare, precum şi cu dispozitive electronice pentru controlul deplasării maşinii cu ițe. Un dispozitiv ergonomic tactil, cu display touchscreen, oferă operatorului posibilitatea de a regla cu uşurință parametrii principalelor funcții ale maşinii. Reglajele sunt foarte precise, cea mai mică ajustare a acestora putând fi observată imediat în calitatea țesăturii obținute. Unul dintre avantajele gradului înalt de automatizare este acela că pot fi folosite chiar şi pentru țeserea firelor de calitate inferioară. În premieră mondială, liderul numărul unu în domeniu a prezentat „bijuteria familiei“, pe al cărei banner de promovare scria cu litere de o şchioapă *OMNIplus Summum running at 2011 picks per minute*. Şi acest lucru se întâmpla în situația în care unele firme concurente nu puteau realiza decât viteze modeste şi, implicit, productivități scăzute (*Sultex A9500* – 1 300 rpm; *Toyota JAT710* – 1 250 rpm). Maşina de țesut *OMNIplus Summum Air Jet* (fig. 3), destinată produselor din bumbac, va înlocui treptat *OMP 800* şi va constitui noua platformă a evoluției ulterioare în segmentul Air Jet. Specialiştii care au vizitat standul au apreciat la aceste maşini noul sistem „revoluționar“ de inserare şi

Fig. 3

platforma electronică Picanol BlueBox. Noul model OMNIplus Summum Air Jet este dotat cu o nouă platformă electronică, care dispune de un microprocesor de mare performanță şi o capacitate superioară de memorare, precum şi de o tehnologie de detectare de la distanță şi de un design astfel construit, încât să poată face față celor mai grele condiții de lucru. Platforma *Picanol BlueBox* este net superioară tuturor platformelor similare, construite de firmele concurente. Noul sistem de inserție, cu regulatoare electronice de presiune, are un rezervor de aer separat pentru fiecare canal de țesut şi un rezervor unic de aer pentru duzele releu. Toate acestea îi oferă maşinii de țesut multiple avantaje în exploatare şi o mare flexibilitate. Setările optime făcute sistemului permit funcționarea maşinii la performanțe maxime, cu cel mai mic consum de aer posibil şi fără compromisuri în privința performanței, flexibilității şi consumului de energie. Combinată cu recunoscuta robustețe a maşinilor Picanol, platforma BlueBox oferă performanțe maxime pe piața mondială a maşinilor de țesut cu jet de aer.

- ***În domeniul tricotajelor*** *– Shima Seiki, Stoll, Protti, Mayer & Cie, Merz, Karl Mayer, Jakob Müller, Maceba, Staubli, Comez, Groz-Beckert, Santoni Group, Loepfe, Kern-Liebers, Memminger-IRO, Jumberca, Monarch, Fukuhara, Albi, Qin Hong Hu, Terrot* etc. s-au regăsit printre liderii tehnologici cu cele mai multe inovații. Deşi numărul expozanților şi vizitatorilor a fost mai mic cu 9% decât la ediția precedentă de la München, ultimul salon din capitala catalană s-a încheiat cu rezultate ce au depăşit cu mult aşteptările liderului mondial japonez *Shima Seiki Mfg. Ltd*. Având în vedere condițiile vitrege cauzate de crizele economice şi financiare la nivel global şi de faptul că majoritatea covârşitoare a producției textile se află în momentul de față în China şi Hong Kong, preşedintele firmei, domnul Masahiro Shima, a declarat că locul de desfăşurare ales, Barcelona – Spania, nu a oferit companiei nipone satisfacțiile legate de preocupările sale privind raportul optim cost-eficiență. În ciuda acestor condiții aparent nefavorabile, firma din Wakayama, având vechi interese în Europa – inclusiv în Spania, dar şi pe alte piețe din afara Asiei de Est, a ales să expună la Fira de Barcelona, nu pentru a răspunde cererilor venite din partea Europei, ci pentru a aduce un omagiu tradiționalelor ediții ale ITMA, prin prezentarea celor mai noi tehnologii de tricotare, şi pentru a-şi păstra poziția absolută de lider mondial. Adeptă, încă de la înființare, în 1953, a strategiei manageriale Ever Onwar, ea a participat la evenimentul din apropiere de Placa dei Rei din motive de ordin tactic, sub deviza *„Soluții pentru diversitate“*. În consecință, liderul tehnologic mondial *Shima Seiki* a prezentat o gamă de produse care reflectă dihotomia pieței maşinilor de tricotat rectilinii. Anticipând profilul vizitatorilor, gigantul nipon a căutat sa includă în ofertă maşini de tricotat de mare productivitate, destinate exportului, precum şi maşini de tricotat pentru producătorii orientali şi pentru satisfacerea pieților de consum locale. Din acest motiv, compania Shima Seiki a expus maşini de tricotat noi, destinate producției de panouri conturate şi produse complexe. În plus, corporația asiatică a avut ocazia de a-şi demonstra rolul de lider inovator în domeniu, prin expunerea în premieră mondială a unui număr impresionant de modele noi de maşini caracterizate printr-o finețe diversificată şi soluții noi brevetabile (*Mach 2X153, SSR 112, Mach 2SIG* etc.), dotate cu display touchscreen, pentru a uşura deservirea maşinii de către un operator cu nivel de instruire mediu (fig. 4). De fapt, din cele 13 modele expuse, 11 exponate au fost complet noi. Profesioniştii au remarcat prima maşina de tricotat rectilinie din lume cu finețea 21 E – capabilă să producă panouri conturate, asemănătoare cu cele produse pe maşinile de tricotat tip Cotton, şi o maşină prototip dotată cu două fonturi suplimentare dispuse în V, prevăzută cu platine de presare. Specialiştii firmei Shima Seiki au apreciat că toate aceste noutăți au creat un contrast puternic cu restul expozanților de maşini de tricotat rectilinii, unii dintre aceştia

Fig. 4

venind pentru prima dată, iar standurile lor fiind, în esență, lipsite de noi tehnologii. Conducerea de vârf a gigantului nipon a remarcat faptul că a existat un interes echilibrat pentru mașinile de tricotat panouri conturate și produse complete și o creștere notabilă a interesului pentru noile dotări ale stațiilor grafice 3D design workstation *SDS-ONE APEX3 (Flat knitting, Textile, Print, Circular knitting)* și ale noilor sisteme de monitorizare, control și protecție în procesul de tricotare *CAD/CAM Systems (P-CAM 100/160/200, Apparel CAD Systems*) – pentru care cererea s-a dublat, comparativ cu interesul manifestat la salonul de acum 4 ani, din capitala Bavariei. Această cerere este atribuită clienților și se bazează pe nevoia lor de a satisface ceințele piețelor de consum din diferite zone geografice ale globului. S-a remarcat un interes deosebit pentru realizarea unor mostre cu desene color apropiate ca aspect de cele pictate, utilizând mașini de tricotat de finețe mare, pe care pot fi produse tricoturi cu ochiuri foarte mici.

Al doilea lider tehnologic mondial în domeniul mașinilor de tricotat rectilinii este firma *H. Stoll GmbH & Co. KG*. Participarea companiei din Reutlingen la târgul textil din capitala Cataloniei, s-a realizat sub mottoul *„Istoria noastră, viitorul vostru*“. Ca la fiecare salon, a prezentat o serie de perfecționări ce vizează îmbunătățirea operației de tricotare pe mașinile de tip *CMS*. Unul dintre punctele de atracție l-a constituit expunerea mașinilor de tricotat rectilinii *CMS 502 HP* și *CMS 502 HP multigage*, echipate cu sisteme de came integrate de tricotare/transfer mai compact. Mașinile sunt prevăzute cu un program de optimizare a cursei căruciorului cu lacăte. Aceste două perfecționări duc la o creștere a productivității mașinii cu circa 10%. Noul soft universal prietenos *Argyle* pentru proiectarea desenelor și programelor de tricotare *M1plus Stoll* s-a bucurat de un interes major din partea participanților. Ultima versiune de soft combinată cu perfecționările prezentate pot duce reducerea cu 95% a timpului de proiectare și de realizare a tricotului. Un alt subiect important oferit de firma Stoll a fost prezentarea noilor mașini cu ace având indicativul 4L și 3L, cu un cârlig mai mare decât în cazul acului de tricotat pentru prelucrarea firelor voluminoase, ceea ce duce la îmbunătățirea condițiilor de depunere și de prindere a firelor și o siguranță mai mare a operației de tricotare. În plus, forma și dimensiunile platinelor de închidere-aruncare au fost schimbate, iar lacătul lor de acționare a fost adaptat utilizării unui ac cu cârlig mai mare. Acul 3L se aplică la mașina CMS 520C, iar acul 4L este disponibil pentru mașinile de tricotat CMS 530 HP, CMS 822 HP și CMS 502.

- ***În domeniul finisajului textil și al nețesutelor*** – inovații remarcabile, la cel mai înalt nivel, au prezentat liderii strategici *JiangsuYingYang nonwoven, Dilo Group + Temafa Machines, NCS nonwoven, Rieter Perfojet, Bruckner Group, A. Monforts Textilmaschinen GmbH*, *Neumag Saurer, Matthys-Machines, Thies, Polymer Group* etc. La salonul din apropiere de El Camp Nou – Futbol Club Barcelona, liderii strategici ai domeniului au fost concurați de firme mai mici, apărute relativ recent, cum ar fi *V-Lap, FibeRio Technology Corporation*. Liderul mondial în nețesute *JiangsuYingYang Nonwoven Machinery Co. Ltd*, un consorțiu chinez înființat în anul 1993, cu hale industriale pe o suprafață de 66 000 m², este, fără îndoială, cel mai mare producător de mașini textilele nețesute de pe glob. Numai în 2010 a instalat peste 300 de linii moderne de fabricarea covoarelor nețesute, geotextilelor, asphalt felt substrate, synthetic leather substrate, glue-free adding, spray-bonded wadding, mimic floss etc. De-a lungul anilor, s-a dovedit faptul că succesele gigantului din Jiangsu se datorează flexibilității și know-how-lui acumulat în domeniul tehnologiilor de vârf de fabricare a liniilor tehnologice pentru nețesute.

  Grupul YingYang colaborează permanent cu centre de cercetare-dezvoltare-inovație și cu universități de prestigiu din China. Numai în ultimele 18 luni, a angajat 40 de tineri absolvenți din universitățile cu care are contracte de CDI. Liderul mondial chinez în nețesute a fost prezent, la cea de-a 16-a ediție a târgului textil de la Fira de Barcelona, o gamă largă de produse noi și tehnologii avansate, susținând filozofia companiei bazată pe elasticitate și experiență de producție. Dezvoltate pe un principiul conform căruia tehnologia inovării are ca menire îmbunătățirea calității vieții oamenilor, inovațiile recente susțin, reinventează sau revoluționează experiența utilizatorilor în interacțiunea prietenoasă cu mediul. Gigantul chinez promovează cu prioritate noi tehnologii ecologice, adică acordă un interes deosebit zonei green. La salonul din apropiere de Palau de la Musica Catalana, liderul chinez a prezentat o gamă largă de produse, printre care: *YYL-HY Stiff Waddings,YYL-ZT Getextiles Production Line, Roller press for cement production line, EPS-4600 Vulcaniziing drying bed, YYKB Bale Opener, YYKS Opening Machine, YYBL-FZ Felt Production Line, Stone Crushing Line – China* etc.

  Un alt medaliat cu aur în acest domeniu, care a avut numeroși admiratori la evenimentul din orașul Santei Eulalia, a fost specialistul și expertul mondial numărul unu în mașini de interțesere *DiloGroup* (fig. 5). Gigantul din Eberbach, care – de foarte mulți ani – este un partener cu performanțe de vârf pentru industria nețesutelor – prin liniile complete de producție pe care le asigură sucursalele *Dilo Temafa opening-blending, Dilo*

Spinnbau-carding, Dilo Machines-crosslapping-needling.

Numeroasele realizări ale firmei, care au avut drept scop creşterea productivităţii, îmbunătăţirea omogenităţii stratului fibros şi creşterea eficienţei au dus la succesul incontestabil al corporaţiei. DiloGroup oferă, pentru fiecare tip de interţesere, o soluţie optimă. Multe dintre invenţiile şi realizările grupului din Eberbach au însemnat paşi tehnologici importanţi, cum ar fi tehnologia *Di-Loor* şi *Di-Loop*, tehnica interţeserii tubulare *Beltex* şi *Rontex*. În vârful acestor noi tehnologii rămâne, însă, *Hyperpunch*, cu efectele sale pozitive asupra stratului fibros în timpul interţeserii. Producătorul german este lider şi în ceea ce priveşte inovaţiile tehnologice şi productivitatea maşinilor de interţesere universale standard, din seria *Di-Loom*, cu un număr de curse de peste 3 000 min^{-1} şi desimi ale acelor de peste 32 000 de ace/ml. Dilo şi-a consolidat poziţia de lider tehnologic mondial prin achiziţionarea pachetului prioritar al renumitei firme *Temafa Machines GmbH*, din Bergisch Gladbach. La salonul internaţional din oraşul celebrului Teatre Nacional de Catalunya, compania a expus cu mare succes produsele: *Vlieleger, Vornadelung* şi *Finish-Vernadelung.*

Fig. 5

Profesor asociat **EUGEN-CONSTANTIN RÂPĂ**
Universitatea Tehnică Ghe. Asachi – Iaşi
e-mail: *ecrapa@gmail.com*

WORKSHOP PRIVIND ACHIZIŢIILE PUBLICE ECOLOGICE

În data de 23 februarie 2012, în cadrul proiectului ***„Inovare durabilă pentru textile în Europa de Sud-Est – Tex-EASTile“***, a avut loc workshopul privind achiziţiile publice ecologice, la Hotel Răzvan, din Bucureşti.

Organizat de Camera de Comerţ şi Industrie a Municipiului Bucureşti (CCIB), în parteneriat cu Institutul Naţional de Cercetare-Dezvoltare pentru Textile şi Pielărie (I.N.C.D.T.P.), workshopul s-a desfăşurat pe trei secţiuni, adresându-se agenţilor economici şi instituţiilor publice şi având ca tematică includerea criteriilor de natură ecologică în procedurile de achiziţii publice pentru produse textile şi îmbrăcăminte.

Manifestarea s-a bucurat de un real interes. Peste 45 de persoane de la diferite IMM-uri, autorităţi contractante şi ministere au participat la prelegerile axate pe diverse teme, precum:

- „Conştientizarea IMM-urilor privind legislaţia achiziţiilor publice, pentru a putea răspunde cerinţelor autorităţilor contractante“;
- „Beneficiile ecoetichetării“;
- „Ecodesignul – o soluţie pentru îmbunătăţirea performanţelor de mediu ale produselor textile“;
- În ce măsură producătorul (IMM-ul) „verde“ şi autorităţile publice se întâlnesc din punct de vedere al cererii şi ofertei de produse textile ecologice (de exemplu, la nivelul canalelor de informare/promovare, obstacole întâmpinate etc.).

Workshopul s-a desfăşurat în cadrul proiectului „Inovare durabilă pentru textile în Europa de Sud-Est – Tex-EASTile“, cu codul SEE/A/069/1.1/X, cofinanţat de Uniunea Europeană în cadrul Programului de Cooperare Transnaţională din Sud-Estul Europei 2007–2013. Informaţii suplimentare despre proiect pot fi găsite pe pagina web a proiectului www.texeastile.eu.

Redacţia

Materii prime

EMANA – UN NOU FIR CU PROPRIETĂȚI INTELIGENTE

Emana este noul fir obținut din poliamida 6.6, care încorporează un aditiv brevetat, cu proprietăți de termoreglare şi îmbunătățire a microcirculației sanguine, atunci când se află în contact cu pielea mai mult de şase ore. „*Acest aditiv exploatează acțiunea radiației în infraroşu îndepărtat*“ – explica Daniel Franco, reprezentantul firmei ***Rhodia***, din Brazilia, producătoare de fire *Emana*, cu ocazia celui de-*al 50-lea Congres al fibrelor sintetice*, organizat la Dornbirn, în Austria.

Studiile ştiințifice efectuate de un laborator independent din Brazilia, au demonstrat că, în comparație cu alte produse, îmbrăcămintea sport produsă din fire *Emana* îmbunătățeşte capacitatea de reglare a temperaturii corpului şi reduce acumularea acidului lactic, un factor generator de oboseală musculară. Aceleaşi studii indică un confort sporit şi o reducere a celulitei, în urma creşterii elasticității pielii. Trebuie remarcat şi faptul că proprietățile inteligente ale firului nu se deteriorează prin spălare repetată.

„*Domeniul infraroşu îndepărtat este caracterizat prin energie scăzută şi penetrare redusă, neproducând daune colaterale țesuturilor biologice... Cu toate acestea, radiația interacționează puternic cu corpul omenesc prin intermediul moleculelor de apă, care reprezintă 70% din masa corporală a omului*“ – a afirmat Daniel Franco.

Beneficiind de principalelele caracteristici ale poliamidei – tuşeul moale, uşurința în îngrijire, rezistența şi elasticitatea, ***Rhodia*** oferă clienților de pe piața articolelor de îmbrăcăminte sport şi a articolelor de lenjerie o largă flexibilitate a culorii şi modelelor.

Emana a fost certificată conform Standardului Oeko-Tex 100, clasa I, ceea ce indică absența unor substanțe dăunătoare în componența acestui produs.

Smarttextiles and nanotechnology, decembrie 2011, p. 13; ianuarie 2012, p. 11

Noi tehnologii

PROCEDEU DE ELECTROFILARE A PROTEINEI DE MĂTASE

Universitatea Tufts şi ***Massachussetts Institute of Technology*** au brevetat un nou proces de producere a biomaterialelor din mătase, cum ar fi fibrele, peliculele, spumele şi păturile fibroase, fără folosirea solvenților organici.

Înaintea procesului de electrofilare, este necesară realizarea unui amestec dintr-un polimer biocompatibil – cum ar fi oxidul de polietilenă, cu o proteină din mătase. Procesul este descris în Brevetul de invenție US Patent Publication 8 071 722, din decembrie 2011.

În natură, filarea fibrei de proteină se face, de exemplu, de către viermii de mătase şi păianjeni, şi se bazează pe formarea unor soluții concentrate de faze liotropice metastabile, care sunt forțate, apoi, să iasă în aer prin mici duze.

Producția fibrelor din soluții proteice s-a bazat, de obicei, pe utilizarea proceselor de filare umedă şi uscată. Electrofilarea reprezintă o abordare alternativă de formare a fibrei proteice, care are potențialul de a genera fibre foarte fine pentru diverse aplicații, cum ar fi ingineria biomaterialelor şi a țesuturilor.

Electrofilarea a fost folosită pentru obținerea unor fibre foarte fine, cu diametrul de ordinul nanometrilor, folosind o proteină de tip elastină recombinată, o proteină asemănătoare mătăsii obținute din viermi de mătase din gogoşi de *Bombyx Mori* şi din fire de păianjen din *Nephila clavipes.* Acestea pot fi electrofilate în fibre cu diametre de ordinul nanometrilor, dacă, mai întâi, sunt solubilizate într-un solvent organic, de tipul hexafluoro-2-propanol.

Amestecurile de mătase au fost foarte mult studiate, mai ales din persepctiva formării peliculei. Pentru a obține o îmbunătățire a stabilității termice sau mecanice, ori a proprietăților membranei peliculelor de mătase, au fost folosite amestecuri cu poliacrilamidă, alginat de sodiu, celuloză, chitosan, alcool polivinilic, polimeri acrilici şi polietilen glicol.

Din păcate, cu niciunul dintre aceste amestecuri nu s-au înregistrat succese în rezolvarea unor probleme legate de procesarea sau reprocesarea proteinei de mătase, cum ar fi fragilitatea.

Se afirmă că metoda organică fără solvenți, descrisă în brevetul US Patent 8 071 722 poate realiza acest lucru.

Smarttextiles and nanotechnology, ianuarie 2012, p. 4

NOI TEHNOLOGII DE FINISARE

Printre coloranții şi finisajele textile oferite de firma ***Clariant*** se află soluții textile tehnice adecvate mai multor domenii – de la cel militar şi al serviciilor de urgență la cel al aplicațiilor pentru lucrul în condiții de mediu extreme. Acestea cuprind agenți de hidrofobizare fără fluor, tehnologii noi de ignifugare Pekoflam, în conformiate cu standardele Oeko-Tex, dar şi diferite sisteme de peliculizare. La ***ITMA 2011***, au fost lansate peste 25 de inovații în domeniul produselor, proceselor şi aplicațiilor acestora.

Finisajul *Foam Eco Care*, realizat de Clariant reprezintă un nou reper în domeniul finisajelor neşifonabile. În colaborare cu ***Cotton Incorporated***, Clariant a realizat acest finisaj pe bază de spumă, îmbunătățind astfel calitatea țesăturii şi scurtând procesele de producție, ceea ce a aduce importante beneficii în privința economisirii de apă, energie şi timp.
Amestecul compozit microîncapsulat *Nuva N1811* prezintă performanțe superioare în ceea ce priveşte caracterul hidrofug, rezistența la pătare şi durabilitatea. Tehnologia permite reticularea şi cristalizarea eficientă a catenelor laterale fluorurate, ceea ce face ca, în ansamblu, finisarea să fie foarte eficientă.
În cooperare cu ***Lipotec SA***, Clariant a elaborat produsul cosmetic microîncapsulat *Quiospheres* (fig. 1), pentru aplicații textile. Microcapsulele sunt proiectate printr-o tehnologie care face posibilă o aplicare uniformă pe țesături sau pe articolele de îmbrăcăminte, conferind o stare de confort şi de bine. Eliberarea sa treptată are loc prin reacția enzimelor naturale din piele şi a noilor molecule active din capsule. Transferul substanțelor cosmetice în piele se realizează printr-o tehnologie în două etape.

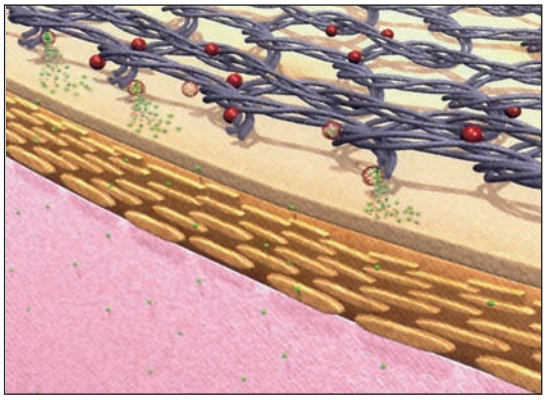

Fig. 1

Primul pas îl constituie transferul microcapsulelor, printr-o reacție chimică între pielea noastră şi microcapsule. Al doilea pas constă în eliberarea treptată şi transferul substanțelor cosmetice încapsulate într-un înveliş integral cosmetic şi biocompatibil, care poate interacționa cu enzimele naturale ale pielii, permițând eliberarea lor în piele. ***Lipotec*** a realizat o serie de noi peptide cu proprietăți biomimetice. Acestea imită moleculele naturale ale pielii, îmbunătățindu-i funcționalitatea. Atunci când articolul de îmbrăcăminte intră în contact cu pielea, începe să elibereze treptat substanțele cosmetice încorporate. Cu cât produsul este purtat mai mult timp, cu atât starea de bine este mai intensă. Țesătura astfel realizată are o bună rezistență la spălare, iar microcapsulele îşi păstrează eficiența pe parcursul a cel puțin 20 de cicluri de spălare la 70°C. Până în prezent au fost dezvoltate două produse: *Quiospheresmoist* şi *Quiospheresslim*. *Quiospheresmoist* are doi ingredienți activi, şi anume antarcticina – o glicoproteină descoperită inițial în Oceanul Antarctic, cu rol de protecție şi regenerare a pielii şi cu proprietăți antiîmbătrânire, datorită intensificării procesului de sinteză a colagenului, şi Xpertmoist – o peliculă moleculară cu un efect puternic hidratant, ce conferă pielii o senzație plăcută. *Quiospheresslim* are, de asemenea, doi ingredienți activi, respectiv o combinație lipozomică de ingrediente de slăbire – Liporeductyl, şi o tripeptidă care previne şi combate celulita şi are efect lipoliptic şi venotonic, activând microcirculația şi îmbunătățind aspectul pielii. Relistase este o peptidă nouă, care măreşte elasticitatea şi impermeabilitatea pielii, prin inhibarea excesului de activitate a elastazei. Relistase ajută la refacerea integrității tridimensionale a pielii, prin stimularea sintezei colagenului şi prin creşterea elasticității şi a rezistenței la rupere.

Sursa: www.clariant.com

NOI APLICAȚII ALE RANFORSĂRILOR TEXTREME

Compania britanică ***Composites Evolution*** a dezvoltat o nouă variantă pentru ranforsările *TeXtreme*, bazată pe fibrele naturale *Biotex*.
La expoziția internațională *Composites Europe,* care a avut loc în toamna anului 2012, la Stuttgart, Germania, în centrul expozițional New Stuttgart Trade Fair Centre, au fost expuse trei proiecte, în cadrul cărora s-au folosit ranforsările *TeXtreme spread tow*. Pe baza unei tehnologii unice de țesere a benzilor, furnizată de compania suedeză ***Oxeon***, au fost produse benzi țesute dintr-un amestec de fibre de in şi polipropilenă, cu bune proprietăți de rezistență. În legătură cu aceasta, Brendon Weager, director tehnic al companiei ***Composites Evolution*** afirma: *„În cadrul acestui proiect au fost dezvoltate benzi țesute cu proprietăți excelente, durabile din punct de vedere ecologic“.*
Pentru elaborarea acestora, ***Institutul de Cercetare Fraunhofer,*** din Germania, a inițiat un proiect destinat producerii unor structuri de susținere, care conțin benzi țesute din polipropilenă şi din fibre de sticlă. În acelaşi scop, firma ***Ticona*** – din Germania, parteneră în acest proiect, a furnizat benzi țesute, din care s-a realizat o nouă variantă a ranforsărilor *TeXtreme*.
La expoziția *Composites Europe,* compania ***Manz Automation Tübingen GmbH,*** din Germania, a prezentat o nouă maşină de fabricat benzi țesute din carbon *DD TeXtreme Spread Tow*, aceste benzi fiind solicitate de către compania suedeză ***Oxeon***.
Folosind noi variante de *TeXtreme*, partenerii implicați în aceste proiecte au obținut progrese continue în producerea părților compozite ultrauşoare.
Cu toate că ranforsările *TeXtreme* se bazează, în general, pe fibre de carbon, în prezent există o serie de preocupări pentru dezvoltarea producției acestora, ceea ce va permite o utilizare mai largă în industria compozitelor.

Smarttextiles and nanotechnology, noiembrie 2011, p. 9

NOI MATERIALE COMPOZITE DIN NANOCELULOZĂ

Cercetătorii din cadrul Institutului de cercetări pentru materiale ***EMPA***, din Elveția, au elaborat un proces de producere a pudrei nanocelulozice, folosită ca materie primă pentru fabricarea compozitelor polimerice. Aceste compozite pot fi folosite la realizarea componentelor uşoare destinate industriei auto sau ca membrane şi materiale filtrante în aplicații biomedicale.

În ultimul timp, nanoceluloza a suscitat un interes considerabil atât pentru domeniul industrial, cât şi pentru cel ştiințific, fiind percepută ca un nou biomaterial. Potențialele aplicații ale nanocelulozei includ tehnologia medicală, industria alimentară şi cea farmaceutică.

Celuloza este un biopolimer compus din două lanțuri lungi de glucoză cu proprietăți structurale unice, abundența ei fiind, practic, inepuizabilă. Ea se găseşte în pereții celulari ai plantelor, având rolul unui schelet de susținere. Celuloza prezintă o rezistență maximă la tensionare şi poate fi modificată din punct de vedere chimic în diferite moduri, schimbându-şi în acest fel şi caracteristicile. În plus, celuloza este biodegradabilă.

În căutarea unor noi materiale polimerice, cu anumite caracteristici dorite de utilizatori, specialiştii în ştiința materialelor au dezvoltat compozite de mare performanță, în care sunt încorporate nanofibre de celuloză. Utilizate sub formă de materiale cu structură uşoară, aceste compozite au proprietăți mecanice asemănătoare oțelului, iar sub formă de biospumă nanoporoasă ele oferă o alternativă la materialele izolatoare tradiționale.

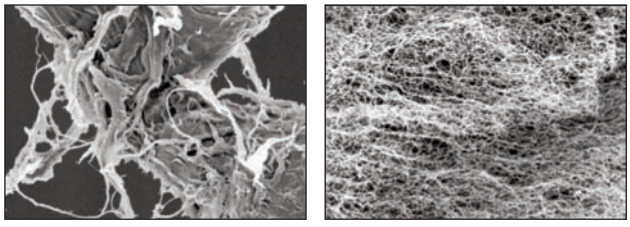

Fig. 1

Celuloza clasică este folosită la scară industrială, în special în industria celulozei, a lemnului şi a hârtiei. În prezent, cercetarea se concentrează pe izolarea celulozei sub formă de nanofibre (fig. 1). Aşa-numita nanoceluloză constă din fibre sau cristale cu diametrul mai mic de 100 nm. Oamenii de ştiință speră că vor reuşi să utilizeze nanoceluloza pentru a crea noi materiale cu greutate redusă şi cu o rezistență mecanică ridicată, ideale pentru crearea structurilor uşoare.

Experții din cadrul laboratoarelor EMPA au izolat, din celuloza de lemn, nanofibre de celuloză cu lungimea de câțiva micrometri şi grosimea de câțiva nanometri, strâns interconectate. Fibrele au o arie a suprafeței extrem de mare, unde se pot produce reacții chimico-fizice cu apa, substanțele chimice organice şi anorganice şi cu unii compuşi polimerici.

Prin urmare, nanofibrele de celuloză pot fi folosite ca materii prime, stabile şi extrem de reactive, pentru diverse aplicații tehnice, prezentând o serie de avantaje suplimentare, datorită caracteristicilor lor biodegradabile. Aceste aplicații includ consolidarea biopolimerilor destinați producerii unor materiale de construcție sigure din punct de vedere ecologic, a materialelor uşoare pentru industria auto şi a membranelor şi materialelor filtrante pentru industria ambalajelor şi biomedicină.

Inițial, nanoceluloza izolată din celuloză de lemn se află sub formă de suspensie apoasă. După uscarea materialului, fibrele de celuloză se lipesc unele de altele şi formează aglomerări rigide, pierzându-şi astfel unele proprietăți mecanice remarcabile.

Din acest motiv, cercetătorii de la Empa au căutat să dezvolte un nou proces de uscare a nanocelulozei, prin care să se evite formarea aglomerărilor şi rigidizarea materialului. Pentru a realiza acest lucru, celuloza a fost tratată folosind o tehnică uşor de implementat la scară mare şi complet inofensivă, adecvată unor aplicații din industria alimentară. Metoda împiedică fibrilele de celuloză să formeze aglomerări şi să se lipească între ele.

Rezultatele obținute în urma redispersiei pe bază de apă, arată că pudra nanocelulozică uscată are aceleaşi proprietăți remarcabile ca şi celuloza care nu a fost uscată sau modificată. Prin urmare, noul produs poate fi o alternativă atrăgătoare la suspensiile de celuloză convențională destinate sintezei materialelor nanocompozite biologice. Suspensiile utilizate în prezent sunt alcătuite din apă, în proporție de peste 90%, fapt ce conduce la costuri foarte mari de transport şi la creşterea pericolului de degradare, prin acțiunea bacteriilor şi a ciupercilor. În plus, manipularea suspensiilor apoase de celuloză necesită, de obicei, schimbarea solvenților pe parcursul procesării chimice.

Activitatea de dezvoltare a unor procese de producție noi şi de identificare a aplicațiilor nanocelulozei ca materie primă pentru fabricarea compozitelor polimerice a fost distinsă cu Premiul Cercetării Empa 2011. Într-un proiect de colaborare cu ***Universitatea Tehnologică Luleå***, din Suedia, cercetătorul Christian Eyholzer şi colaboratorii săi au folosit noua pudră nanocelulozică pentru a consolida adezivi, hidrogeluri şi substanțe sintetice biodegradabile.

Smarttextiles and nanotechnology, decembrie 2011, p. 5